7th International Conference on Nonlinear Vibrations, Localization and Energy Transfer

Bruno Cochelin

Publications du LMA

N° 160 - Juillet 2019

ISSN 1159-0947
ISBN 978-2-909669-26-7

RÉSUMÉS ÉTENDUS / EXTENDED ABSTRACTS

7th International Conference on

NONLINEAR VIBRATIONS, LOCALIZATION AND ENERGY TRANSFER

1st - 4th July 2019, Marseille (France)

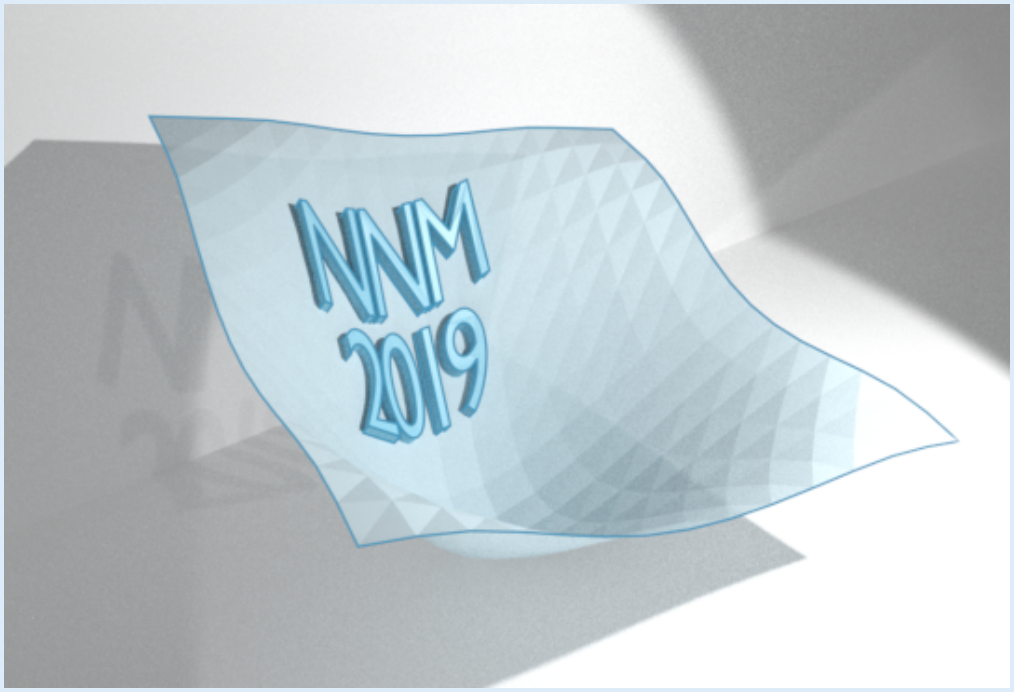

Publications du LMA

N° 160 - Juillet 2019

ISSN 1159-0947
ISBN 978-2-909669-26-7

RÉSUMÉS ÉTENDUS / EXTENDED ABSTRACTS

7th International Conference on

NONLINEAR VIBRATIONS, LOCALIZATION AND ENERGY TRANSFER

1st - 4th July 2019, Marseille (France)

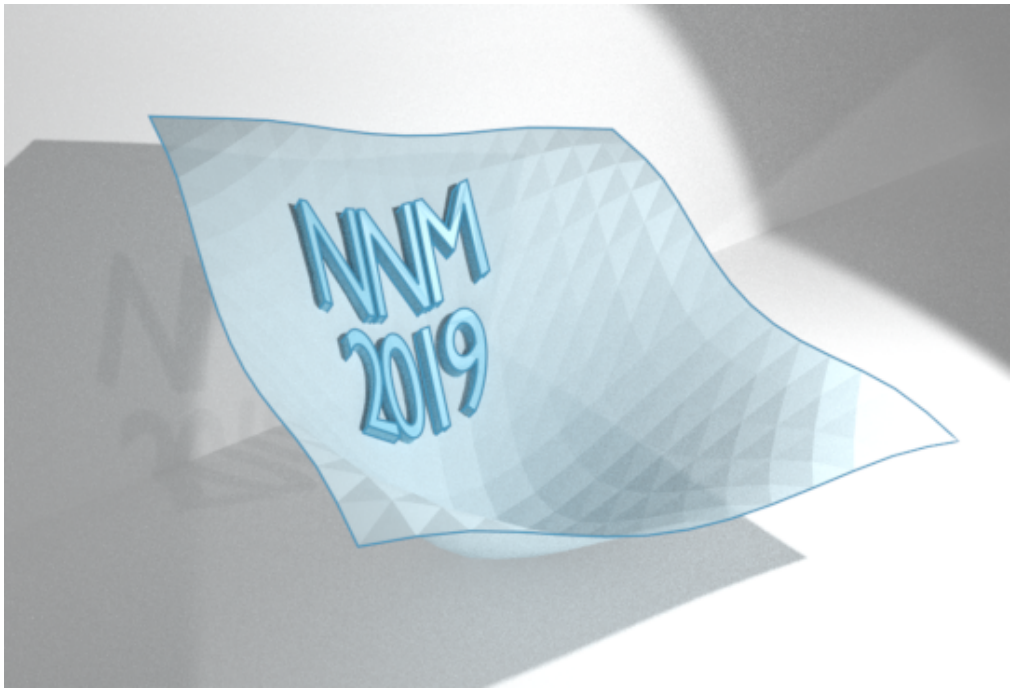

Foreword

Dear Participants,

It's a great pleasure to welcome all of you in Marseille for the seventh edition of the "International Conference on Nonlinear Vibrations, Localization and Energy Transfer". I am glad that the conference comes back to the south of France after the first gathering in Frejus (2004) and the successful editions that were successively held in Samos Island (2006), Frescati (Rome, 2009), Haifa (2012), Istanbul (2014) and Liège (2016).

The purpose of our conference is more than ever to promote exchange and discussions between scientists from all around the world about the latest research developments in the area of nonlinear vibrations, with a particular emphasis on the concept of nonlinear normal modes and targeted energy transfer. We preserve the usual format, with 30 minutes communications within plenary sessions, and we hope many fruitful discussions will ensue and animate lunch hour and coffee breaks. I have no doubt that you will enjoy the scientific content of this event and, in particular, the special session about nonlinear aspects in Musical Acoustics that will illustrate the variety of applications of the concepts, methods, and tools that we are interested in.

Beyond the scientific aspects, the social program is intended to give you a taste of the Provencal *savoir vivre*, and I expect that you will enjoy our city of Marseille and the local peculiarities that make it so unique.

Finally, I would like to warmly thank all the people that have contributed to the success of this conference, the scientific committee, all the sponsors and of course all the Keynotes speakers, oral presenters and poster sessions participants. Special thanks to the local organizing committee, and in particular to Annie, Elena, Marie-Madeleine, Stéphanie, Alain and Michel from the LMA for their help.

Marseille, June 2019

Bruno Cochelin
NNM20129 Chair

Sponsors

Aix-Marseille University
https://www.univ-amu.fr/en

Centrale Marseille Engineering School
https://www.centrale-marseille.fr/en

French National Centre for Scientific
Research
http://www.cnrs.fr/en

Federation for Research
Fabri de Peiresc
http://www.federation-peiresc.cnrs.fr/

Laboratory of Excellence
Mechanics & Complexity
https://labex-mec.univ-amu.fr/?q=en

Aix Marseille Provence Metropole
https://www.ampmetropole.fr/

HGL Dynamics
http://www.hgl-dynamics.com/

Ideol
https://www.ideol-offshore.com/en

Scientific committee

M. Allen	Univ. Wisconsin-Madison
L. Bergman	Univ. of Illinois at Urbana-Champaign
O. Gendelman	Technion
O. Gottlieb	Technion
G. Kerschen	Univ. Liège
W. Lacarbonara	La Sapienza, Rome
C.H. Lamarque	ENTPE, Lyon
S. Lenci	Univ. Politecnica delle Marche
L.I. Manevitch	Russian Academy of Sciences
Y. Mikhlin	Kharkiv Polytechnical Institute
G. Rega	La Sapienza, Rome
F. Romeo	La Sapienza, Rome
S.W. Shaw	Michigan State Univ.
C. Touzé	ENSTA ParisTech, Palaiseau
A.F. Vakakis	Univ. of Illinois at Urbana-Champaign
K. Worden	Univ. of Sheffield

Organizing committee

B. Cochelin, Chairperson	ECM, LMA, Marseille
S. Bellizzi	CNRS, LMA, Marseille
R. Cote	AMU, LMA, Marseille
P.O. Mattei	CNRS, LMA, Marseille
E. Sarrouy	ECM, LMA, Marseille
F. Silva	CNRS, LMA, Marseille
C. Vergez	CNRS, LMA, Marseille

Contents

Identification & ROM

Monday, 1st July 2019

Chairman: A.F. Vakakis

Nonlinear System Identification: Current Status and Challenges Ahead

G. Kerschen, J.P. Noël

University of Liège
Aerospace and Mechanical Engineering Department
Liège, Belgium
g.kerschen@ulg.ac.be

Abstract Even if we are entering the age of virtual prototyping, *experimental testing* and *system identification* still play a key role because they help the structural dynamicist reconcile numerical predictions with experimental investigations. The past decade witnessed a shift in emphasis in nonlinear system identification, accommodating the growing industrial need for a first generation of tools capable of addressing complex nonlinearities in larger-scale structures. The objective of this presentation is to survey some of the key developments which arose in the field and to present the remaining challenges.

System identification refers herein to the development (or the improvement) of mathematical models from input and output measurements performed on the real structure using vibration sensing devices [1]. This presentation, which is based on the two review papers [2,3], provides first a brief historical perspective of the progress of nonlinear system identification starting from the seminal work of Masri and Caughey [4].

After this historical perspective, it is shown that the identification process may be regarded as a progression through three steps, namely detection, characterization and parameter estimation, as outlined in Figure 1. Once nonlinear behavior has been detected, a nonlinear system is said to be characterized after the location, type and functional form of all nonlinearities throughout the system are determined. The parameters of the selected model are then estimated using linear least-squares fitting or nonlinear optimization algorithms depending upon the method considered.

1. Detection: *Is there?* Ascertain if nonlinearity exists in the structural behaviour, *e.g.*, yes.

2. Characterization: *Where? What? How?*

   (a) Locate the nonlinearity, *e.g.*, at the joint;

   (b) determine the type of nonlinearity, *e.g.*, Coulomb friction;

   (c) select the functional form of the nonlinearity, *e.g.*, $g(q,\dot{q}) = c\,\mathrm{sign}(\dot{q})$.

3. Parameter estimation: *How much?*

   Calculate the coefficients of the nonlinearity model and quantify their uncertainty, *e.g.*, in a probabilistic sense, $c \sim \mathcal{N}(5.47, 1)$.

Figure 1: Identification process for nonlinear structural models.

Figure 2: Decommissionned F-16 aircraft at Saffraanberg Airforce Base.

The three steps are illustrated using a real-life aerospace structure, i.e., the F-16 aircraft in Figure 2, for which a detailed measurement campaign was carried out in 2014 in collaboration with Siemens Industry Software [5]. It is shown that the F-16 possesses very interesting nonlinear dynamics, including complex nonlinear stiffness and damping between the wing and the payload.

The presentation concludes by discussing future research directions. Specific attention is paid to experimental continuation techniques, the physical realization of numerical continuation. It exploits feedback control strategies to stabilize the measured response, enabling both stable and unstable branches to be measured.

References

[1] K. Worden and G. Tomlinson, *Nonlinearity in Structural Dynamics: Detection, Identification and Modelling*, Institute of Physics Publishing, Bristol and Philadelphia, 2001.

[2] G. Kerschen, K. Worden, A.F. Vakakis and J.C. Golinval, *Past, present and future of nonlinear system identification in structural dynamics*, Mechanical Systems and Signal Processing 20, 505-592, 2006.

[3] J.P. Noel, G. Kerschen, *Nonlinear system identification in structural dynamics: 10 more years of progress*, Mechanical Systems and Signal Processing 83, 2-35, 2017.

[4] S.F. Masri and T.K. Caughey, *A nonparametric identification technique for nonlinear dynamic problems*, Journal of Applied Mechanics 46, 443-447, 1979.

[5] T. Dossogne, J.P. Noel, C. Grappasonni, G. Kerschen, B. Peeters et al., Nonlinear ground vibration identification of an F-16 aircraft - Part II: understanding nonlinear behaviour in aerospace structures using sine-sweep testing, Proceedings of the IFASD conference, Saint Petersburg, Russia, 2015.

Nonlinear modal analysis based on complete statistical independence

M. Champneys[1], **K. Worden**[1] **and N. Dervilis**[1]

[1]The University of Sheffield
Sheffield, UK
mdchampneys1@sheffield.ac.uk

Abstract A recent study proposes an extension to the Nonlinear modal analysis framework presented by Worden and Green in [1]. The focus of the current investigation is to advance the method by developing a quantitative measure of modal separation and by considering alternate correlation metrics that are able to detect correlations at any order.

Extensions of linear modal analysis to the nonlinear case have been proposed by several researchers; notably the frameworks from Rosenberg [2] and the geometrically more general work from Shaw and Pierre [3]. A recent paper [1] has put forward a new data-driven approach, leveraging statistical independence to optimise the parameters of a Shaw-Pierre mapping to the nonlinear modal coordinates. For a 2Dof system subject to a cubic transformation, this approach gives a transformation of the form of equation 1 and equation 2 as an objective function.

$$\mathbf{u} = \begin{bmatrix} a_{11} & a_{21} \\ a_{21} & a_{22} \end{bmatrix} \begin{bmatrix} x_1 \\ x_2 \end{bmatrix} + \begin{bmatrix} b_{11} & b_{21} & b_{31} & b_{41} \\ b_{21} & b_{22} & b_{32} & b_{42} \end{bmatrix} \begin{bmatrix} x_1^3 \\ x_1^2 x_2 \\ x_1 x_2^2 \\ x_2^3 \end{bmatrix} \tag{1}$$

$$j = Cor(u_1, u_2) + \mid \{a_1\} \cdot \{a_2\} \mid + \sum \mid \text{pairwise dot products of the } \{b_i\} \mid \tag{2}$$

In the study, problems arose where the best (lowest cost) transformations found by the heuristic optimisation were not as attractive as less optimal ones when judged by eye. It was suggested that this may owe to the fact that only statistical correlations up to the 2nd order were considered in the optimisation objective function. In order to address this problem, recent work has investigated ways that the results from the forward mapping may be improved.

In [1], the correlation metric used was the Pearson correlation coefficient (Cor). However this formulation is of limited use due to the fact that only correlations up to the 2nd order can be evaluated. The alternate metrics considered by this study are Spearman's rank monotonicity test (Spr) equation, and the Mutual information (MI). These have the advantage of being able to detect monotonic relationships and correlations to any order respectively.

$$\mathrm{Spr}(X, Y) = \frac{\mathrm{Cov}(r_X, r_Y)}{\sigma_{r_X} \sigma_{r_Y}} \tag{3}$$

$$\mathrm{MI}(X, Y) = -\sum_X \sum_Y P(X, Y) \log(P(X, Y)) \tag{4}$$

In order to provide a qualitative measure of mode separation a new approach is presented. First the spectra of the modal responses are estimated by the Welch method. These spectra are then convolved sequentially into a single signal. Finally a thresholding algorithm is used to detect prominent peaks in the convolved spectra. This approach has the desirable property of generating a unimodal signal only when the modal responses are themselves unimodal.

Some initial results are illustrated in figures 1 and 2. By requiring the convolved spectra to have a single peak, better separated modes are identified despite less optimal objective scores.

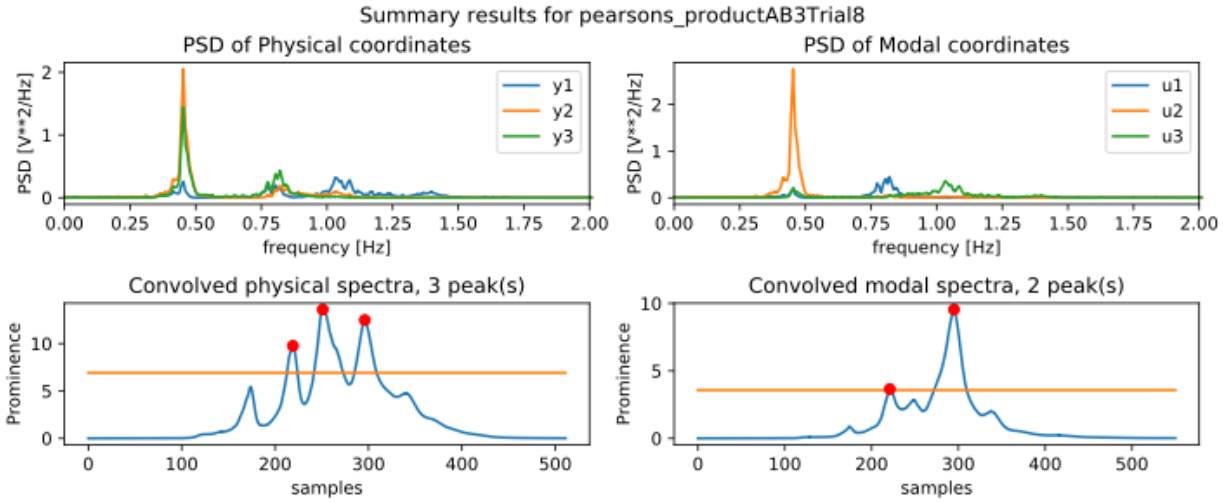

Figure 1: Modal decomposition of 3Dof Duffing system using Pearson's correlation metric - Cubic transformation

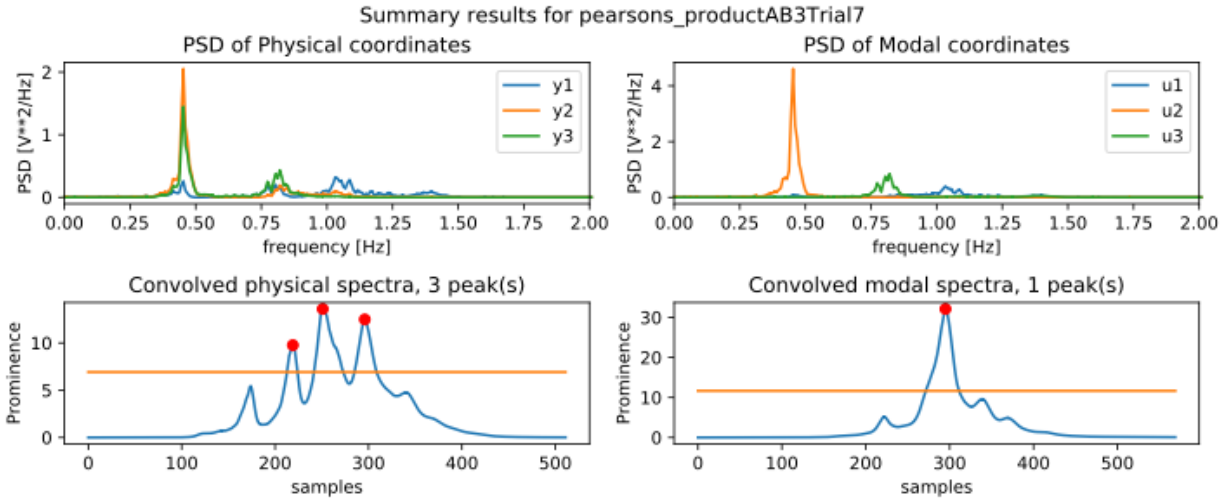

Figure 2: Modal decomposition of 3Dof Duffing system using Pearson's correlation metric - Cubic transformation subject to single peak constraint

Much remains to be done in regards to analysis of the current method. Potential avenues for investigation include; alternate formulations of the objective as a constrained optimisation problem, investigation into ways that computational cost of the metrics might be reduced and wider questions regarding the analytical uniqueness of the NNMs that are computed using this method.

References

[1] K. Worden and P. L. Green, "A machine learning approach to nonlinear modal analysis," in *Dynamics of Civil Structures, Volume 4*, F. N. Catbas, Ed. Cham: Springer International Publishing, 2014, pp. 521–528.

[2] R. M. Rosenberg, "The normal modes of nonlinear n-degree-of-freedom systems," *Journal of applied Mechanics*, vol. 29, no. 1, pp. 7–14, 1962.

[3] S. W. Shaw and C. Pierre, "Normal modes for non-linear vibratory systems," *Journal of Sound and Vibration*, 1993.

Advances to Testing and Model Updating for Geometrically Nonlinear Structures

M. Allen[1], C. VanDamme[1] and M. Kwarta[1]

[1] *Engineering Physics Department, University of Wisconsin-Madison, Madison, WI, USA*
msallen@engr.wisc.edu

Abstract - Model correlation and updating is an important part of the development process of state of the art aircraft, launch vehicles and many other systems. Even though finite element software is highly capable, it still far from reliable when it comes to predicting the actual dynamics of complicated structures such as these. It is necessary to make many approximations around joints, mechanisms, simplifications for details such as sandwich structures, neglecting manufacturing variations, etc…. Furthermore, the current state of the art neglects nonlinearities in the dynamic response. This work seeks to advance the relatively new field of model updating for nonlinear systems. The nonlinear normal modes (NNMs) of the structure are used as a basis for model updating, with new stepped-sine approach used to measure the NNMs and a model updating scheme to update the parameters of a Nonlinear Reduced Order Model (NLROM) for the structure

For the geometrically nonlinear systems that are the focus of this work, the NLROM has the following form [1], where *A* and *B* are the constant coefficients of the quadratic and cubic polynomials respectively, ζ_r and ω_r are the damping ratio and natural frequency of the *r*th mode and $\boldsymbol{\varphi}_r$ is the *r*th mass normalized mode shape.

$$\ddot{\theta}_r + 2\zeta_r\omega_r\dot{\theta}_r + \omega_r{}^2\theta_r + \theta_r(\mathbf{q}) = \boldsymbol{\varphi}_r{}^{\mathrm{T}}F(t) \tag{1}$$

$$\theta_r(\mathbf{q}) = \sum_{i=1}^{m}\sum_{j=i}^{m} B_r(i,j)q_iq_j + \sum_{i=1}^{m}\sum_{j=i}^{m}\sum_{k=j}^{m} A_r(i,j,k)q_iq_jq_k \tag{2}$$

When modeling linear structure such as launch vehicles or aircraft, it is typically necessary to perform tests to update the FEM such that it reflects the correct dynamics, which are captured by ζ_r, ω_r and $\boldsymbol{\varphi}_r$. For a nonlinear structure, the coefficients *A* and *B* that define nonlinearity in the ROM depend on many parameters of the FEM, such as the boundary stiffnesses, material properties, precise curvature of the geometry, etc… and hence we anticipate that it will be necessary to employ testing and model updating to bring the NLROM into agreement with measurements.

The presentation will discuss the authors' latest approach to model updating for these types of structures. The first step involves experimentally estimating the nonlinear normal mode(s) (NNMs) of the system. To do this, the structure is excited near but not precisely at resonance (in order to circumvent difficulty associated with tuning the input so near the point of maximum where the response, where the system is prone to fall off of the resonance. Then the known linear modes of the structure are used with a simplified model to extrapolate to the precise NNM. This approach can speed up stepped-sine testing considerably. The method is illustrated in Figure 1, for real experimental measurements near the first NNM of a nominally flat clamped-clamped beam that is base excited by a shaker. The measurements appear to be very near the NNM because the nonlinear FRFs for this structure are nearly parallel to the actual NNM curve near resonance. The other pane illustrates this for simulated measurements from a curved beam that exhibits both hardening and softening nonlinearities.

Once the NNMs have been measured, the NNMs of the NLROM can be computed and compared. Many iterations may be required to adjust the model parameters until the NNMs come into agreement. This work employs a new algorithm that can significantly accelerate model updating by using a multi-harmonic balance approach in which the gradients of the NNMs with respect to the NLROM parameters are available analytically. Specifically, the gradient of the harmonic amplitudes, **z**, with respect to model parameters, **p**, is given by the following closed form expression in terms of the gradient of the internal forces $\tilde{\mathbf{f}}$ with

respect to the model parameters. For an NLROM the parameters are the nonlinear stiffness coefficients, A and B, and so these are known in closed form. The other matrices are part of the harmonic balance method [2] and are similarly known.

$$\left[\frac{\partial \mathbf{z}}{\partial \mathbf{p}}\right] = -\left[\mathbf{A}(\omega) - \mathbf{\Gamma}(\omega)^{+}\frac{\partial \tilde{\mathbf{f}}}{\partial \tilde{\mathbf{x}}}\mathbf{\Gamma}(\omega)\right]^{-1}\left[\frac{\partial \mathbf{A}(\omega)}{\partial \mathbf{p}}\mathbf{z} - \mathbf{\Gamma}(\omega)^{+}\frac{\partial \tilde{\mathbf{f}}}{\partial \mathbf{p}}\right] \tag{3}$$

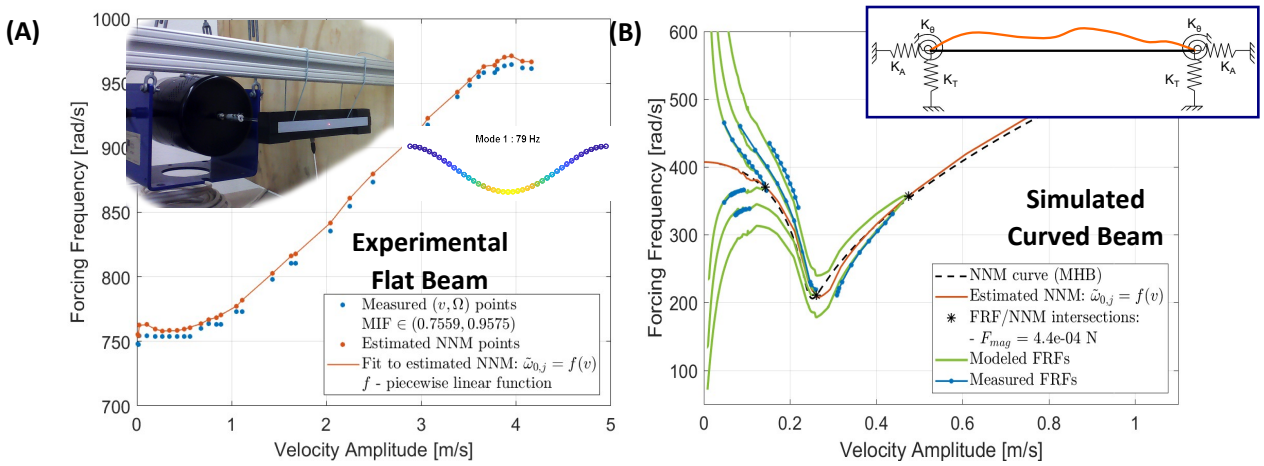

Figure 1. (A) Experimental demonstration of the proposed algorithm to measure NNMs. A series of measurements (blue) are taken near resonance and the single nonlinear resonant mode approximation is used to estimate the NNM (red). (B) Simulated experiments for a curved beam. The nonlinear frequency response is also computed from the measured NNM and compared to simulated measurements (blue).

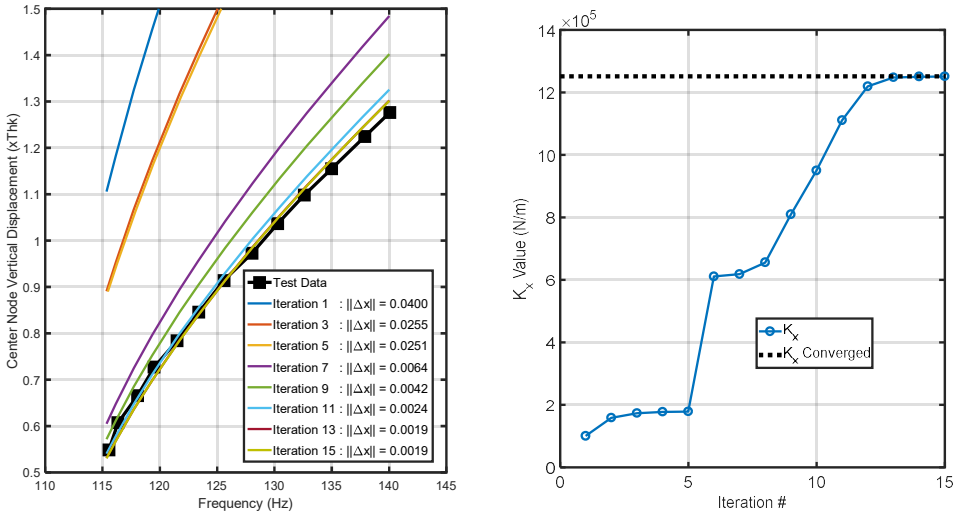

Figure 2. Sample results for nonlinear model updating applied to experimental measurements from a clamped-clamped beam similar to that in Fig. 1. The NNM of the NLROM converges quickly to the measured NNM as the parameters are updated.

References

[1] J. J. Hollkamp and R. W. Gordon, *Reduced-order models for nonlinear response prediction: Implicit condensation and expansion*. Journal of Sound and Vibration 318 (2008) 1139-1153.

[2] T. Detroux, L. Renson, L. Masset, and G. Kerschen, *The harmonic balance method for bifurcation analysis of large-scale nonlinear mechanical systems*. Computer Methods in Applied Mechanics and Engineering 296 (2015) 18-38.

Multi-input phase resonance testing of a nonlinear wing-engine structure using control-based continuation

L. Renson

Department of Engineering Mathematics,
University of Bristol, UK.
l.renson@bristol.ac.uk

Abstract Control-based continuation (CBC) is a general and systematic method that proved useful to identify the nonlinear normal modes (NNMs) of conceptually-simple structures directly during experimental tests. The accurate identification of the NNMs of more complex structures can, however, require the application of multiple input forces. CBC is here extended to multi-input experiments and demonstrated on a wing-engine structure.

Nonlinear normal modes (NNMs) are families of periodic responses of the unforced undamped system that have been successfully exploited to interpret the nonlinear dynamic behaviour of forced and damped systems. For instance, NNMs are found to capture the amplitude-dependence of the resonance frequency of many harmonically-forced systems, which is valuable from an engineering perspective because this is where displacements are often maximum and the structure is at the greatest risk of failure.

NNMs can be identified experimentally through a phase quadrature condition between the system response and the applied excitation. At quadrature, external input forces exactly counterbalance the internal damping forces and hence the system responds as the underlying conservative system. Experimentally finding and tracking this phase quadrature condition is commonly referred to as phase resonance testing. Identified NNMs can, in turn, be exploited for parameter estimation or compared to theoretical predictions for model updating and validation [1].

The phase resonance testing of complex nonlinear structures raises a number of challenges. The quadrature condition often lies close to a saddle-node bifurcation. As such, reaching quadrature requires to test the physical structure on the verge of instability, i.e. where the system's response is particularly sensitive to perturbations and untimely transition to other behaviours can occur. Another difficulty is that quadrature can give results that are significantly different from the true NNM, in particular, when the excitation applied to the system is limited to one input force, as is frequently used in practice [4].

Control-based continuation (CBC) is a testing method that uses feedback control to change the linearisation of the dynamics such that unstable responses of the underlying uncontrolled system can be made stable. The controller also maintains the experiment around a prescribed operating point, thus avoiding untimely transitions between coexisting behaviours. As such, CBC has the potential to be a general and systematic tool to identify NNMs. The method was, for instance, exploited to track phase quadrature conditions in the forced response of several single-degree-of-freedom systems subjected to external harmonic excitations [2, 3]. Although these successful results attest of the power of this method, CBC has been so far limited to conceptually simple experiments with single-input excitation.

The objective of this work is to further develop CBC such that it can be applied to more complex experiments including multiple inputs. The presence of several inputs offers the flexibility to exploit one or several exciters to control the experiment. The effects of this choice on the controller design and the complexity of CBC are discussed. The presence of detrimental interactions between the different sources of excitation through the tested structure is also analysed.

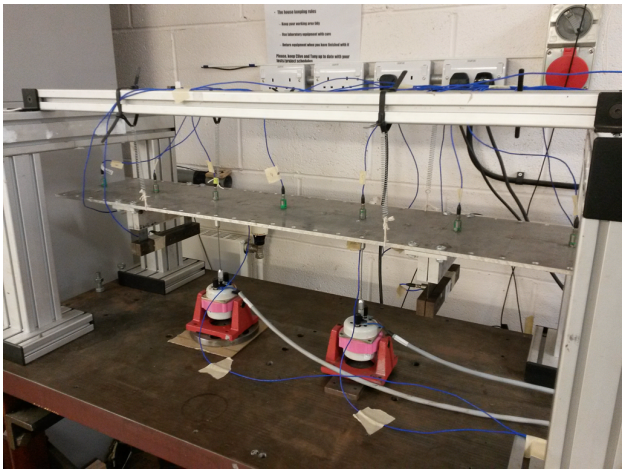

Figure 1: Nonlinear wing-engine structure used to demonstrate the extension of CBC to experiments with multiple input excitations and perform phase-resonance testing.

To validate the extension of CBC to multiple inputs, CBC is tested on a wing-engine structure (Figure 1). This structure is composed of an aluminum plate to which two masses are suspended through a nonlinear mechanism. A linear state feedback controller designed using optimal control techniques and a local linear model of the experiment is sufficient to apply CBC to this multi-input experiment. This further demonstrates that no sophisticated (nonlinear) control strategies are necessary for CBC to work. CBC is then exploited to carry out multi-input phase resonance tests and extract the NNMs of the structure. NNMs identified using either one or two input forces are compared. Controller invasiveness is analysed in both configurations of the excitation.

Acknowledgements

The financial support of the Royal Academy of Engineering (RF1516/15/11) is gratefully acknowledged.

References

[1] M. Song, L. Renson, J.-P. Noël, B. Moaveni, G. Kerschen. (2018) Bayesian model updating of nonlinear systems using nonlinear normal modes. *Struct. Control Health Monit.* 25:e2258.

[2] L. Renson, A. Gonzalez-Buelga, D.A.W. Barton, S.A. Neild. (2016) Robust identification of backbone curves using control-based continuation. *J. Sound. Vib.* 367:145-158.

[3] L. Renson, D.A.W. Barton, S.A. Neild. (2017) Experimental Tracking of Limit-Point Bifurcations and Backbone Curves Using Control-Based Continuation. *Int. J. Bif. Chaos* 27(01):1730002.

[4] L. Renson, T.L. Hill, D.A. Ehrhardt, D.A.W. Barton, S.A. Neild. (2018) Force appropriation of nonlinear structures. *Proc. R. Soc. A* 474, 20170880.

Methods & Concepts

Monday, 1st July 2019

Chairman: L. Manevitch

Basic mechanisms of escape of a harmonically forced classical particle from a potential well.

Oleg Gendelman

Faculty of Mechanical Engineering, Technion – Israel Institute of Technology,

Haifa, 3200003, Israel, ovgend@technion.ac.il

Abstract Various models and systems involving the escape of periodically forced particle from the potential well demonstrate a common pattern. The minimal forcing amplitude required for the escape exhibits sharp minimum for the excitation frequency below the natural frequency of small oscillations in the well. Current work explains this regularity by detailed exploration of the transient dynamics of the escape in a number of benchmark potential wells.

Escape from the potential well under external forcing is invoked for description of numerous important processes and phenomena in physics, chemistry and engineering. Very incomplete list of such processes and phenomena includes dynamics of molecules and absorbed particles, celestial mechanics and gravitational collapse, energy harvesting, physics of Josephson junctions, transient resonance dynamics of oscillatory systems, and even such deceivingly remote topic as capsize of ships. Another important engineering phenomenon related to the escape processes is a dynamic pull-in in microelectromechanical systems.

It is known for a long time [1] that the critical force amplitude required for the escape of harmonically forced particle from various potential wells exhibits a sharp minimum at certain frequency below the frequency of small oscillations in the well. Qualitatively similar escape curves in frequency – voltage domain were observed in the problem of dynamic pull-in in MEMS excited by the alternating current.

In current work, we explain this regularity by considering the escape from three benchmark potential wells, described by the following potential functions:

$$U_0(q)=\begin{cases}-\frac{1}{2}+\frac{q^2}{2}, |q|\le 1\\ 0,\ |q|>1\end{cases};\quad U_\varepsilon(q)=\begin{cases}-\frac{1}{2}+\frac{q^2}{2}-\frac{\varepsilon\alpha q^4}{4}, |q|\le q_m\\ 0,\ |q|>q_m\end{cases};\ U_4(q)=\frac{q^2}{2}-\frac{q^4}{4} \qquad (1)$$

Thus, three different potential functions with increasing complexity are considered: truncated parabolic well, truncated weakly nonlinear well and strongly nonlinear quadratic-quartic potential. For the truncated parabolic well, exact solution is available and the minimum forcing required for the escape tends to zero at the resonant frequency. Addition of even small nonlinearity qualitatively modifies the dynamics. The minimum escape forcing becomes nonzero and shifts towards smaller frequencies. Interestingly, strongly nonlinear model exhibits quite similar properties, at least in the vicinity of main resonance. For the nonlinear wells, the analytic treatment relies on the approximation of isolated resonance [2] and is performed with the help of appropriate transformations to action-angle variables. Results for the escape thresholds for the nonlinear wells are presented in Figure 1.

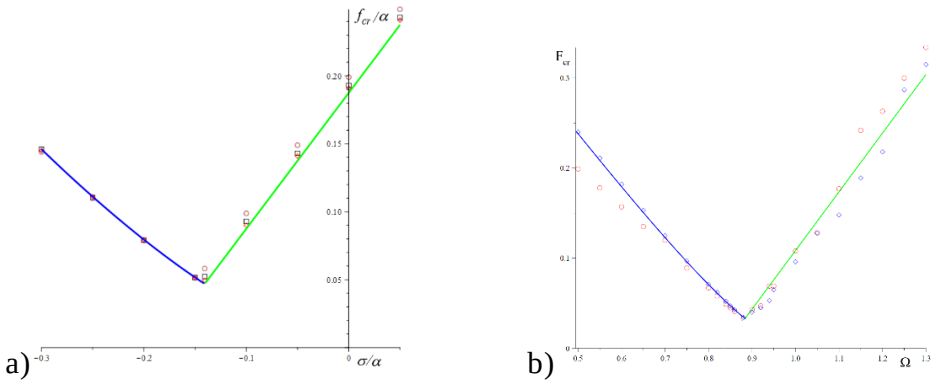

Figure 1 Escape threshold versus the excitation frequency; a) weakly nonlinear truncated well; b) strongly nonlinear well. Dots, circles and diamonds stay for numeric results.

For both nonlinear models one reveals two qualitatively different scenarios of the escape transition. They are illustrated for the strongly nonlinear well in Figure 2.

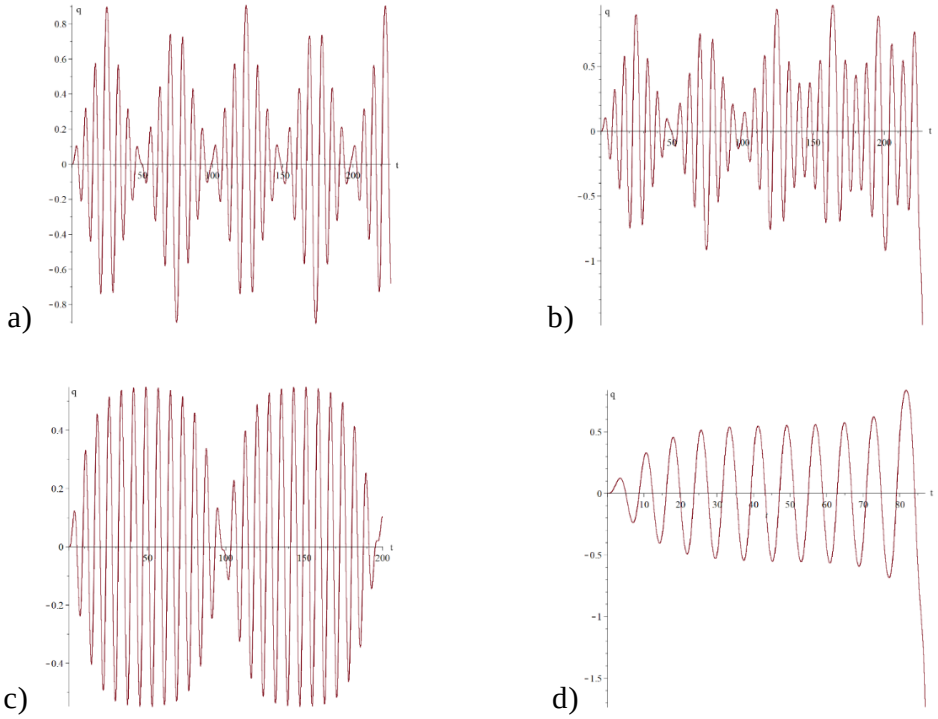

Figure 2. Escape mechanisms: a)-b) –the maximum, c) –d) – the dynamical saddle.

Both in transitions 2a)-2b) and 2c)- 2d) the forcing amplitude differs by about 1%. Still, in the latter case the maximum response energy immediately before the escape achieves only about a half of the well depth. The abrupt increase occurs due to a dynamical heteroclinic bifurcation that reveals itself when details of the transient escape dynamics are considered.

References

[1] L.N.Virgin, R.H. Plaut, C.C. Cheng, *Prediction of Escape from a Potential Well under Harmonic Excitation.* International Journal of Non-Linear Mechanics. 21, 357-365, 1992**.**

[2] O.V.Gendelman, *Escape of a harmonically forced particle from an infinite-range potential well: a transient resonance.* Nonlinear Dynamics. 93, 79-88 2018.

Perturbation methods, algebra and nonlinear vibrations

C.-H. Lamarque[1], **A. Ture Savadkoohi**[1]

[1]Univ Lyon, ENTPE, LTDS UMR CNRS 5513
Vaulx-en-Velin, France
lamarque@entpe.fr, alireza.turesavadkoohi@entpe.fr

Abstract A technique based on exploiting Gröbner bases [1] of multivariable polynomials for detection of periodic solutions is introduced. It is based on generating Gröbner bases and verifying the possibility of determining/defining polynomials of approximated L^2-norms of solutions which belong to ideals generated by the Gröbner bases.

To track periodic solutions of nonlinear (quite often polynomial nonlinearities) smooth second order differential systems (i.e. nonlinear vibrations of nonlinear mechanical systems) perturbation methods have been developed (KBM averaging, Normal Form, Multiple scales, etc.: [2–19]). These approximated methods lead to algebraic polynomial equations. One can obtain approximations of periodic solutions by solving systems of algebraic equations with unknown coefficients (coefficients of truncated Fourier series for examples) and given parameters. Numerical techniques are used to solve these algebraic equations at given parameters' values such as Newton-Raphson methods, or continuation methods [20, 21] if solutions are tracked versus one (or several, which is not usually the case in practice) parameter(s). Nevertheless finding all solutions, and especially the isolated branches of solutions is always a challenge. For systems with k degrees of freedom (dof), $k \geq 1$, these perturbation methods tends to provide approximated values of coefficients of truncated Fourier series and then to provide frequency-response curves, finally the response corresponds to an approximation of L^2 norm of a periodic response of each dof. We present an approach based on using algebra methods. The main idea is to exploit Gröbner bases of multivariate polynomials. Contrary to the approach of Grolet and Thouverez [22], we do not try to obtain a parametrization of the nonlinear vibrations versus one particular variable which satisfies a polynomial equation. Here, the main idea is to test the belonging of a polynomial of the approximated L^2-norm to the ideal generated by the set of polynomial equations issuing from the analytical approximated response. We consider the cases of single dof systems. Let us assume that a perturbation/approximated method provides N polynomial equations. Then, a general algorithm is described to generate a Gröbner bases and to test the possibility to constraint a polynomial (to be determined) of the approximated L^2-norm of the solution of single dof systems to belong to ideals generated by the Gröbner basis. This approach is presented via some simple examples (Duffing oscillator at first) treated by Harmonic Balance method as an example of the perturbation method. Then, we explain how to extend the method to two dof systems. It is enough to understand possible generalization to n dof systems. The method could be extended to non polynomial nonlinearities. Limitations/potential of the method are discussed. Moreover, open questions and perspectives will be given.

References

[1] A. Bostan, F. Chyzak, M. Giusti, R. Lebreton, G. Lecerf, B. Salvy, E. Schost, *Algorithmes efficaces en Calcul Formel*, published by the Authors, 2017.

[2] N. M. Krylov; N. N. Bogolyubov, *Introduction to non-linear mechanics*. Princeton Univ. Press, 1947.

[3] D. R. Smith, *Singular-Perturbation Theory*. Cambridge: Cambridge University Press, 1985.

[4] N. Bogoliubov, *Asymptotic Methods in the Theory of Non-Linear Oscillations*, Paris: Gordon & Breach, 1961.

[5] Maurice Roseau, Vibrations in Mechanical Systems: Analytical Methods and Applications. Springer-Verlag, Berlin, 1987.

[6] J.K. Hale, *Oscillations in nonlinear systems*, McGraw-Hill, 1963

[7] A.H. Nayfeh, *Perturbation methods*, Wiley, 1973

[8] P. H. Coullet, E. A. Spiegel, *Amplitude Equations for Systems with Competing Instabilities*, SIAM Journal on Applied Mathematics, 43 (4), 776-821, 1983.

[9] C. Hayashi, *Forced Oscillations in Nonlinear Systems*, Tokyo, Nippon Printing and Publishing, 1953.

[10] M. Urabe, *Galerkin's procedure for nonlinear periodic systems*, Archive of Rational Mechanics and Analysis, 20, 120-152, 1965.

[11] H. Poincaré, *Les méthodes nouvelles de la mécanique céleste (vol. 2)*, Paris, Gauthier-Villars, 1893.

[12] G.D. Birkhoff, *Dynamical systems*, A.M.S. Coll. Publications, vol. 9, (1927). Reprinted 1966.

[13] C. Elphick, E. Tirapegui, M. E. Brachet, P. Coullet, G. Iooss, *A simple global characterization for normal forms of singular vector fields*, Physica D, 29, 95-127, 1987.

[14] J. Guckenheimer, P. Holmes, *Nonlinear oscillations, dynamical systems and bifurcations of vector fields*, Applied Mathematical Science, vol.42, Springer, Berlin, Heidelberg, New York, 1983.

[15] F. G. Gustavson, *On constructing formal integrals of an hamiltonian system near an equilibrium point*, Astronomical Journal, 71, 670-686, 1966.

[16] G. Iooss, M. Adelmeyer, *Topics in Bifurcation Theory and Applications*, Advanced Series in Nonlinear Dynamics, vol. 3, World Scientific, Singapore, 1992.

[17] J. Moser, C. L. Siegel, Lectures on celestial mechanics. Springer-Verlag, New York, Heidelberg, Berlin, 1971.

[18] R. Rand, D. Armbruster, *Perturbation Methods, Bifurcation Theory and Computer Algebra*, SPrineger Verlag, 1987

[19] A.H. Nayfeh and D.T. Mook, *Nonlinear Oscillations*. Wiley, New York, 1979.

[20] B. Cochelin, C. Vergez, *A high order purely frequency-based harmoni cbalance formulation for continuation of periodic solutions*, Journal of Sound and Vibration 324, 243262, 2009.

[21] L. Renson, G. Kerschen and B. Cochelin, *Numerical computation of nonlinear normal modes in mechanical engineering*, Journal of Sound and Vibration 364, 177-206, 2016.

[22] A. Grolet, F. Thouverez, *Computing multiple periodic solutions of nonlinear vibration problems using the harmonic balance method and Gröbner bases*, Mechanical Systems and Signal Processing 52-53(1), 529-547, 2015.

Nonlinear cable's moving boundary problem: boundary modulation vs. quasi-static drift

T.D. Guo[1,2], G. Rega[2]

[1]College of Civil Engineering, Hunan University, Changsha, China
guotd@hnu.edu.cn

[2]Department of Structural and Geotechnical Engineering,
Sapienza University of Rome, Rome, Italy
giuseppe.rega@uniroma1.it

Abstract A nonlinear suspended cable excited by a boundary motion is attacked in two different formulations, i.e., the boundary modulation formulation and the quasi-static drift formulation.

Cable's nonlinear vibration [1] excited by a kinematic boundary motion of a support (deck or tower) is important for cable-stayed structures, and also, theoretically, an interesting fundamental dynamics problem. Indeed, it can be regarded as one of the two key building blocks - the other one being the support dynamics excited by cable tension - for the boundary modulation concept [2], which allows to deal with the two-way (cable-support) coupled problem. This presentation focuses on two different approaches for attacking the first (support-to-cable) coupling problem, i.e., the boundary modulation approach [2] and the quasi-static drift formulation [3][4]. Their conditional equivalence will be analytically established, and differences, limitations will also be reported. Furthermore, an interesting logical connection between the common empirical shape function [3] and the new rationally derived one, will be discussed. A cable with boundary motion is formulated as

$$\ddot{w}+2c\dot{w}-w''-\alpha\left(w''+y''\right)\left[s_d\left(t\right)\cdot\sin\beta_0+\int_0^1\left(y'w'+0.5w'^2\right)\mathrm{d}x\right]=0 \tag{1}$$

where β_0 is boundary motion inclination, $w(x,t)$ and $s_d(t)$ represent the cable's and the support's displacements, respectively. The cable's non-dimensional stiffness is α, and initial sag is $y(x)=4fx(1-x)$, where the sag-to-span ratio is $f=b/l$, with b, l denoting the sag and span. The cable's boundary conditions at $x=0$ and $x=1$ are $w(0,t)=0, w(1,t)=s_d\left(t\right)\cos\beta_0$. A single-mode cable is chosen, and ω_m is its dominant frequency. The support motion is assumed to be $s_d\left(t\right)=Y_0\,e^{\mathrm{i}\Omega_d t}/2+cc.$, $\Omega_d=2\omega_m+\varepsilon^2\sigma_1$, which means the cable is excited parametrically.

In the boundary modulation formulation, one key assumption is introduced, i.e., the moving boundary is too weak to affect cable's linear modal dynamics while its effects are only on cable's higher order dynamics [2], i.e., $O(w)\sim O(\varepsilon), O(s_d)\sim O(\varepsilon^2)$. Thus, the moving boundary can be transformed analytically to a weak boundary modulation term on cable's slow dynamics through a standard multi-scale expansion ($w(x,t)=\sum\varepsilon^j w_j\left(x,T_0,T_2\right)$). After finding the solvability condition at the order $O\left(\varepsilon^3\right)$, we get the corresponding reduced model

$$D_2A_m=-\mu_mA_m-\frac{\mathrm{i}}{2\omega_m}\Gamma_mA_m\left|A_m\right|^2-\frac{\mathrm{i}}{2\omega_m}\underbrace{\left[\kappa_{S1}\left(\beta_0\right)+\kappa_{S2}\left(\beta_0\right)\right]}_{\kappa_S}\bar{A}_mY_0e^{\mathrm{i}\sigma_1T_2} \tag{2}$$

Here, A_m is cable's dominant modal amplitude appearing in $w_1=A_m\left(T_2\right)\phi_m\left(x\right)e^{\mathrm{i}\omega_mT_0}+cc.$, and the boundary modulation coefficient $\kappa_{S1}\left(\beta_0\right)$, $\kappa_{S2}\left(\beta_0\right)$ can be analytically derived.

In the quasi-static drift formulation, as the cable's standard boundary condition (fixed at both ends) has been relaxed, a modification induced by the moving boundary is introduced, i.e.,

$$w = \psi_0(x)\, s_d(t) \cos\beta_0 + \phi_m(x)\, q_m(t) \tag{3}$$

where the quasi-static drift function $\psi_0(x)$ satisfies $\psi_0(0)=0$ and $\psi_0(1)=1$, and the elastic mode shape $\phi_m(x)$ satisfies $\phi_m(0)=\phi_m(1)=0$. Two empirical drift functions are $\psi_0(x)=x$ [3] and $\psi_0(x)=x^2$ [4]. By substituting Eq.(3) into Eq.(1) and using Galerkin discretization technique, we get (similar ordering assumption is also used $O(w)\sim O(q_m)\sim O(\varepsilon), O(s_d)\sim O(\varepsilon^2)$)

$$\ddot{q}_m + 2\mu\dot{q}_m + a_1 q_m - a_2 q_m^2 - a_3 q_m^3 + a_4 \ddot{s}_d + a_5 \dot{s}_d - a_6 s_d + a_7 q_m s_d + O(\varepsilon^4) = 0 \tag{4}$$

Using a proper multi-scale expansion ($q_m(t)=\sum \varepsilon^j q_{mj}(T_0,T_2), j=1,2,3,\cdots$), the reduced model is established through finding the solvability condition

$$D_2 B_m = -\mu B_m - \frac{\mathrm{i}}{2\omega_m}\underbrace{\left(3a_3 + \frac{10a_2^2}{3\omega_m^2}\right)}_{\tilde{\Gamma}_m}\left|B_m\right|^2 B_m - \frac{\mathrm{i}}{2\omega_m}\underbrace{\left(-\frac{a_6}{2} - \frac{a_4 a_2 \Omega_d^2 - a_5 a_2}{3\omega_m^2}\right)}_{\tilde{\kappa}_S}\bar{B}_m Y_0 e^{\mathrm{i}\sigma_1 T_2} \tag{5}$$

Here B_m is the cable's dominant modal amplitude appearing in $q_{m1} = B_m(T_2)e^{\mathrm{i}\omega_m T_0} + cc.$ The coefficients $a_1 \sim a_7$ can be analytically derived. A full comparative study will be based upon these two different reduced models (Eq.(2) and Eq.(5)), as illustrated in Fig. 1 below.

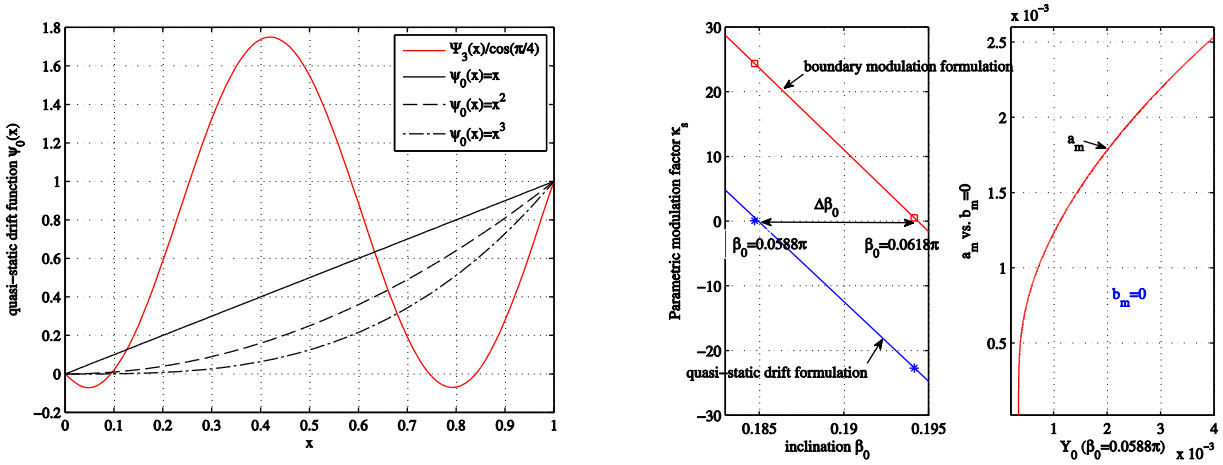

Figure 1: Different shape functions, and two formulation comparisons: μ=0.001, ω_m= 4.21369, σ_1=0.0. $\psi_0=x$ (*), $\psi_0=\Psi_3/\cos(\beta_0)$ (□)

References

[1] G. Rega, Nonlinear vibrations of suspended cables - Part I: Modeling and analysis, *Applied Mechanics Reviews* 57, 443-478, 2004.

[2] T.D. Guo, H.J. Kang, L.H. Wang, Y.Y. Zhao, Cable's mode interactions under vertical support motions: Boundary resonant modulation, *Nonlinear Dynamics* 84, 1259-1279, 2016.

[3] L.H. Wang, Y.Y. Zhao, Large amplitude motion mechanism and non-planar vibration character of stay cables subject to the support motions, *Journal of Sound and Vibration* 327, 121-133, 2009.

[4] C.T. Georgakis, C.A. Taylor, Nonlinear dynamics of cable stays. Part I: Sinusoidal cable support excitation, *Journal of Sound and Vibration* 281, 537-–564, 2005.

Mass detection through symmetry breaking in a MEMS array

S. Baguet[1], C. Grenat[1], C.H. Lamarque[2] and R. Dufour[1]

[1]Univ Lyon, INSA-Lyon, CNRS UMR5259, LaMCoS
Villeurbanne, France
Sebastien.Baguet@insa-lyon.fr, Clement.Grenat@insa-lyon.fr, Regis.Dufour@insa-lyon.fr

[2]Univ Lyon, ENTPE, CNRS UMR5513, LTDS
Vaulx-en-Velin, France
Claude.Lamarque@entpe.fr

Abstract In this contribution, an original mass sensing technique exploiting the nonlinearities of a symmetric array of coupled MEMS (micro electro-mechanical systems) resonators is proposed. It is shown that the nonlinear normal modes (NNMs) of the system are modified after a symmetry-breaking event, with the creation of isolated branches of NNMs. This modification is used to produce easy-to-detect jumps in amplitude when an additional mass is dropped on the resonator.

Due to their small size and high sensitivity, MEMS resonators are very good candidates for mass sensing devices. Classical MEMS-based sensing techniques rely on detecting a shift in frequency induced by an external perturbation (acceleration, addition of mass, ...) in a single MEMS resonator. The need for parallel mass sensing and highly sensitive devices led to the development of MEMS arrays [1] and alternative mass sensing techniques based on nonlinear phenomena [2–4].

In this paper, an array of two coupled electrostatically-actuated MEMS resonators is considered, as sketched in Figure 1a). The two beams 1 and 2 are identical with the following design and material properties: h=300nm, b=160nm, l=10μm, E=1.69 10^{11}N/m^2, ρ=2330kg/m^3, a quality factor Q=5000 and identical gaps g=200nm between two adjacent beams. Each beam i is subjected to lateral vibrations w_i due to nonlinear harmonic electrostatic forces generated by the adjacent beam and electrode. The model is similar to the two-beam model detailled in [4]. The spatial dependence is removed with a Galerkin method using the linear undamped eigenmodes. The continuation and stability analysis of the underlying NNMs is performed with the harmonic balance method using 5 harmonics [5].

In the case of a perfectly symmetric configuration (symmetric voltages, no additional mass), the system exhibits two main (pure) NNM branches corresponding to the out-of-phase and in-phase motions of the beams respectively, see Figure 1b). A branch point (BP) bifurcation is found on the in-phase NNM. After this BP, the in-phase NNM becomes unstable and a stable mixed NNM appears, whose modal shape is an asymmetric mix of the two pure modal shapes.

When a small mass δm=$10^{-4}m$, with m the mass of one microbeam, is added on beam 1, the system becomes asymmetric and the symmetry breaking turns the BP of Figure 1b) into an imperfect bifurcation, see Figure 2. As a result, the in-phase and mixed NNMs are transformed into an asymmetric (different on each beam) in-phase pure NNM and an isolated NNM (INNM) which is detached from the pure NNMs. A starting point for the continuation of the INNM is obtained by performing a bifurcation tracking with respect to δm from the BP of Figure 1 (δm=0) until δm=$10^{-4}m$ corresponding to the limit points (LP) of Figure 2. It is worth noting that the two plots of Figure 2 are switched if δm is added on beam 2 instead of beam 1.

The nonlinear forced response curves (NFRCs) of this asymmetric array are composed of a main NFRC supported by the pure NNMs and of isolated solutions (ISs) detached from the main NFRC and supported by the INNMs and possibly by the pure NNMs. Therefore, in the

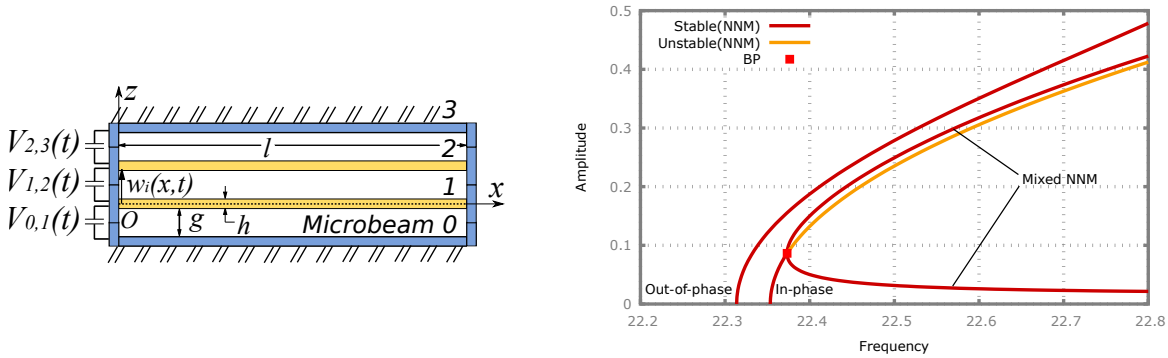

Figure 1: Left: Two-beam MEMS array. Right: NNMs of the symmetric array.

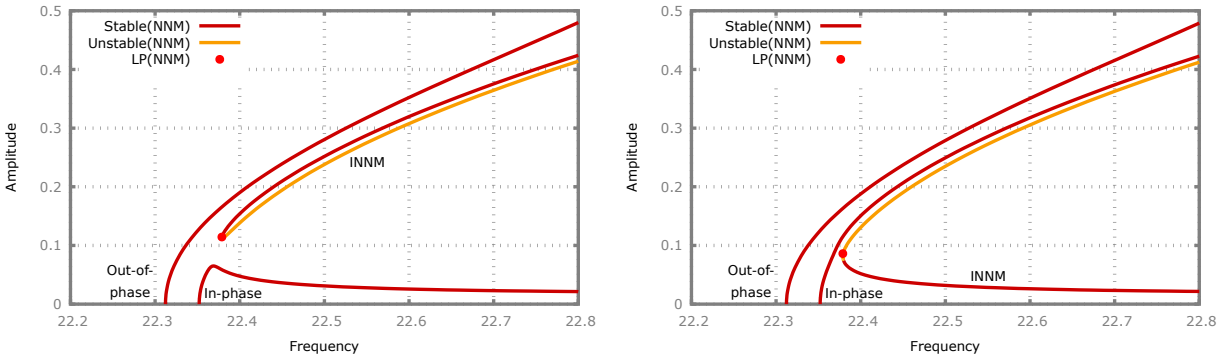

Figure 2: NNMs of the asymmetric array. Left: Beam 1. Right: Beam 2.

case of in-phase response, the main NFRC of beam 1 has a much lower amplitude than beam 2. This localization of motion resulting from symmetry breaking can be exploited for mass detection. Real devices are likely to be inherently asymmetric due to manufacturing defects for instance. In this case, the mass detection is based on the reversal of localization of motion that occurs when the added mass exceeds the level of asymmetry.

References

[1] S. Gutschmidt and O. Gottlieb, *Nonlinear dynamic behavior of a microbeam array subject to parametric actuation at low, medium and large dc-voltages*, Nonlinear Dynamics 67(1), 1-36, 2012.

[2] M.I. Younis and F. Alsaleem,F, *Explorationofnewconceptsfor mass detection in electrostatically-actuated structures based on nonlinear phenomena*, J. Comput. Nonlinear Dyn. 4(2), 021010 (2009).

[3] J.F. Rhoads, S.W. Shaw, and K.L. Turner, *Nonlinear dynamics and its applications in micro- and nanoresonators*, J. Dyn. Syst. Meas. Contr., 132(3):034001, 2010.

[4] S. Baguet, V. N. Nguyen, C. Grenat, C-H. Lamarque, and R. Dufour, *Nonlinear dynamics of micromechanical resonator arrays for mass sensing*, Nonlinear Dynamics 95 (2), 1203-1220, 2019.

[5] C. Grenat, S. Baguet, R. Dufour, and C-H. Lamarque, *Bifurcation analysis of nonlinear normal modes with the harmonic balance method*, ENOC 2017, 9th European Nonlinear Dynamics Conference, Budapest, Hungary, 2017.

[6] T. L. Hill, S. A. Neild, and A. Cammarano, *An analytical approach for detecting isolated periodic solution branches in weakly nonlinear structures*, Journal of Sound and Vibration, 379, 150-165, 2016.

Port-Hamiltonian Representation of Dynamical Systems. Application to Self-Sustained Oscillations in the Vocal Apparatus

F. Silva[1], T. Hélie[2] and V. Wetzel[1,2]

[1] Aix Marseille Univ., CNRS, Centrale Marseille, LMA, Marseille, France
silva@lma.cnrs-mrs.fr

[2] S3AM Team, UMR STMS 9912, IRCAM-CNRS-SU, Paris, France
{thomas.helie,victor.wetzel}@ircam.fr

Abstract Phonation is a natural example of nonlinear dynamical system with self-sustained oscillations, here resulting from the controlled nonlinear coupling between the deformable vocal folds and the airflow expired from the lungs through the glottis and the vocal tract. As a proof of concept, we propose a minimal model of the full vocal apparatus using the port-Hamiltonian representation that emphasises on the structure of a system (on the separation between the behaviour of the subsystems and their interconnection) and on the power exchanges. Numerical results on bifurcations are qualitatively discussed in relation to voice pathologies.

Motivations The physics of voice production has motivated a wide variety of models, from full-featured numerical ones (mainly based on FEM for vocal folds and FVM for the airflow) to reduced order models focusing on the essential phenomenon underlying the phonation. A large body of work in the latter category relies on the description of the glottal aerodynamics from the late 1950 that is based on experiments in rigid static larynx-like ducts. However phonation intrinsically implies the vibration of the vocal folds periodically closing the glottis. There is a significant paradox in those simplified models: the vocal folds move as a consequence of the power exchanged with the glottal flow, but the description of the latter assumes that it does not receive or provide any power to the folds. This power imbalance in the models introduces a bias in the analysis of the coupling occurring in the larynx and of the instability leading to voice production.

Port-Hamiltonian systems (PHS) The port-Hamiltonian theory combines the views of the (geometric) Hamiltonian mechanics and of port-based modelling approach, emphasising the separation between the behaviour of components and their interconnection. The *lingua franca* of this theory is energy : port-Hamiltonian systems are open passive systems that can store, dissipate and exchange power with their neighbourhood. Energy-storage is defined by the Hamiltonian $H(x)$ as a function of state variables x. This dependency, formulated as the Hamiltonian gradient $\nabla_x H$, expresses the *effort* of the energy-storing component. Conversely, the evolution of this component is described by the *flux* variable $\dot{x}$. Effort and flux are power dual variables, i.e., they jointly define the *energy flow* $dH/dt = \dot{x} \cdot \nabla H(x)$.

Dissipating components are described by dissipation variable w and their constitutive laws $z(w)$, such that the dissipated power is $\mathcal{P}_{\text{diss}} = w \cdot z(w) \geq 0$. Finally, external interactions are classically described in terms of inputs u (also called efforts) and output y (fluxes) that are dual with respect to the external power: $\mathcal{P}_{\text{ext}} = y \cdot u$ (≥ 0 when the system yields power).

The geometric structure (Dirac structure, see [1]) accounting for the interconnection of the

subsystems is then described by a matrix S relating efforts to fluxes:

$$\begin{pmatrix} \dot{x} \\ w \\ y \end{pmatrix} = S(x, w) \begin{pmatrix} \nabla H \\ z(w) \\ u \end{pmatrix}. \tag{1}$$

When the interconnection is conservative, the power balance is ensured provided that the matrix S is skew-symmetric ($e \cdot S \cdot e = 0$ for any effort e).

Minimal port-Hamiltonian model of the vocal apparatus The vocal apparatus is modelled as the interconnection of vocal folds, glottal flow, vocal tract and a subglottal pressure supply. Every component is designed minimally with an emphasis on the dual pairing on the interconnection ports. For instance, each vocal fold is considered to be a single-d.o.f. oscillator with an elastic cover, and is submitted to pressure on the upstream and downstream faces, and interacts with the flow at the glottal face. Reciprocally, the glottal flow is modelled as the simplest kinematics of potential incompressible flow of inviscid air preserving the continuity of the normal velocity on the surface of the vocal folds (see details in Ref. [2]). Downstream the glottis, the flow separates from the folds into a jet that spreads and dissipates its kinetic energy into heat. Finally, the vocal tract is represented as seen by the larynx, i.e. by means of its input impedance describing the acoustic feedback on the larynx.

The full vocal apparatus is obtained by conservative interconnection of the previous subsystems. For the sake of conciseness, the resulting Hamiltonian and matrix S are not reported here but can be efficiently computed using the Python package PyPHS [3] designed for the symbolic manipulation of PHS systems.

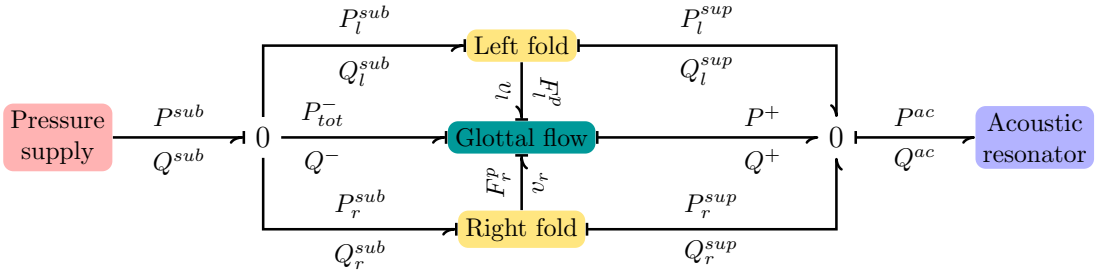

Figure 1: Components of the vocal apparatus. The interconnection takes place via pairs of effort (P) and flux (Q) variables.

Numerical results Time-domain simulations are performed using the numerical scheme designed after the principles of the port-Hamiltonian theory [4], i.e. preserving power balance, but also being more consistent than standard integrators (e.g., RK45, ...). Time-domain simulations and bifurcation analysys evidence the ability of the model to produce oscillating regimes above some pressure threshold, and quasi-periodic vibrations to possible intermittency when vocal folds are detuned.

References

[1] A. van der Schaft and D.Jeltsema, *Port-Hamiltonian Systems Theory: an Introductory Overview*, Now Publishers Inc., 2014.

[2] T. Helie and F. Silva, *Self-oscillations of a Vocal Apparatus: A Port-Hamiltonian Formulation*, 3rd GSI, Paris, 2017.

[3] A. Falaize, *PyPHS: Passive modeling and simulation in python.* Website **https://afalaize.github.io/pyphs/**.

[4] N. Lopes, *Approche passive pour la modélisation, la simulation et l'étude d'un banc de test robotisé pour les instruments de type cuivre*. PhD thesis, UPMC, Paris, 2016.

NES & TET

Tuesday, 2nd July 2019

Chairman: O. Gendelman

Stochastic Design Optimization in Nonlinear Vibrations

Keynote Lecture

Samy Missoum

Aerospace and Mechanical Engineering Department
University of Arizona
Tucson, Arizona, 85721, USA
smissoum@email.arizona.edu

Abstract The design optimization of problems involving nonlinear dynamics is tedious because of their inherent sensitivity to uncertainties and the presence of discontinuities. Traditional methods in design optimization are not sufficient to overcome the hurdles encountered in these problems. This lecture will provide an overview of current difficulties in design optimization and uncertainty propagation. It will also present a new framework for the stochastic optimization of nonlinear vibration problems.

Nonlinear dynamics phenomena have been studied and leveraged in several areas of science and engineering. For instance, nonlinear energy sinks (NESs) [1] have become extremely popular in vibration mitigation. Nonlinearities are also important in the development of metamaterials [2] where the tailoring of local nonlinearities can lead to performances and behaviors not encountered in nature. The use of nonlinearities has markedly extended the realm of design possibilities and, in conjunction with strides in additive manufacturing, it is an area that has yet to deliver its full potential.

However, the design, and in particular the optimal design, of dynamical systems exhibiting a nonlinear behavior is particularly tedious for several reasons. First, "jump" behaviors lead to discontinuous responses, which present major hurdles for traditional optimization methods. In the area of nonlinear vibrations, a typical example is provided by the NES efficiency, which is discontinuous when the activation threshold is reached. Related to the presence of discontinuities, the second difficulty is the potentially high sensitivity of the responses to design and loading uncertainties. Finally, high dimensional problems involving computationally intensive function evaluations also represent a major hurdle. Therefore, dedicated design optimization approaches are needed to tackle the specificities of nonlinear vibration problems.

This lecture will discuss the sensitivity of the dynamic behavior to uncertainties by providing examples of jump behaviors that can strongly impact the choice and the efficiency of optimization or uncertainty propagation techniques. For instance, the non-smoothness of the responses prevents the use of gradient-based optimization methods or topology optimization approaches that rely on the computation of adjoint-based sensitivities. Discontinuities also prevent the use of approximations, referred to as surrogates or metamodels (e.g., Kriging, Polynomial Chaos Expansion), that typically enable optimization or uncertainty quantification.

A general stochastic optimization framework for nonlinear dynamic problems, which attempts to address the aforementioned difficulties, will be presented. In particular, a solution scheme to the following optimization problem will be provided [3, 4]:

$$\begin{aligned} \max_{\boldsymbol{\mu}^d} \quad & \mathbb{E}(F(\mathbf{X^d}, \mathbf{X^a})) \\ s.t. \quad & \mathbb{P}((\mathbf{X^d}, \mathbf{X^a}) \in \Omega) \leq P_T \\ & \boldsymbol{\mu}^d_{min} \leq \boldsymbol{\mu}^d \leq \boldsymbol{\mu}^d_{max} \end{aligned} \tag{1}$$

where $\mathbb{E}(F)$ is the expected value of a performance metric F. $\mathbf{X^d}$ are random design variables (e.g., nonlinear stiffness) with hyperparameters $\boldsymbol{\mu}^d$ (e.g., means of distributions) and $\mathbf{X^a}$ are "environmental" random variables (e.g., loading conditions). Ω is a domain of unwanted behaviors (e.g., no NES activation) and P_T is a probability threshold. The key features of the solution scheme are the use of "machine learning" techniques such as clustering and support vector machines (SVM) classifier for the purpose of automatically detecting discontinuities and identifying the boundary, defined through an SVM, segregating various dynamic behaviors. An adaptive sampling scheme, which helps reduce the number of function calls, has been developed for the refinement of the SVM boundary thus enabling the optimization and the calculation of statistical moments and probabilities.

Several examples will be presented: one set of examples will deal with the optimal design of NESs for simple problems as well as for the mitigation of nonlinear aeroelastic vibrations in the sub- and supercritical regimes [5]. Another set of examples will present the design optimization of chains of nonlinear resonators for the mitigation of vibrations using band gap and dissipation effects.

References

[1] A. Vakakis, O.V. Gendelman, L. Bergman, M. McFarland, G. Kerschen, Y.S. Lee, *Nonlinear targeted energy transfer in mechanical and structural systems*, Springer Science & Business Media 156, 2008

[2] P.A. Deymier, *Acoustic metamaterials and phononic crystals*, Springer Science & Business Media, 173, 2013

[3] E. Boroson, S. Missoum, *Stochastic optimization of nonlinear energy sinks*, Structural and Multidisciplinary Optimization 55, 633-646, 2017

[4] E. Boroson, S. Missoum, P.O. Mattei, C. Vergez, *Optimization under uncertainty of parallel nonlinear energy sinks*, Journal of Sound and Vibration 394, 451-464, 2017

[5] B. Pidaparthi, S. Missoum, *Stochastic optimization of nonlinear energy sinks for the mitigation of limit cycle oscillations*, AIAA Journal, to appear (https://doi.org/10.2514/1.J057897), 2019

Experimental Study of Global Response of a Model Airplane with a Strongly Nonlinear Store on Each Wing

K. Moore[1], A. Mojahed[2], J. Dalisay[2], L. Bergman[2], A. Vakakis[2]

[1]University of Nebraska-Lincoln
Lincoln, Nebraska, USA
kmoore@unl.edu

[2]University of Illinois at Urbana-Champaign
Urbana, Illinois, USA
mojahed2@illinois.edu, dalisay2@illinois.edu, lbergman@illinois.edu,
avakakis@illinois.edu

Abstract Global dynamics of a model airplane with a strongly nonlinear store attached to each wing under impulsive loading is studied for several combinations of locked and unlocked stores.

Following methods introduced in [1-2], we investigate the effects of local, strongly nonlinear attachments, in this case a store (e.g., an auxiliary fuel tank or missile), attached to each wing, on the global dynamics of a model airplane [3] (Figure 1). The stores are constructed and installed such that, when locked, they contribute only a mass effect to the dynamics, while when unlocked they impart strong nonlinearity to the dynamic response of the plane. The system is studied experimentally, under impulsive excitation to one of the wings, in three configurations: with (a) both stores locked (the baseline linear system); (b) one store unlocked; and (c) both stores unlocked. The measured responses reveal that the unlocked stores drastically affect the participation of the first and second modes of the plane despite being local attachments. These global effects are further investigated by projecting the measured responses of configurations (b) and (c) onto the linear modes of the plane (i.e., with both stores locked, configuration (a)), computed using an experimentally-updated finite element model. These are used to compute the instantaneous total energy of each projected linear modal response. This reveals that, when only one store is unlocked (configuration (b)), the first and second projected modal responses decay at significantly faster rates than the first and second modal responses observed for the linear baseline system (configuration (a)). However, when both stores are unlocked (configuration (c)), the first projected modal response again decays at an increased rate, whereas the second projected modal response closely follows the second modal response of the linear baseline system. These results suggest that, when both stores are unlocked, their modal responses interfere both constructively and destructively depending on the locations of the measurements, resulting in this somewhat counterintuitive outcome of greater effective modal damping with one unlocked store than with two.

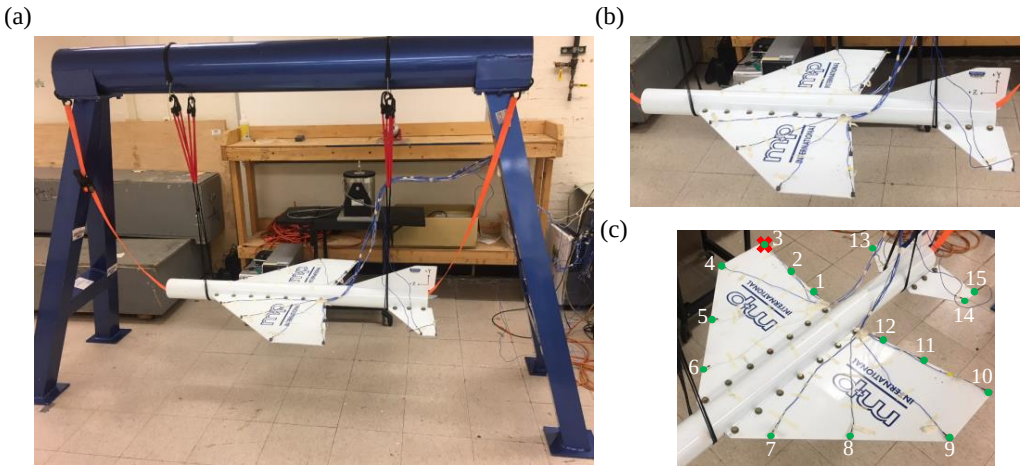

Figure 1: (a) Support structure with the suspended plane fully instrumented, (b) zoomed-in view of the suspended plane, and (c) the instrumentation scheme used for the experimental measurements with green circles and the red cross indicating accelerometer and impact locations, respectively.

References

[1] K.J. Moore, M. Kurt, M. Eriten, D.M. McFarland, L.A. Bergman, A.F. Vakakis, *Direct Detection of Nonlinear Modal Interactions from Time Series Measurements*, Journal of Mechanical Systems and Signal Processing, Special Issue on Exploring Nonlinear Benefits in Engineering. https://doi.org/10.1016/j.ymssp.2017.09.010. (In press)

[2] K.J. Moore, M. Kurt, M. Eriten, D.M. McFarland, L.A. Bergman, A.F. Vakakis, *Time Series Based Nonlinear System Identification of Modal Interactions Caused by Strongly Nonlinear Attachments*, Journal of Sound and Vibration, 438, 13-32, 2019. DOI: 10.1016/j.jsv.2018.09.033.

[3] K. J. Moore, A. Mojahed, L.A. Bergman, A. F. Vakakis, *Local Nonlinear Stores Induce Global Effects in the Dynamics of an Experimental Model Plane, AIAA Journal*. (Submitted)

From resonant to unstable dynamics control via nonlinear energy sinks

Guilhem MICHON[1], Leonardo SANCHES[2]

[1]Université de Toulouse, ICA, CNRS, ISAE-Supaero, Toulouse, France
guilhem.michon@isae-supaero.fr

[2]leonardo.sanches@isae-supaero.fr

Abstract

Passive vibration control has been the theme of numerous scientific works along decades for reducing vibrational amplitudes or user's discomfort when aerospatial structures are concerned. Tuned Vibration Absorbers are a good alternative for this purpose by synchronizing its natural frequency to the specific target vibration frequency of the primary dynamical system. When one desires to reduce multiple frequencies, multimodal vibration absorbers are used. Nonetheless, their efficiency is sensitive to variations of the main system's frequency.

To face this sensitivity issue, essential nonlinear elastic forces have been considered for the tuned vibration absorber which are denominated as Nonlinear Energy Sink (NES). Indeed, these nonlinear attachments can lead to an irreversible energy transfer from the primary system toward the NES which are known as target energy transfer. An important feature of this kind of device is that there is no preferable frequency of oscillations because of their intrinsic nonlinear nature. Therefore, the NES is able to capture the energy from a large broadband resonant condition.

Most of the works so far have dealt with a nonlinear attachment represented by a cubic stiffness. The feasibility on how to obtain a purely cubic stiffness has been presented in [1]. Beyond this, others type of nonlinear functions has been evaluated analytically and some has been explored experimentally; among these, magnetic-strung mechanisms [2] and a vibro-impact NES with non-smooth nonlinear functions [3]. Figure 1 illustrates different NES developed and explored experimentally.

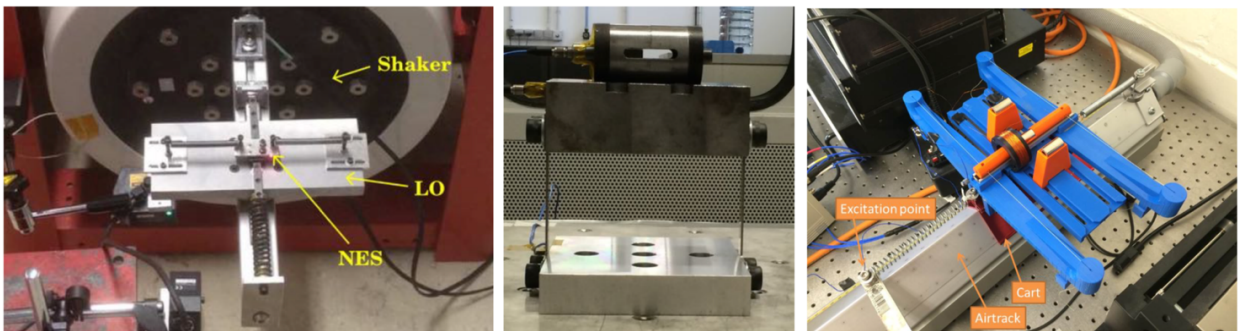

Fig.1 – Examples of cubic NES, Vibro-Impact NES and Magnet-strung NES designed for resonant conditions

Therefore, depending on the NES characteristics, the primary structure under a forcing excitation can respond with a steady-state amplitude or even reach a strong modulated response regime (SMR). These different regimes depend on the amplitude level of the

response. Moreover, undesired nonlinear phenomena can appear such as jumps or isolated responses. The response regime is not robust to the excitation characteristics.

Even if the comprehension about the use of NES for vibration amplitude control at resonant conditions is well understood, important development for applying them for controlling instabilities are necessary. Different from a resonant condition, an instability is characterized by the veering of two natural frequencies that submits the structure to high amplitude and divergent oscillations. Since the structure is no more able to dissipate the input energy, high amplitude is reached which leads to its total destruction. Among others, the dynamical instabilities on aerospatial structures addressed are aeroelastic flutter, helicopter ground resonances or shimmy landing gear instabilities.

Concerning NES application for instabilities control, the previous design rules developed for resonant structures are not valid anymore. NESs have been studied when applied to passive control of these instabilities. In [4], a NES was used to control the limit cycles of a Van der Pol oscillator, to suppress aeroelastic instabilities [5] and divergent oscillations of the ground resonance of helicopters [6]. Figure 2 highlight some of the referred works.

The main objective of this paper is to highlight the differences on the design of NES for controlling resonant and unstable phenomena. Moreover, the main perspectives for a successfully achievement of NES design will be pointed out.

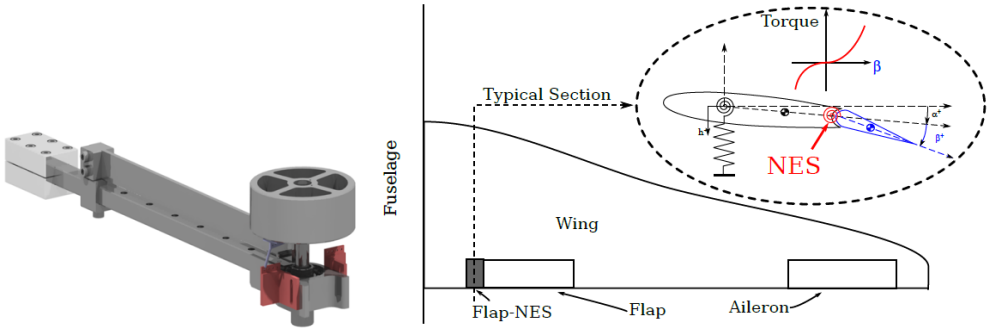

Fig.2 – Embedded NES on aeronautical structure for Instability control

References

[1] E. Gourc, G. Michon, S. Seguy, and Alain Berlioz. Experimental investigation and design optimization of targeted energy transfer under periodic forcing. Journal of Vibration and Acoustics, 136(2):021021, 2014.

[2] G. Pennisi, B.P. Mann, N. Naclerio, C. Stephan, G. Michon, Design and experimental study of a Nonlinear Energy Sink coupled to an electromagnetic energy harvester, Journal of Sound and Vibration, Volume 437, 2018, Pages 340-357.

[3] G. Pennisi, C. Stephan, E. Gourc, and G. Michon. Experimental investigation and analytical description of a vibro-impact nes coupled to a single-degree-of-freedom linear oscillator harmonically forced. Nonlinear Dynamics, pages 1–16, 2017.

[4] O. Gendelman, T. Bar, Bifurcations of self-excitation regimes in a van der pol oscillator with a nonlinear energy sink, Physica D, Volume 239(3), pages 220–229, 2010.

[5] Amar. Nonlinear passive control of an aeroelastic airfoil, simulations and experimentations. PhD Thesis. 2017, Toulouse University.

[6] J. F. Pafume Coelho, Contrôle Passif Nonlinéaire du Phénomène de Résonance Sol des Hélicoptères, PhD Thesis, 2017, Toulouse University.

Dynamic instability mitigation by means of nonlinear energy sinks in mechanical systems having one or two unstable modes

B. Bergeot[1] **and S. Bellizzi**[2]

[1]INSA CVL, Univ. Orléans, Univ. Tours, LaMé EA 7494
Blois, France
baptiste.bergeot@insa-cvl.fr

[2] Aix Marseille Univ, CNRS, Centrale Marseille, LMA UMR 7031
Marseille, France
bellizzi@lma.cnrs-mrs.fr

Abstract The presentation is divided into two parts. The first part presents a general method to predict the steady-state regimes of a multi-degree-of-freedom mechanical system (the primary system) having one unstable mode coupled to a set of nonlinear energy sinks (NESs). In the second part the primary system has two unstable modes and it is coupled to one NES. Preliminary numerical results and analytical treatments of this situation are presented.

In the context of passive mitigation of dynamic instabilities, it is now established that the Nonlinear Energy Sinks (NESs) are good candidate to consider especially when low frequency and high level are concerned [1, 2]. The operation of the NESs is based on the concept Targeted Energy Transfer (TET). A basic NES generally consists of a light mass, an essentially nonlinear spring and a viscous linear damper. Because of its essentially nonlinear stiffness, a NES can engage in resonance over a broad frequency range. Whether for a system under impulsive, harmonic or broadband frequency excitation or whether for an auto-oscillating system, TET results from nonlinear mode bifurcations. In general, the phenomenon of TET can be described as a 1:1 resonance capture [3].

This work considers auto-oscillating systems as primary system and it is divided into two parts described below.

1 Prediction of steady-state regimes of a multi-degree-of-freedom unstable dynamical system coupled to a set of nonlinear energy sinks

Here the primary system is a multi-degree-of-freedom (multi-DOF) unstable mechanical systems undergoing cubic nonlinearities and coupled to M NESs. We assume in this section that the primary system has only one mode which can become unstable through Hopf bifurcation.

We propose an analytical method to predict the steady-state regimes of the coupled system. The method begins using the biorthogonal transformation to diagonalize the primary system written in the state-space form. Afterwards, the dynamics of the diagonalized system is reduced keeping only the unstable mode and ignoring the stable modes. Then the slow-flow of the system is obtained using the complexification-averaging (CA-X) method within the assumption of a 1:1 resonance capture around the frequency of the unstable mode. The resulting slow-flow possesses a small parameter related to the mass of the NES and, in the framework of Geometric Singular Perturbation Theory (GSPT) [4], it defines a $(2M, 1)$-fast–slow system. The slow variable characterizes the unstable mode of the primary system whereas the $2M$ fast variables describe the NESs motions (amplitude and phase). It is shown that the Critical Manifold (CM) of the slow-flow can be reduced to a one dimensional parametric curve evolving in a multidimensional space. A similar form of the CM is obtained considering a network of parallel NESs [5]. The knowledge of the stability properties of the critical manifold and the fixed point of the slow-flow

(position and stability) makes it possible to predict the response regimes. Finally, the method is applied to the prediction of the steady-state responses of an airfoil undergoing an aeroelastic instability coupled the a set of NESs (from one to four). Theoretical results are compared, for validation purposes, to direct numerical integration of the system. The comparison shows a good agreement.

2 Mitigation by means of nonlinear energy sinks of friction-induced vibrations in a mechanical system having two unstable modes

In this part, the primary system has two unstable modes and, as a first step, it is linear and coupled to only one NES. Our objective is to investigate the solutions in the vicinity of two simultaneous 1:1-1:1 resonances to the natural frequencies of the two unstable modes.

The procedure described above is performed again except that now the two unstable modes must be kept. Moreover, in spite of the presence of the NES coupling, we assume that each variable associated to the primary system (resulting to the biorthogonal transformation) oscillates at one single frequency contrary to the degrees of freedom associated to the NES which must be split as a sum of two terms to capture frequency components with respect to the two unstable modes. Within this assumptions, the CA-X method is applied leading to a slow-flow (in the real domain) which takes the form of a $(4, 2)$-fast–slow system. The slow variables characterize the two unstable modes of the primary system whereas the 4 fast variables describe the NESs motion (amplitude and phase of the two frequency components).

Preliminary analytical results, again based on GSPT, are presented. For example the CM, which appears as a 6-dimensional parametric surface, is determined as well as fixed points of the slow-flow and their stability. These results are validated by comparison to numerical simulation of the system.

References

[1] O. V. Gendelman, A. F. Vakakis, L. A. Bergman, D. M. McFarland, Asymptotic analysis of passive nonlinear suppression of aeroelastic instabilities of a rigid wing in subsonic flow, SIAM Journal on Applied Mathematics 70 (5) (2010) 1655–1677. doi:10.1137/090754819.

[2] A. Luongo, D. Zulli, Aeroelastic instability analysis of nes-controlled systems via a mixed multiple scale/harmonic balance method, Journal of Vibration and Control 20 (13) (2013) 1985–1998. doi:10.1177/1077546313480542.

[3] O. V. Gendelman, L. I. Manevitch, A. F. Vakakis, R. M'Closkey, Energy Pumping in Nonlinear Mechanical Oscillators: Part I—Dynamics of the Underlying Hamiltonian Systems, Journal of Applied Mechanics 68 (1) (2001) 34. doi:10.1115/1.1345524.

[4] C. K. R. T. Jones, Geometric singular perturbation theory, in: R. Johnson (Ed.), Dynamical Systems, Vol. 1609 of Lecture Notes in Mathematics, Springer Berlin Heidelberg, 1995, pp. 44–118. doi:10.1007/BFb0095239.

[5] B. Bergeot, S. Bellizzi, Asymptotic analysis of passive mitigation of dynamic instability using a nonlinear energy sink network, Nonlinear Dynamics 94 (2) (2018) 1501–1522. doi:10.1007/s11071-018-4438-0.

Poster session 1

Tuesday, 2nd July 2019

Chairman: B. Cochelin

Basins of attraction of high-dimensional systems: case study of periodically excited sympodial tree

N. Andonovski[1], **S. Lenci**[1] **and I. Kovacic**[2]

[1]Polytechnic University of Marche
Ancona, Italy
n.andonovski@pm.univpm.it

Centre of Excellence for Vibro-Acoustic Systems and Signal Processing CEVAS, Faculty of Technical Sciences, University of Novi Sad
Novi Sad, Serbia
ivanakov@uns.ac.rs

Abstract Detecting basins of attraction is a fundamental part of a global analysis, often not performed due to the lack of analytical methods or hardware limitations of numerical techniques. In fact, what is required for numerical methods in four dimensions or more is High Performance Computing to give results in reasonable time. To overcome some of these shortcomings, we have developed the software to build basins of attraction of high-dimensional systems, illustrating its capabilities on a case study of a periodically excited three degree-of-freedom sympodial tree.

In practical applications, it is not sufficient to know only the stability of particular attractors. Supplementary information about their robustness, which is closely related to the structure of basins of attraction, is needed. This entails performing a global analysis and quantifying a basin compactness by integrity measures [1].

Our primary goal is to explore the global behavior (including practical stability) of various strongly nonlinear systems with six state-space dimensions (6D). To do so, it is necessary to employ High Performance Computing frameworks, as numerical computations of full basins in 6D is a challenging task. The Simple Cell Mapping (SCM) method [2] is an adequate choice for these computations as it offers possibilities to parallelize the most resource demanding part of basin computation - the integration of equations of motion of dynamical systems associated with a large number of initial conditions.

In this work, a software that we have developed is used as a part of a global analysis for the model of a sympodial tree with first-level branches [3] to underline the complex behaviour of basins of attraction and to show how attractors are not equally robust. This is helpful in understanding the resilience of trees to various natural conditions and environmental excitations.

The motion of the sympodial tree shown in Fig. 1 is mathematically modeled by choosing the generalised coordinates as being the absolute angles φ, ψ_1, ψ_2 (Figure 1b) and also introducing the dimensionless parameters $D_1/D = \lambda^{1/2}$, $l_1/l = \lambda^{1/2s}$, $m_1/m = \lambda^{4/3}$, $\kappa = k_1/k$, $\zeta = b/2l\sqrt{3/km}$ and $\beta = b_1/b$, leading to the following equations of motion [3]:

$$\begin{aligned}
&-2\kappa(\psi_1+\psi_2) - 4\beta\zeta(\dot{\psi}_1+\dot{\psi}_2) \\
&-3\lambda^{5/3}\dot{\psi}_2^2\sin(\alpha-\varphi+\psi_2) + 2(1+\kappa)\varphi + 4(1+2\beta)\zeta\dot{\varphi} \\
&+3\lambda^{5/3}\dot{\psi}_1^2\sin(\alpha+\varphi-\psi_1) + 2(1+6\lambda^{4/3})\ddot{\varphi} \\
&+3\lambda^{5/3}\ddot{\psi}_1 cos(\alpha+\varphi-\psi_1) - 3\lambda^{5/3}\ddot{\psi}_2\cos(\alpha-\varphi+\psi_2) &= 2M\cos(\Omega t), \qquad (1)\\
&2\kappa\varphi + 4\beta\zeta\dot{\varphi} + 3\lambda^{5/3}\dot{\varphi}^2\sin(\alpha+\varphi-\psi_1) - 2\kappa\psi_1 \\
&-4\beta\zeta\dot{\psi}_1 - 3\lambda^{5/3}\ddot{\varphi}\cos(\alpha+\varphi-\psi_1) - 2\lambda^2\ddot{\psi}_1 &= 0, \qquad (2)\\
&2\kappa\varphi + 4\beta\zeta\dot{\varphi} - 3\lambda^{5/3}\dot{\varphi}^2\sin(\alpha-\varphi+\psi_2) - 2\kappa\psi_1 \\
&-4\beta\zeta\dot{\psi}_2 - 3\lambda^{5/3}\ddot{\varphi}\cos(\alpha-\varphi+\psi_2) + 2\lambda^2\ddot{\psi}_2 &= 0. \qquad (3)
\end{aligned}$$

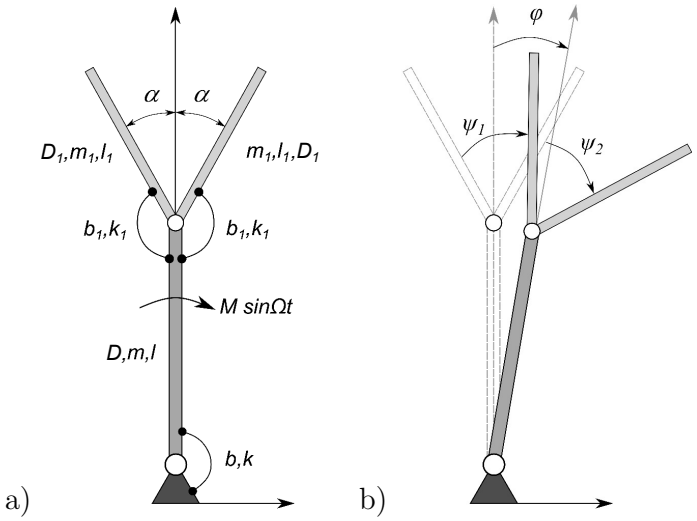

Figure 1: Model of sympodial tree with first-level branches, a) model properties, b) generalized coordinates.

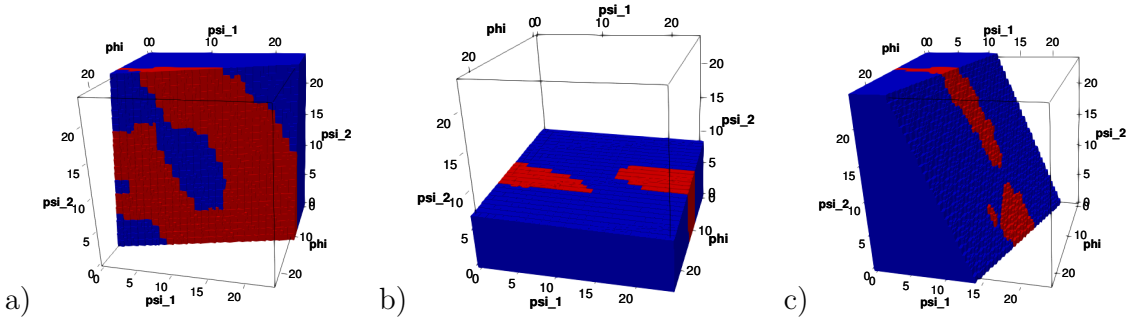

Figure 2: 3D basin cross-section $\varphi, \psi_1, \psi_1, \dot{\varphi} = 12, \dot{\psi_1} = 11, \dot{\psi_2} = 11$, sliced with various 2D planes.

The tree model with the parameter values $\beta = 1/2$, $\kappa = 0.3$, $\zeta = 0.03$, $\alpha = 20°$, $\lambda = 1/2$, $s = 3/2$, the excitation amplitude $M = 0.5$ and frequency $\Omega = 1.57$ has both one periodic (PA) and one quasi-periodic (QP) attractor, which coexist simultaneously. The three-dimensional cross-sections of their basin corresponding to the generalized coordinates are presented in Fig. 2 (the blue cells belong to the PA basin and the red cells to the QP one), where the initial generalized velocities are fixed at $\dot{\varphi} = 12, \dot{\psi_1} = 11, \dot{\psi_2} = 11$. They are sliced with various planes to underline the basins structure.

Although it is evident that the steady state of the PA is more robust than the QP one, a deeper analysis is needed to draw specific conclusions. It is required to compute integrity measures for various values of relevant system parameters, to obtain the so-called "erosion profiles" [1]. They would underline the evolution of basin regions that are considered "safe" from a practical point of view, uncovering the robustness of the examined dynamical system.

References

[1] G. Rega and S. Lenci. Identifying, evaluating, and controlling dynamical integrity measures in non-linear mechanical oscillators. *Nonlinear Analysis: Theory, Methods & Applications*, 63(5):902–914, 2005.

[2] C.S. Hsu. *Cell-to-Cell Mapping: A Method of Global Analysis for Nonlinear Systems.* Springer-Verlag, New York, 1987.

[3] I. Kovacic, M. Zukovic, and D. Radomirovic. Sympodial tree-like structures: from small to large-amplitude vibrations. *Bioinspiration & Biomimetics*, 13(2):026002, 2018.

A state-space approach to output-only identification of nonlinear systems with load estimation

T.J. Rogers[1], **K. Worden**[1] **and E.J. Cross**[1]

[1]Dynamics Research Group,
Department of Mechanical Engineering,
University of Sheffield
Sheffield, UK
tim.rogers@sheffield.ac.uk

Abstract The nonlinear Bayesian state-space model provides a natural framework for modelling of dynamic systems. The particle filter is an efficient tool for working with such systems; however, one of the key challenges is when inputs to a system are non-Gaussian. This paper shows how a latent force approach can be combined with the particle filter in a step towards removing the assumption of Gaussian white noise as an input to the system of interest.

The problem of output-only identification of dynamic systems is by no means a new challenge; there remain many open questions in the realm of linear systems and work on nonlinear systems is, in reality, only just beginning. Methods for identification of linear systems have revolved around the use of modal methods such as stochastic subspace identification [1, 2]. Nonlinear systems fail to exhibit modes in the same way as a linear system (if at all!) contributing to the impossibility of using these methods in the presence of any (except maybe the weakest) nonlinearity. One key assumption made in many of these methods is that the system is under a Gaussian white noise excitation. This assumption becomes stronger and therefore, more problematic with a nonlinear system, where there can exist changes in resonant frequency and other phenomena not seen in linear systems.

Previously, the authors have shown the effectiveness of treating the identification problem as a Bayesian state-space model where the forcing can be treated as a latent state [3]. Using this method, distributions over the unknown parameters of the system are recovered alongside a distribution over possible time histories of the forcing. Here, the extension of this work to a nonlinear example is shown.

A Duffing oscillator is considered, by now a very familiar system to the dynamics community [4] and is used to demonstrate the methods in this work. Moving to this nonlinear system leads to a nonlinear Bayesian state-space model. Unlike the linear case which may be solved with the Kalman filter [5] and Rauch-Tung-Striebel [6] smoothing equations the system is intractable — no closed form solution exists. Instead the system must be approximated, Sequential Monte Carlo methods or particle filters provide an elegant solution for this [7–9],

$$x_t \sim f_\theta\left(x_t \,|\, x_{t-1}, u_{t-1}\right) \tag{1a}$$
$$y_t \sim g_\theta\left(y_t \,|\, x_t, u_t\right) \tag{1b}$$

Here, x_t is a vector of some hidden (latent) states at time t, the evolution of which is governed by $f_\theta\left(x_t \,|\, x_{t-1}, u_{t-1}\right)$. u_t is a vector of 'control' inputs to the model at time t; in structural dynamics this would generally be the force input to the oscillator. These states are related to a vector of observed variables y_t through the probabilistic model defined by $g_\theta\left(y_t \,|\, x_t, u_t\right)$. In this formulation $f_\theta\left(x_t \,|\, x_{t-1}, u_{t-1}\right)$ is the transition density of the model and $g_\theta\left(y_t \,|\, x_t, u_t\right)$ the observation density of the model. The Duffing oscillator defined as,

$$m\ddot{y} + c\dot{y} + ky + k_3 y^3 = F \tag{2}$$

parameterised by its mass m, damping c, linear stiffness k, and cubic stiffness k_3; the oscillator has a displacement, velocity and acceleration $\ddot{y}, \dot{y}$, and y. It is also subjected to an external force F. A Gaussian Process [10] is used as a Bayesian prior over the forcing function in time, this is converted to a state-space representation [11] along with the dynamic system to formulate $f_\theta\left(x_t \,|\, x_{t-1}, u_{t-1}\right)$. Through this reformulation, a joint state-space model between the dynamics and the loading is formed as in [12] but with nonlinear dynamics. The use of particle MCMC [13] is explored to solve this partially-observed nonlinear state-space system and recover the forcing alongside the parameters of the model.

Acknowledgements

The author gratefully acknowledge the support of the Engineering and Physical Sciences Research Council, UK for this work through grant numbers, EP/J016942/1 and EP/S001565/1.

References

[1] B. Peeters and G. De Roeck. Stochastic system identification for operational modal analysis: a review. *Journal of Dynamic Systems, Measurement, and Control*, 123(4):659–667, 2001.

[2] E. Reynders. System identification methods for (operational) modal analysis: review and comparison. *Archives of Computational Methods in Engineering*, 19(1):51–124, 2012.

[3] T. J. Rogers, K. Worden, G. Manson, U. T. Tygesen, and E. J. Cross. A Bayesian filtering approach to operational modal analysis with recovery of forcing signals. In *Proceedings of the 7th International Conference on Uncertainty in Structural Dynamics (USD2018)*, 2018.

[4] I. Kovacic and M. J. Brennan. *The Duffing Equation: Nonlinear Oscillators and Their Behaviour*. John Wiley & Sons, 2011.

[5] R. E. Kalman. A new approach to linear filtering and prediction problems. *Journal of basic Engineering*, 82(1):35–45, 1960.

[6] H. E. Rauch, C. Striebel, and F. Tung. Maximum likelihood estimates of linear dynamic systems. *AIAA journal*, 3(8):1445–1450, 1965.

[7] S. Särkkä. *Bayesian Filtering and Smoothing*, volume 3. Cambridge University Press, 2013.

[8] A. Doucet and A. M. Johansen. A tutorial on particle filtering and smoothing: Fifteen years later. *Handbook of nonlinear filtering*, 12(656-704):3, 2012.

[9] T. B. Schön, A. Svensson, L. Murray, and F. Lindsten. Probabilistic learning of nonlinear dynamical systems using sequential Monte Carlo. *Mechanical Systems and Signal Processing*, 104:866–883, 2018.

[10] C. E. Rasmussen and C. K. I. Williams. *Gaussian Processes for Machine Learning*. Citeseer, 2006.

[11] J. Hartikainen and S. Särkkä. Kalman filtering and smoothing solutions to temporal Gaussian process regression models. In *Machine Learning for Signal Processing (MLSP), 2010 IEEE International Workshop on*, pages 379–384. IEEE, 2010.

[12] J. Hartikainen and S. Sarkka. Sequential inference for latent force models. *arXiv preprint arXiv:1202.3730*, 2012.

[13] C. Andrieu, A. Doucet, and R. Holenstein. Particle Markov chain Monte Carlo methods. *Journal of the Royal Statistical Society: Series B (Statistical Methodology)*, 72(3):269–342, 2010.

Edge states and frequency response in nonlinear model of forced-damped valve spring

Majdi Gzal* **and Oleg Gendelman†**

Faculty of Mechnical Engineering, Technion - Israel Institute of Technology

Haifa, Israel

* majdi.gzal@technion.ac.il , † ovgend@technion.ac.il

Abstract The nonlinear dynamics of the valve spring of an internal combustion engine is mathematically modeled and investigated. Exact solutions in the form of time-periodic and spatially localized edge states are derived. The stability of the system is analyzed using the Floquet theory. Comparison of the analytical solution with numerical simulations and experimental test results conducted on an actual valve spring yields an excellent agreement.

Nonlinearity and discreteness are inherent in many systems in nature, e.g. Josephson junction networks, Bose-Einstein condensates, micro-mechanical devices and optical devices. This interplay between nonlinearity and discreteness supports time-periodic and spatially localized solutions which are often referred to as discrete breathers (DBs) [1].

Exact solutions for symmetric discrete breathers are derived for the Hamiltonian model [2] and for the case of a homogenous external forcing with restitution coefficient less than unity, where it is the only source of damping in the model [3]. The stability of the periodic solutions is investigated using Floquet's theory by observing the movement of the eigenvalues of the monodromy matrix in the complex plane [4].

The purpose of our current work is to develop an exact solution and stability threshold for edge states in finite non-homogenous forced-damped chain with vibro-impact nonlinearity.

The proposed model given in Figure 1 presents a finite non-homogenous one-dimensional mass-spring-damper discrete chain. Periodic displacement (shown in Figure 2), which mimics the actual camshaft profile, is applied to the upper end of the chain while the other end is fixed. The zeroth mass experiences an impact that satisfies the Newton impact law with restitution coefficient less than unity. There are two damping sources in this model, one at the contact and the other due to internal damping of the spring material. The nonlinearity of the model originates from the periodic impact interactions.

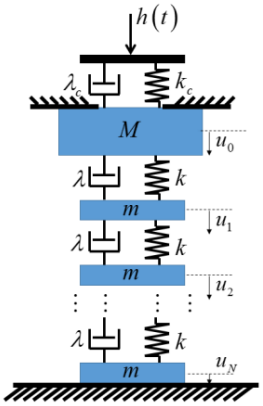

Figure 1: The nonlinear mass-spring-damper chain under periodic excitation.

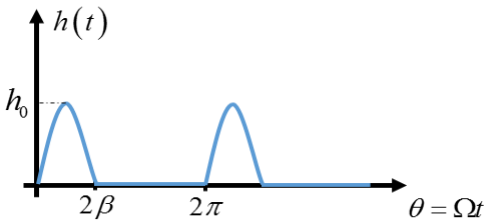

Figure 2: The applied displacement mimics a general Camshaft profile.

Considering the periodicity of the excitation $h(t)$, its hybrid behavior can be modeled as a continuous form using Fourier Series as follows:

$$h(t) = a_0 + \sum_{r=1}^{\infty}\left[a_r \cos(r\Omega t) + b_r \sin(r\Omega t)\right] \tag{1}$$

Following Gendelman [3], the non-smooth bounding condition at the impact can be eliminated by representing it as an external loading force:

$$\begin{aligned} &M\ddot{u}_0 + \lambda(\dot{u}_0 - \dot{u}_1) + k(u_0 - u_1) + k_c u_0 + \lambda_c \dot{u}_0 = \lambda_c \sum_{r=1}^{\infty} r\Omega\left[-a_r \sin(r\Omega t) + b_r \cos(r\Omega t)\right] + \\ &+k_c\left[a_0 + \sum_{r=1}^{\infty}\left[a_r \cos(r\Omega t) + b_r \sin(r\Omega t)\right]\right] + 2p\sum_{j=-\infty}^{\infty}\delta\left(t - \phi + j\frac{2\pi}{\Omega}\right) \\ &m\ddot{u}_n + \lambda(2\dot{u}_n - \dot{u}_{n-1} - \dot{u}_{n+1}) + k(2u_n - u_{n-1} - u_{n+1}) = 0 \\ &u_N = 0 \end{aligned} \tag{2}$$

where $2p$ represents the change in the linear momentum, ϕ is the phase lag between the external forcing and the impact and $\delta(x)$ is the Dirac-delta function.

The edge state solution of Equation (2) has the following form:

$$\begin{aligned} &u_n = u_{n,0} + \sum_{r=1}^{\infty} C_{n,r}\cos\left(r\Omega(t-\phi)\right) + \sum_{r=1}^{\infty} S_{n,r}\sin\left(r\Omega(t-\phi)\right) \\ &u_{n,0} = U_0\left(1 - \frac{n}{N}\right); \\ &C_{n,r} = A_r f_r^n + B_r f_r^{-n};\ \ S_{n,r} = D_r g_r^n + E_r g_r^{-n} \end{aligned} \tag{3}$$

The obtained solution is characterized by a strongly localized at the edge of the chain as shown in Figure 3. Finally, the analytical solution is compared with numerical simulations and experimental data obtained from analysis of actual automotive valve spring (Figure 4).

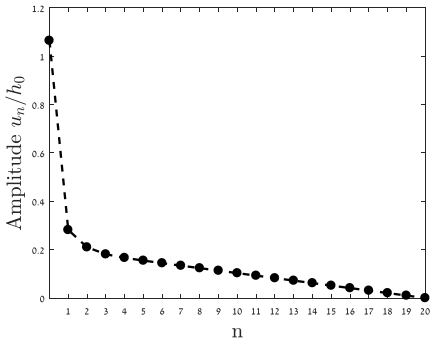

Figure 3: The edge state profile.

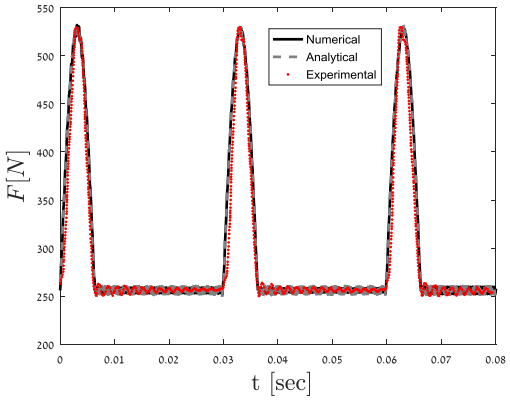

Figure 4: Spring force: comparison of the exact solution with numerical simulations and experimental test results.

References

[1] S. Flach, A. V. Gorbach, *Discrete breathers: Advances in theory and applications*, Phys. Rep. 467 (1) (2008) 1–116.

[2] O.V. Gendelman, L.I. Manevitch, *Discrete breathers in vibro-impact chains: analytic solutions*, Phys. Rev. E 78 (2) (2008) 026609.

[3] O.V. Gendelman, *Exact solutions for discrete breathers in a forced-damped chain*, Phys. Rev. E 87 (6) (2013) 062911.

[4] A.H. Nayfeh, B. Balachandran, *Applied Nonlinear Dynamics: Analytical, Computational, and Experimental Methods*, Wiley-Interscience, New York (1995).

Solitary waves in a non-integrable chain with double-well potentials

A. Katz Shmuel[1], B. Sefi Givli [2]

[1] Faculty of Mechanical Engineering, Technion
Haifa, Israel
katzshm@campus.technion.ac.il

[1] Faculty of Mechanical Engineering, Technion
Haifa, Israel
givli@technion.ac.il

Abstract We study solitary waves in a 1-D lattice of identical masses that are interact by nonlinear springs of double-well potentials. Based on analytical treatment, combined with numerical simulations, we are able to reveal important insights. For example, the solitary wave is indifferent to the energy barrier that separates the two energy wells, and the shape of the wave can be described by means of two scalar properties of the spring potential.

In general, a 1-D lattice with nonlinear interaction between neighbour masses can support propagation of solitary waves. We study special lattice where the neighboring masses interact through springs with double-well potentials, also termed bistable springs. The double-well potential consists of two disjoint intervals of convex energy, "Phase-I" and "Phase-II", separated by a concave "spinodal" region. This results in a nonlinear, non-monotonous force-strain curve, consisting of two branches with positive stiffness, separated by a branch with negative stiffness. We note the fundamental difference between the system studied here, where double-well potentials govern the *interactions* between neighbours, and the lattice with *onsite* double-well potential, where each mass lies in a double-well potential. In the latter, kink waves (or transition waves), rather than solitary waves, may propagate for very long distances, even in the presence of dissipative mechanisms.

Lattices with double-well-potential interactions have been studied extensively, but not in the context of solitary waves. The Lattice with double-well is prototypical to the behavior of elastoplastic materials, super elasticity, shape-memory effect, plasticity, fracture, hysteresis in material behavior, and more. The *dynamic* behavior of bistable lattices has also been extensively studied, usually by means of modeling inertial dynamics directly, or by assuming simplified evolution strategies or kinetic relations. In addition, the unique nonlinear behavior associated with the double-well-potential has led to the development of a new class of metamaterials, i.e. materials that exploit local instabilities for enhanced performance. These studies have demonstrated the advantages of such architected materials in the context of energy absorption, mechanical/acoustic filtering and tailored bandgaps, transformation of mechanical signals, origami-based metamaterials and other applications.

In a recent work [1], we showed that, governed by the ratio of Phase II to Phase I stiffness, a 1D lattice with double-well-potential interactions may exhibit two fundamentally different dynamic responses following impact. For a softening media (phase-II is softer than phase-I) most of the energy of the impact translates into transition of the first few springs from Phase I to Phase II. However, for a hardening media (phase-II is stiffer than phase-I) a solitary wave, which propagates faster than the speed of sound associated with phase-I, is formed. Further, it was shown that the *height* of the solitary wave is indifferent to the energy barrier separating between phase-I and phase-II. In this study we extend and generalize the results presented in [1], and show that: (i) The entire solitary-wave solution is indifferent to the energy barrier

which separates Phase I and Phase II. (ii) The *shape* of the solitary wave is governed by a non-dimensional parameter which reflects the relative significance of the spinodal region in the double-well potential.

The above results are obtained analytically based on padé approximations and are validated by means of extensive numerical simulations that relax the simplifications adopted in the analytical treatment. In particular, the analytical analysis adopts a trilinear approximation for the force-strain behavior of the interaction forces and derives a quasi-continuum approximation based on Padé approximants of the differential operator. These steps enable a straight-forward analytical treatment and the derivation of an explicit solution. In addition, the numerical simulations suggest that the analytical insights apply to bistable lattices with non-trilinear interactions as well. We note that a similar analytical approach has been applied in [2–4] for studying solitary waves in a lattice with bilinear force-strain interactions (convex potentials).

References

[1] S. Katz, S. Givli, Solitary waves in a bistable lattice, Extreme Mechanics Letters. 22, 106–111, 2018.

[2] L. Truskinovsky, A. Vainchtein, Solitary waves in a nonintegrable Fermi-Pasta-Ulam chain, Phys. Rev. E. 90, 042903, 2014.

[3] A. Vainchtein, Solitary wave propagation in a two-dimensional lattice, Wave Motion. 83, 12–24, 2018.

[4] L. Truskinovsky, A. Vainchtein, Strictly supersonic solitary waves in lattices with second-neighbor interactions, Physica D: Nonlinear Phenomena. 389, 24–50, 2019.

Low-dimensional Nonlinear Modes computed with PGD/HBM and Reduced Nonlinear Modal Synthesis for Forced Responses

L. Meyrand[1], **E. Sarrouy**[1] **and B. Cochelin**[1]

[1]Aix Marseille Univ, CNRS, Centrale Marseille, LMA
Marseille, France
meyrand@lma.cnrs-mrs.fr, sarrouy@lma.cnrs-mrs.fr, cochelin@lma.cnrs-mrs.fr

Abstract This work proposes an algorithm allowing to perform a fast and light computation of branches of damped Nonlinear Normal Modes (dNNMs). Based on a previous work about undamped NNMs (uNNMs), it couples Proper Generalized Decomposition (PGD) features, harmonic balance and prediction-correction continuation schemes. After recalling the main contributions of the method applied on an example with cubic nonlinearities, the issue of a reduced nonlinear modal synthesis is briefly addressed.

The differential equations governing the motion of a nonlinear dynamical system can usually take the following form after a spatial discretization, where the nonlinear efforts $\mathbf{f}_{\text{nl}}(\mathbf{x}, \dot{\mathbf{x}})$ are separated from the linear ones:

$$\mathbf{M}\ddot{\mathbf{x}}(t) + \mathbf{C}\dot{\mathbf{x}}(t) + \mathbf{K}\mathbf{x}(t) + \mathbf{f}_{\text{nl}}(\mathbf{x}(t), \mathbf{x}(t)) = \mathbf{f}_e(t) \quad (\text{dim.: } N) \tag{1}$$

Assuming the Rosenberg's framework [4], an undamped NNM is a set of limit cycles of Eq. (1) from which dissipative and external forcing terms are put to zero. Shaw and Pierre extended this first definition of NNMs to the case of dissipative systems: a (damped) NNM is a two-dimensional invariant manifold in the phase space [5]. Hence, one wants to obtain a dNNM by computing a set of pseudo-periodic solutions of Eq. (1) with $\mathbf{f}_e(t) = \mathbf{0}$.

A frequential reduced algorithm coupling a PGD approach with an harmonic balance method (HBM) is implemented to make a quick and compact dNNM computation. The first step of the PGD process is separating the variables, here space and time:

$$\mathbf{x}(t) \approx \sum_{j=1}^{m} \mathbf{p}_j q_j(t) \Leftrightarrow \mathbf{x}(t) \approx \mathbf{P}\mathbf{q}(t) \text{ with } \mathbf{P} = [\mathbf{p}_1, \ldots, \mathbf{p}_m] \tag{2}$$

$m \ll N$ is a positive integerand denotes the number of PGD modes $(\mathbf{p}_j, q_j(t))$ used for $\mathbf{x}$ decomposition. $\mathbf{P}$ is the $(N \times m)$-sized matrix of the m PGD mode shapes $\mathbf{p}_j$, and $\mathbf{q}(t)$ is the vector containing the time dependence of each PGD mode. Then a spatial subproblem $\mathcal{S}_m$ and a temporal subproblem $\mathcal{T}_m$ are defined from specific weak formulations [1]. The calculus, its notations and operators are detailed in [3]. Given the spatial matrix $\mathbf{P}$, $\mathcal{T}_m$ is a set of m ordinary differential equations of order 2. A complex HBM [2] is then implemented to obtain another nonlinear algebraic system for $\mathcal{T}_m$ from the following solution form:

$$\mathbf{q}(t) = \frac{\mathbf{a}_0}{\sqrt{2}} + \sum_{k=1}^{H} e^{-k\beta t}[\mathbf{a}_k \cos(k\omega t) + \mathbf{b}_k \sin(k\omega t)] \tag{3}$$

β-dependant linear terms can easily be separated from the classic undamped HBM matrices. Given the temporal part $\mathbf{q}(t)$, the spatial subproblem $\mathcal{S}_m$ is a $N \times m$ nonlinear algebraic system which takes into account the damping ratio β into the definition of its operators. The PGD/HBM solver is obtained by integrating $\mathcal{S}_m$ and $\mathcal{T}_m$ into an alternated directions solver. This PGD/HBM solver is eventually embedded into a continuation scheme as a corrector in order to build the dNNM branch. The choice of predictor is left to the user.

The first point of the branch is described with only one PGD mode which contains the shape and the frequency of the underlying linear damped mode with a null amplitude. When the error criterion can no longer be met through the continuation, the size of the description m is incremented and some new spatial and temporal information is added to the PGD description. Unlike Grolet and Thouverez [1] who initialized $\mathbf{q}(t)$ with random values, we propose to process $\mathcal{T}_m$ first based on the shape on the next damped linear modes. The full algorithm adds new modal data on the fly, only when it is necessary with respect to the error criterion.

It should be noted that two variants have been implemented: oPGD (optimized PGD) recomputes the whole $\mathbf{P}$ matrix at each point of the branch whereas pPGD (progressive PGD) only computes the last shape $\mathbf{p}_{m+1}$ when it is introduced. Although oPGD generally needs less PGD modes than pPGD, the computational cost is higher.

The method is here applied on a cantilever beam with a cubic spring at its free end investigated in [3]. A 1% modal damping is added on each linear mode. The Frequency-Energy Plot given on Fig. 1 illustrates the hardening effect of the cubic nonlinearity while the conservative mechanical energy grows and the damping-energy dependence of the NNM.

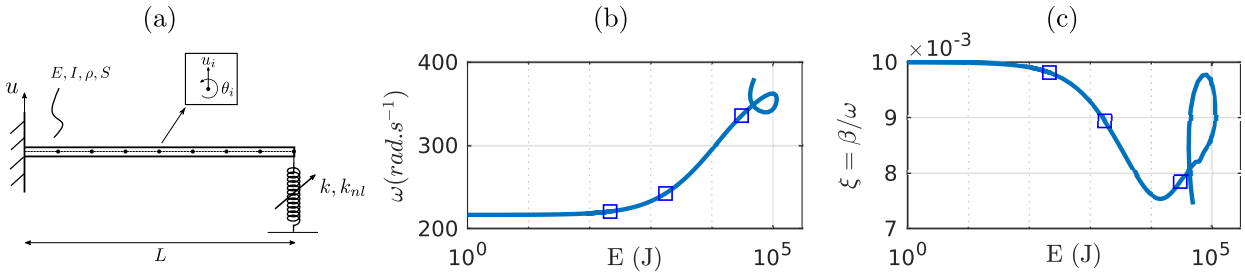

Figure 1: (a) Schematic diagram of beam+cubic spring (b) Main branch of dNNM1 (c) Damping ratio with respect to energy. Squares: Solution points where a PGD mode is added.

Eventually, this compact description of NNMs can be embedded into a reduced modal synthesis solver in order to quickly build Frequency Response Functions by looking for $\mathbf{x}$ solution of Eq. (1) as follows:

$$\mathbf{x}(t) = \mathbf{P}(s)\left(\frac{\mathbf{a}_0(s)}{\sqrt{2}} + \sum_{k=1}^{H}[\mathbf{a}_k(s)\cos\left(k(\omega t+\phi)\right) + \mathbf{b}_k(s)\sin\left(k(\omega t+\phi)\right)]\right) \tag{4}$$

where s is an index for the dNNM branch and ϕ is the phase of the response. Although this decomposition is slightly different of the one given in [2], the two equations used to solve for s and ϕ are similar.

References

[1] A. Grolet and F. Thouverez. *On the use of the proper generalised decomposition for solving nonlinear vibration problems*, in ASME 2012 International Mechanical Engineering Congress and Exposition 4, 913-920, 2012.

[2] C. Joannin, B. Chouvion, F. Thouverez. *A reduced-order modeling technique for the study of non-linear vibrations in dissipative systems*, in ISMA2016 - International Conference on Noise and Vibration Engineering, KU Leuven, 2016.

[3] L. Meyrand, E. Sarrouy, B. Cochelin and G. Ricciardi. *Nonlinear normal mode continuation through a Proper Generalized Decomposition approach with modal enrichment*, Journal of Sound and Vibration, Elsevier 443, 444-459, 2018.

[4] R. Rosenberg. *On nonlinear vibrations of systems with many degrees of freedom*, Advances in Applied Mechanics 9, 155-242, 1966.

[5] S. Shaw and C. Pierre. *Non-linear normal modes and invariant manifolds*, Journal of Sound and Vibration 150, 170-173, 1991.

Identification & ROM

Tuesday, 2nd July 2019

Chairman: K. Worden

Capturing nonlinear modal coupling and interactions in reduced-order models

T.L. Hill, V.R. Melanathuru and S.A. Neild

Department of Mechanical Engineering
University of Bristol
Bristol, UK
tom.hill@bristol.ac.uk

Abstract A robust methodology for deriving nonlinear reduced-order models from finite-element models would enable powerful nonlinear techniques to be used to analyse large and complex engineering structures. This work highlights why nonlinear modal coupling leads to challenges in establishing such a methodology. Furthermore, using analytical insights gained from considering simple mechanical systems, it is demonstrated how these challenges may be overcome.

Two popular methods for deriving reduced-order models from finite-element models are the Enforced Modal Displacement (EMD) and Applied Modal Force (AMF) methods [1]. These two approaches can lead to significantly different results due to the way in which membrane-type coupling is captured. Specifically, the EMD method often requires that membrane modes are included in the reduced-order model (ROM) [2], whilst the modal parameters calibrated using the AMF method can be sensitive to the magnitude of the force used [3].

In this work, the AMF method is applied to a simple, analytical model of a mass supported by two orthogonal, linear springs, as shown in Figure 1(a). This mass, m, is free to move in two degrees-of-freedom, x and y. The spring parallel to direction x has a length ℓ_1 and a stiffness k_1, whilst the spring parallel to y has a length ℓ_2 and a stiffness k_2. The parameters used here are $m = 1\,\mathrm{kg}$, $\ell_1 = \ell_2 = 5\,\mathrm{cm}$, $k_1 = 100\,\mathrm{N\,m^{-1}}$ and $k_2 = 15000\,\mathrm{N\,m^{-1}}$.

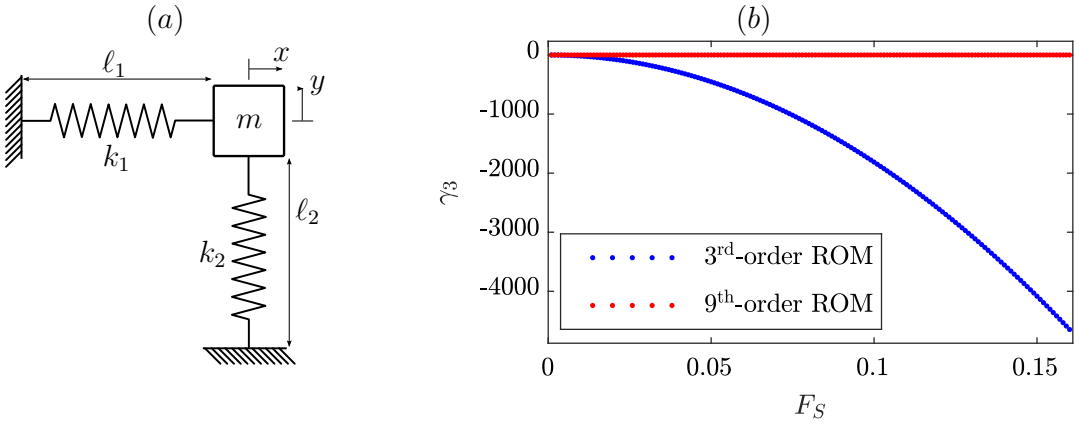

Figure 1: A schematic diagram of the simple oscillator, used to motivate this work, is shown in panel (a). The value of the ROM parameter, γ_3, as the force scale factor, F_S, is varied is shown in panel (b).

The equation of motion of this system may be written

$$\ddot{q}_1 + \omega_{n1}^2 q_1 + 3\alpha_1 q_1^2 + 2\alpha_2 q_1 q_2 + \alpha_3 q_2^2 + 4\beta_1 q_1^3 + 3\beta_2 q_1^2 q_2 + 2\beta_3 q_1 q_2^2 + \beta_4 q_2^3 = f_{q1}\,, \quad (1)$$

$$\ddot{q}_2 + \omega_{n2}^2 q_2 + \alpha_2 q_1^2 + 2\alpha_3 q_1 q_2 + 3\alpha_4 q_2^2 + \beta_2 q_1^3 + 2\beta_3 q_1^2 q_2 + 3\beta_4 q_1 q_2^2 + 4\beta_5 q_2^3 = f_{q2}\,, \quad (2)$$

where the modal coordinates $q_1 = mx$ and $q_2 = my$ have been substituted, and a Taylor expansion, truncated at the third order, has been used to approximate the nonlinear terms. Note that the linear natural frequencies are given by $\omega_{n1}^2 = 100\,\mathrm{rad\,s^{-1}}$ and $\omega_{n2}^2 = 15000\,\mathrm{rad\,s^{-1}}$ – hence the second mode, with a significantly higher frequency, resembles a membrane-type mode. These equations of motion will be treated as the *full-order* system (typically represented by a finite-element method).

To find a reduced-order model describing the dynamics of the first mode of this system, q_1, a suitable parameterised model must be chosen. As the nonlinearity in this full-order system contains quadratic and cubic terms, it appears reasonable to reduce the system to a model containing similar nonlinear terms, i.e.

$$\ddot{q}_1 + \omega_{n1}^2 q_1 + \gamma_2 q_1^2 + \gamma_3 q_1^3 = f_{q1}\,. \tag{3}$$

The AMF method is employed by applying a series of static loads to the first mode of the full-order model (whilst setting the second modal forcing, f_{q2}, to zero) allows the nonlinear parameters of the ROM, γ_2 and γ_3, to be estimated. The blue dots in Figure 1(b) show the estimated value of the cubic parameter, γ_3, as the magnitude of the static loads applied to the full model vary (using scaling F_S). This clearly shows that this nonlinear parameter is sensitive to the magnitude of the applied load, and that the process for calibrating the ROM is not robust.

To understand the cause of this variation, we return to the equation of motion of the second mode, Eq. (2). When the system is static and no load is applied, $\ddot{q}_2 = f_{q2} = 0$, and hence the only remaining variables in Eq. (2) are the modal displacements q_1 and q_2. As such, Eq. (2) represents a constraint between q_1 and q_2, which may be written

$$q_2 = f\left(q_1\right) \approx A_2 q_1^2 + A_3 q_1^3 + \ldots\,, \tag{4}$$

where it has been assumed that the function $f(q_1)$ may be approximated using a polynomial. If this polynomial, describing q_2 in terms of q_1, is truncated at the third-order, substituting this into the first equation of motion, Eq. (1), gives

$$\ddot{q}_1 + \omega_{n1}^2 q_1 + \gamma_2 q_1^2 + \gamma_3 q_1^3 + \gamma_4 q_1^4 + \gamma_5 q_1^5 + \gamma_6 q_1^6 + \gamma_7 q_1^7 + \gamma_8 q_1^8 + \gamma_9 q_1^9 = f_{q1}\,. \tag{5}$$

This is representative of a 9^{th}-order ROM (i.e. a ROM where the nonlinearity is expressed up to the 9^{th}-order) which is in contrast to the 3^{th}-order ROM shown in Eq. (4). The variation of the γ_3 parameter of the 9^{th}-order ROM, with the force scale factor F_S, is represented by a red dots in Figure 1(b). This clearly shows that the 9^{th}-order ROM is significantly more robust to variations in the force scale factor than the 3^{th}-order ROM.

When applying the AMF method, the 3^{th}-order ROM is typically adopted. These results demonstrate that, due to the strong coupling that may exist between modes that are well-separated in frequency, the parameters of the 3^{th}-order ROM may vary significantly with the magnitude of the applied load. Furthermore, these results suggest that a higher-order of nonlinearity should be adopted in the ROM in order to account for these coupling effects.

Acknowledgements
The authors gratefully acknowledge the support of EPSRC grant EP/R006768/1.

References

[1] M. P. Mignolet, A. Przekop, S. A. Rizzi, S. M. Spottswood, A review of indirect/non-intrusive reduced order modeling of nonlinear geometric structures, Journal of Sound and Vibration 332 (10) (2013) 2437–2460.

[2] S. A. Rizzi, A. Przekop, System identification-guided basis selection for reduced-order nonlinear response analysis, Journal of Sound and Vibration 315 (3) (2008) 467–485.

[3] R. W. Gordon, J. J. Hollkamp, Reduced-order models for acoustic response prediction, Tech. Rep. AFRL-RB-WP-TR-2011-3040, Air force research laboratory (2011).

Finite elements based reduced order models for nonlinear dynamics of piezoelectric structures

O. Thomas[1], **A. Givois**[1,2], **A. Grolet**[1] **and J.-F. Deü**[2]

[1]Arts et Métiers ParisTech, LISPEN EA 7515
8 bd. Louis XIV 59046 Lille, France
olivier.thomas@ensam.eu, arthur.givois@ensam.eu, aurelien.grolet@ensam.eu

[2] Conservatoire National des Arts et Métiers, LMSSC EA 3196,
2 Rue Conté, 75003 Paris, France
jean-francois.deu@lecnam.net

Abstract This paper presents a general methodology to predict the dynamics of geometrically nonlinear electro-mechanical structures with piezoelectric transducers. Modal Reduced Order Models (ROM) are built using a finite-element software thanks to a non-intrusive strategy. The resulting system is solved with the Harmonic Balance Method coupled to an Asymptotic Numerical Method (ANM). The present study focuses on the computation of the ROM and its validation with experiments on a test structure, exhibiting bent nonlinear modes, internal resonances and nonlinear response under parametric excitation.

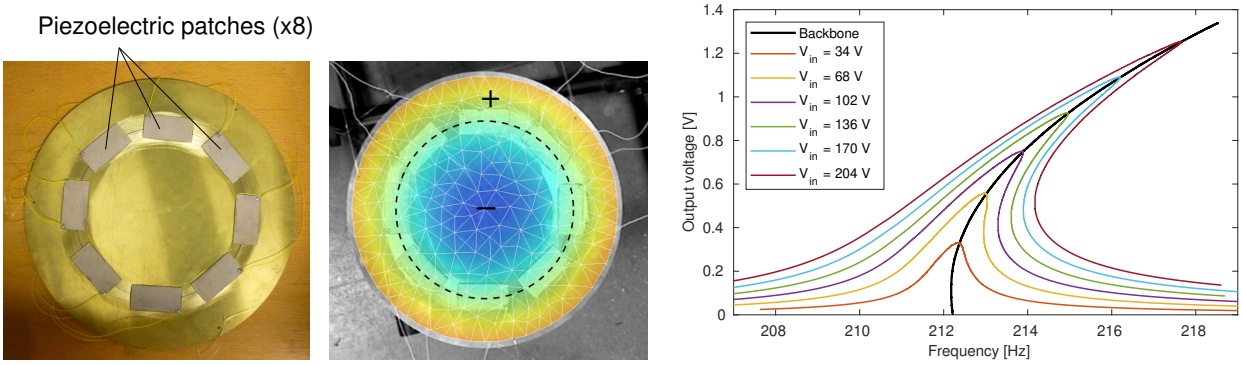

Figure 1: Photograph of the test structure. Deformed shape of the (0,1) mode and experimental nonlinear frequency response in forced and free vibrations (backbone curve) with piezoelectric actuation and detection.

Geometrical nonlinearities, due to large transverse displacements of thin structures, are involved in a large range of applications. Among them, Micro-Electro Mechanical Systems (MEMS) developments has been the focus of numerous studies, whose purpose is to master and use the geometrically nonlinear behaviour (among others, see [5,7,8]). Recent advances in non-intrusive ROM finite element modeling of nonlinear geometric structures offer new perspectives to compute accurate ROM of structures with complex geometries [3]. An application on piezoelectric nanobridges of such a method has been proposed in [2], with a home made finite element code. The purpose of this paper is to extend this approach to a wider range of electromechanical structures, composed of a thin elastic host structures equipped with several piezoelectric patches, for actuation and detection of the vibrations. The modelling proposed here includes: (i) the geometrical nonlinearities (ii) the laminated structure and (iii) the electromechanical transduction with both converse and direct effects.

Following the ideas of [6] for the linear case and [2] for the case with geometrical nonlinearities, we expand the finite element formulation on K eigenmodes of the structures, by writing

the displacement vector $\boldsymbol{U}(t) = \sum_{k=1}^{K} \boldsymbol{\Phi}_k q_k(t)$, where $\boldsymbol{\Phi}_k$ is the k-th. eigenvector with the piezoelectric patches in short circuit and $q_k(t)$ the corresponding modal coordinate. It can be shown that it verifies, $\forall k = 1, \dots K$, $\forall p = 1, \dots P$:

$$\begin{cases} \ddot{q}_k + 2\xi_k \omega_k \dot{q}_k + \omega_k^2 q_k + \sum_{i,j=1}^{K} \beta_{ij}^k q_i q_j + \sum_{i,j,l=1}^{K} \gamma_{ijl}^k q_i q_j q_l + \sum_{p=1}^{P} \chi_k^{(p)} V^{(p)} + \sum_{p=1}^{P} \sum_{i=1}^{N} \Theta_{ik}^{(p)} q_i V^{(p)} = F_k, & \text{(1a)} \\ C^{(p)} V^{(p)} - \sum_{k=1}^{K} \chi_k^{(p)} q_k - \sum_{i,j=1}^{K} \frac{1}{2} \Theta_{ij}^{(p)} q_i q_j = Q^{(p)}. & \text{(1b)} \end{cases}$$

In the above equations, P piezoelectric patches have been considered, whose electrical state is defined by $(V^{(p)}, Q^{(p)})$, respectively the voltage between the electrodes and the electric charge contained in one of the electrodes. The above model is composed of four separated parts: (1) the linear part (that depends on the k-th eigenfrequency in short circuit ω_k, the modal damping factors ξ_k and the modal mechanical forcing F_k), (2) the geometrical nonlinear part (with coefficients β_{ij}^k and γ_{ijl}^k), (3) the linear piezoelectric coupling (defined by the coupling coefficients $\chi_k^{(p)}$ between mode k and patch p) and (4) a less classical part stemming from both the geometrical nonlinearities and the piezoelectric coupling (of coefs. $\Theta_{ij}^{(p)}$), introduced in [2] and responsible of parametric excitation effects in thin structures [7].

In this context, we propose an extension of the method introduced in [4] to compute all coefficients of the above ROM and some validations. A first set of validations is obtained by considering theoretical test cases for which analytical models are at hand (such as a hinged-hinged beam with two symmetrically disposed piezoelectric patches that cover its whole length). Then, some experiments are also considered, on a specially designed test structure, composed of a circular brass plate equiped with eight piezoelectric patches (Fig. 1). Using experimental continuation [1], the free (backbone curves / nonlinear mode) and forced vibrations are obtained for the first axisymmetric mode (Fig. 1), for two companion asymmetric modes involved in internal resonance and also for parametric excitation. In all cases, the piezoelectric patches are used for both actuation and detection.

References

[1] V. Denis, M. Jossic, C. Giraud-Audine, B. Chomette, A. Renault, and O. Thomas. Identification of nonlinear modes using phase-locked-loop experimental continuation and normal form. *Mechanical Systems and Signal Processing*, 106:430–452, 2018.

[2] A. Lazarus, O. Thomas, and J.-F. Deü. Finite elements reduced order models for nonlinear vibrations of piezoelectric layered beams with applications to NEMS. *Finite Elements in Analysis and Design*, 49(1):35–51, 2012.

[3] M. P. Mignolet, A. Przekop, S. A. Rizzi, and S. M. Spottswood. A review of indirect/non-intrusive reduced order modeling of nonlinear geometric structures. *Journal of Sound and Vibration*, 332(10):2437–2460, 2013.

[4] A. A. Muravyov and S. A. Rizzi. Determination of nonlinear stiffness with application to random vibration of geometrically nonlinear structures. *Computers and Structures*, 81(15):1513–1523, 2003.

[5] O. Shoshani, D. Heywood, Y. Yang, T. W. Kenny, and S. W. Shaw. Phase noise reduction in an mems oscillator using a nonlinearly enhanced synchronization domain. *Lournal of Microelectromechanical Systems*, 25(5):870–876, 2016.

[6] O. Thomas, J.-F. Deü, and J. Ducarne. Vibration of an elastic structure with shunted piezoelectric patches: efficient finite-element formulation and electromechanical coupling coefficients. *International Journal of Numerical Methods in Engineering*, 80(2):235–268, 2009.

[7] O. Thomas, F. Mathieu, W. Mansfield, C. Huang, S. Trolier-McKinstry, and L. Nicu. Efficient parametric amplification in mems with integrated piezoelectric actuation and sensing capabilities. *Applied Physics Letters*, 102(16):163504, 2013.

[8] L. G. Villanueva, E. Kenig, R. B. Karabalin, M. H. Matheny, R. Lifshitz, M. C. Cross, and M. L. Roukes. Surpassing fundamental limits of oscillators using nonlinear resonators. *Physical Review Letters*, 110(17):177208, 2013.

Retrieving highly structured models starting from black-box nonlinear state-space models using polynomial decoupling

J. Decuyper[1], **K. Tiels**[2] **and J. Schoukens**[1,3]

[1]Department of Engineering Technology, Vrije Univeristeit Brussel
Brussels, Belgium
jan.decuyper@vub.be

[2]Department of Information Technology, Uppsala University
Uppsala, Sweden
koen.tiels@it.uu.se

[3]Department of Electrical Engineering, Eindhoven University of Technology
Eindhoven, The Netherlands
johan.schoukens@vub.be

Abstract This work discusses a model reduction technique for polynomial nonlinear state-space models. The reduction proceeds by translating the large coupled polynomials into a low number of univariate polynomial functions.

1 Introduction

The use of nonlinear state-space models as a generic nonlinear model structure has proven useful in a variety of applications over recent years. The downside of flexibility is the size of the models, and the large number of parameters required in their description. Moreover, the generic set of equations rely on large multivariate polynomial functions which are hard to interpret. This work discusses a method that involves the decoupling of the polynomial functions in order to retrieve structured models. The size of the models is reduced and the use of univariate functions provides more insight into the nature of the nonlinearity.

2 Approach

The method consists of three steps:

1. Decouple the multivariate polynomial ($\mathbf{f}$) starting from its first-order derivate sampled in a number of operating points [1],

$$\mathbf{f}(\mathbf{x}(t), \mathbf{u}(t)) = \mathbf{W}\mathbf{g}\left(\mathbf{V}^{\mathrm{T}}\begin{bmatrix}\mathbf{x}(t)\\ \mathbf{u}(t)\end{bmatrix}\right), \tag{1}$$

   here $\mathbf{g}$ is a univariate vector function of a set of intermediate variables. The nonlinear mappings of $\mathbf{g}$ are referred to as branches.

2. Exploiting linear dependencies amongst branches, their number is reduced in successive steps. Doing so, model complexity is balanced to accuracy.

3. The decoupled function is plugged back into the nonlinear state-space model and nonlinear optimisation is used to ensure good performance.

3 Results on the Silver box system

The Silver box is an electrical implementation of the forced Duffing oscillator. Polynomial nonlinear state-space (PNLSS) modelling [2] results in the following model,

$$\mathbf{x}(k+1) = \mathbf{A}\mathbf{x}(k) + \mathbf{b}u(k) + \begin{bmatrix} e_{11} & \cdots & e_{17} \\ e_{21} & \cdots & e_{27} \end{bmatrix} \begin{bmatrix} x_1^2(k) \\ x_1(k)x_2(k) \\ x_2^2(k) \\ x_1^3(k) \\ x_1^2(k)x_2(k) \\ x_1(k)x_2^2(k) \\ x_2^3(k) \end{bmatrix} \tag{2a}$$

$$y(k) = \mathbf{c}\mathbf{x}(k) + du(k), \tag{2b}$$

where the nonlinear part (in red) is described using 14 parameters. Without loss of performance the model is reduced to the following form,

$$\mathbf{x}(k+1) = \mathbf{A}\mathbf{x}(k) + \mathbf{b}u(k) + \begin{bmatrix} w_1 \\ w_2 \end{bmatrix} \left[\theta_1 z^3(k) + \theta_2 z^2(k)\right] \tag{3a}$$

$$y(k) = \mathbf{c}\mathbf{x}(k) + du(k), \tag{3b}$$

$$z(k) = \begin{bmatrix} v_1 & v_2 \end{bmatrix} \begin{bmatrix} x_1(k) \\ x_2(k) \end{bmatrix}, \tag{3c}$$

which uses only 6 parameters (corresponding to only 4 d.o.f) in the nonlinear description. The results on a validation data set are shown below. Results are also presented for the Bouc-Wen system, the Van der Pol system and a Li-Ion battery model.

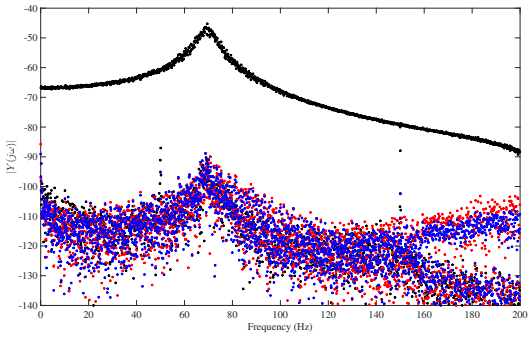

Figure 1: Results of the Silverbox model on a validation data set. Black is the true output, blue is the PNLSS model error, red the reduced model error.

4 Acknowledgements

This work was supported by the Fund for Scientific Research (FWO-Vlaanderen), the Swedish Research Council (VR) via the project NewLEADS – New Directions in Learning Dynamical Systems (contract number: 621-2016-06079), and by the Swedish Foundation for Strategic Research (SSF) via the project ASSEMBLE (contract number: RIT15-0012).

References

[1] P. Dreesen, M. Ishteva, J. Schoukens, *Decoupling multivariate polynomials using first-order information*, SIAM Journal on Matrix analysis and Applications 36, 864-879, 2014.

[2] J. Paduart, L. Lauwers, J. Swevers, K. Smolders, J. Schoukens, R. Pintelon, *Identification of nonlinear systems using Polynomial Nonlinear State Space models*, Automatica 46, 647-656, 2010.

Waves & Localisation

Tuesday, 2nd July 2019

Chairman: C.H. Lamarque

Localization and non-reciprocity in nonlinear dissipative lattices

A. Mojahed[1], O. V. Gendelman[2] and A. F. Vakakis[1]

[1] University of Illinois at Urbana-Champaign
Urbana, USA
avakakis@illinois.edu

[2] Technion – Israel Institute of Technology
Haifa, Israel

Abstract The effect of on-site damping and other physical parameters on breather arrest, energy localization and non-reciprocity in strongly nonlinear semi-infinite lattices is studied. The study is performed for two lattices: (i) a strongly nonlinear uniform semi- infinite lattice and, (ii) an asymmetric strongly nonlinear hierarchical semi-infinite lattice. A more detailed presentation of these results are given in (Mojahed et al., 2018).

Breathers are localized oscillatory wavepackets formed by nonlinearity and dispersion, and breather arrest refers to breather decay and disintegration over a finite "penetration depth" in a dissipative lattice. First, a simplified system of two nonlinearly coupled oscillators under impulsive excitation is considered. The exact relation between the finite number of nonlinear beats (energy exchanges between oscillators), the magnitude of excitation, and the on-site damping is derived. In the next step, these results are correlated to those of the semi-infinite extension of the simplified system, and it was found out that the breather penetration depth is governed by a similar law to that of the finite beats in the simplified system. The comparison between the characteristic curves (corresponding to disappearance of modulated response after a specific finite number of beats) and breather penetration depths is demonstrated in figure 1. The comparison reveals that the 2DOF reduced order model is able to represent the general breather arrest phenomenon in the semi- infinite uniform lattice.

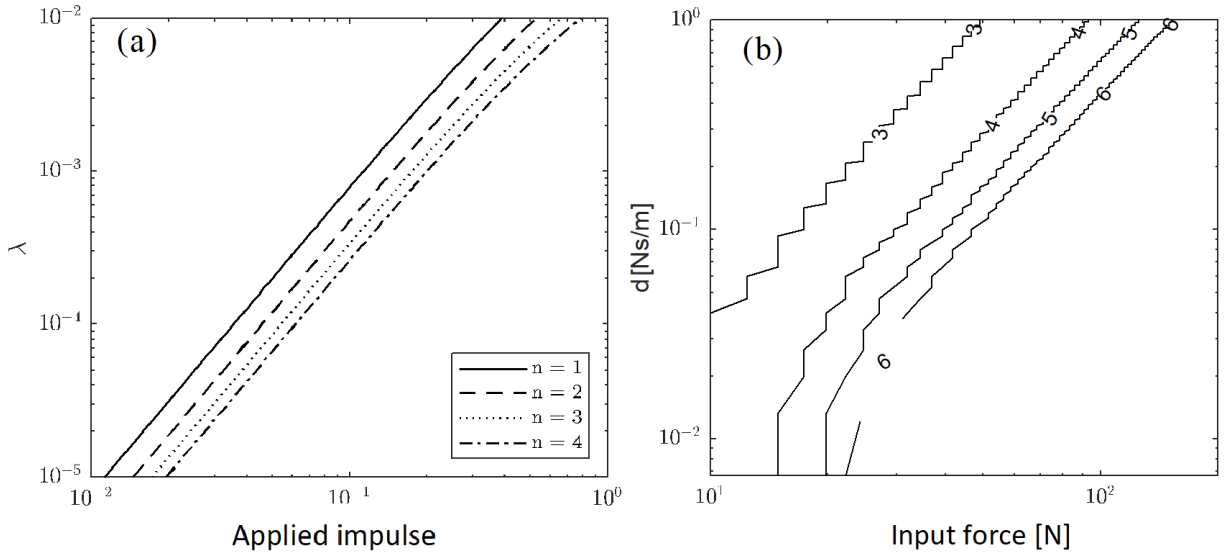

Figure 1: (a) Characteristic curves for specific maximum number of beatings and (b) breather penetration depths in the semi-infinite homogeneous lattice in the parameter space corresponding to (damping-excitation level) in logarithmic scales.

Similarly, for the second nonlinear lattice, energy localization and acoustic non- reciprocity are studied. Due to asymmetric nature of the lattice, depending on from which end the lattice is being excited, one can see energy localization at the excitation site or wave propagation through the lattice from the excitation site. In studying energy localization in this lattice, a very interesting observation in this system is that when the nonlinear coupling stiffness elements are considered non-linearizable, energy localization occurs on the opposite end of the lattice when compared to the similar lattice but with linearizable (small linear stiffness in parallel with the nonlinear stiffness) nonlinear coupling stiffness elements. Figure 2 illustrates the energy localization site for both of the discussed cases, i.e. non-linearizable and linearizable nonlinear coupling.

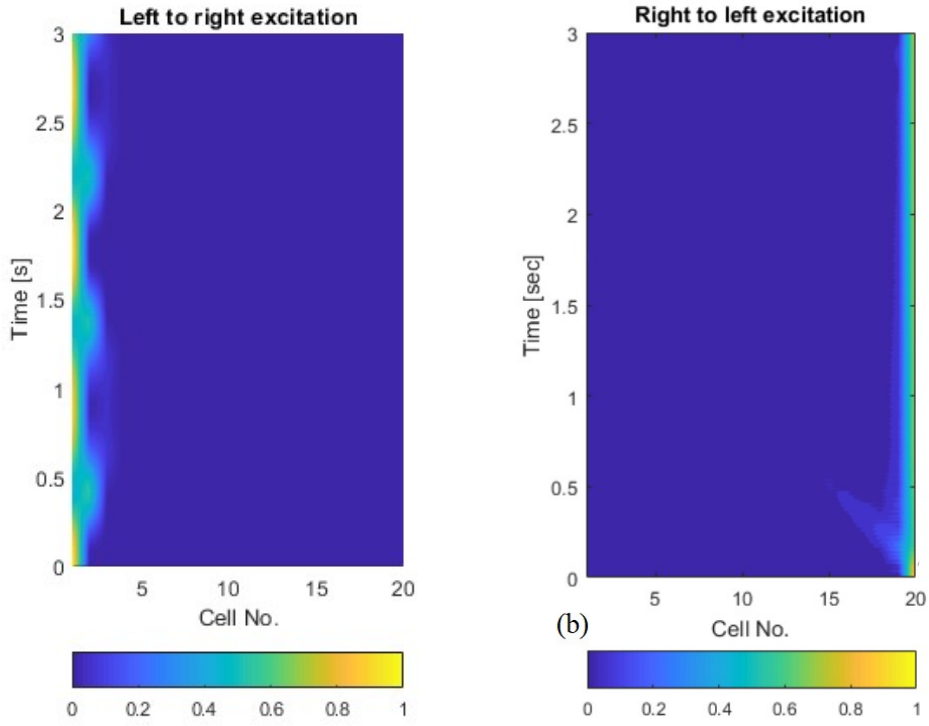

Figure 2: (a) Energy localization on the left end of the lattice (non-linearizable nonlinear coupling). (b) Energy localization on the right end of the lattice (linearizable nonlinear coupling).

The effect of the small linear component in the nonlinear coupling stiffness on the inversion of energy localization site is fully explained through studying the governing nonlinear normal modes (NNMs) [1], of the lattice and the exploring the localized NNMs of this system and their interactions with the nonlinear propagation zones of the lattice.

References

[1] Kerschen, G., Peeters, M., Golinval, J. C., Vakakis, A. F., Nonlinear normal modes, Part I: A useful framework for the structural dynamicist , Mechanical Systems and Signal Processing 23.1, 170-194, 2009.

[2] Mojahed, A., Gendelman, O.V., Vakakis, A.F., Breather arrest, localization and acoustic non-reciprocity in dissipative nonlinear lattices , Journal of Acoustical Society of America (Special Issue on Non-reciprocal and Topological Wave Phenomena in Acoustics) (submitted).

Stationary and Non-stationary Resonant Dynamics of the Finite Chain of Weakly Coupled Pendula

L.I. Manevitch [1], **V.V. Smirnov** [2]

Polymer and Composite Materials Department, N. N. Semenov Institute of Chemical Physics, RAS
Moscow, Russia
[1]manevitchleonid3@gmail.com
[2]vvs@polymer.chph.ras.ru

Abstract We discuss new phenomena of energy localization and transition to chaos in the finite system of coupled pendula without any restrictions on the amplitudes of oscillations. We propose a new approach to the problem based on the recently developed Limiting Phase Trajectory (LPT) concept in combination with a semi-inverse method. The analytic predictions of the conditions providing transition to energy localization are confirmed by numerical simulation.

The system of the coupled pendula is the wide-expanded model in the various field of science [1, 2]. We consider the nonlinear non-stationary dynamics of the sine-lattice [3], which is very useful in some fields of the polymer physics and biophysics. We start from the Hamilton function of the discrete system of coupled pendula with the harmonic-type bonds:

$$H = \sum_{j=1}^{N} \left(\frac{1}{2} \left(\frac{d\varphi_j}{dt} \right)^2 + (1 - \cos(\varphi_{j+1} - \varphi_j)) + \sigma \left(1 - \cos \varphi_j\right) \right), \tag{1}$$

where φ_j is the displacement of the j-th pendulum from its equilibrium position and N is the number of pendula. The dimensionless time t is normalized by the coupling constant while the "gravity" constant σ can be changed in the accordance of the concrete problem.

It can be shown [4] that the non-stationary dynamics of the system under consideration can be studied in the terms of the complex variables $\Psi_j = (1/\sqrt{2\omega})(\omega\varphi_j + id\varphi_j/dt)$. In such a case, the energy of the nonlinear normal mode $\Psi_j = \psi_j \exp(-i\omega t)$ can be written in the form

$$H_r = \sum_{j=1}^{N} \frac{\omega}{2}|\psi_j|^2 + \left(1 - J_0\left(\sqrt{\frac{2}{\omega}}|\psi_{j+1} - \psi_j|\right)\right) + \sigma\left(1 - J_0\left(\sqrt{\frac{2}{\omega}}|\psi_j|\right)\right), \tag{2}$$

where J_0 - the Bessel function of zero order and the eigen frequency of the nonlinear normal mode with the wave number κ can be written as follows

$$\omega^2 = \frac{2}{Q}\left(2J_1\left(2Q\sin\frac{\kappa}{2}\right)\sin\frac{\kappa}{2} + \sigma J_1(Q)\right). \tag{3}$$

Here, the amplitude Q of the oscillations are related to the modulus of the complex variable $|\psi_j| = \sqrt{\frac{\omega}{2}}Q$.

Equation (2) with $\psi_j = \chi \exp(i\kappa j)$ can be considered as the Hamilton function corresponding to the non-stationary dynamics if the amplitude χ is changed at the scale, which is essentially larger than the period of the mode ($T = 2\pi/\omega$). In particular, this occurs when two mode with close wave numbers are excited simultaneously. In such a case, the equations of motion can be obtained accordingly the rule:

$$i\frac{\psi_j}{d\tau} = -\frac{\partial H_r}{\partial \psi_j^*} \tag{4}$$

(the asterisk denotes the complex conjugate function).

It can be shown that equations (4) admit the additional integral of motion $X = \frac{1}{N}\sum_j |\psi_j|^2$. It was shown in [4–6] that the existence of integral X is extremely useful for the analysis of the nonlinear normal modes (NNMs) interaction. Near the edges of the spectrum (3) this process leads to the separation of the chain onto two domains, which are differed by the energy concentration. So we can introduce the "domain variables"

$$\chi_1(\tau) = \frac{1}{\sqrt{2N}}\sum_j \psi_j(\tau)\left(1+\cos\left(\kappa j+\frac{\pi}{4}\right)\right); \quad \chi_2(\tau) = \frac{1}{\sqrt{2N}}\sum_j \psi_j(\tau)\left(1-\cos\left(\kappa j+\frac{\pi}{4}\right)\right).$$

Taking into account integral X one should write the domain variables in the form $\chi_1 = \sqrt{X}\cos\theta\exp(-i\Delta/2), \chi_1 = \sqrt{X}\sin\theta\exp(i\Delta/2)$ and express the domain occupation via the value $R = |\chi_1|^2 - |\chi_2|^2 = X\cos 2\theta$. The accurate analysis of hamiltonian (3) on the phase plane Δ, R shows that there are two threshold values of integral X (see fig. 1(a-c)). Before the first threshold the modes are stable and the periodic redistribution of the energy between domains occurs. If X exceeds the first threshold one of the modes losses its stability, but the energy migration is still possible. Finally, above the second threshold the phase trajectories starting at $R = -1$ can not achieve the value $R = 1$ and vise versa. It means that the energy putting into one part of the chain can not be redistributed along it.

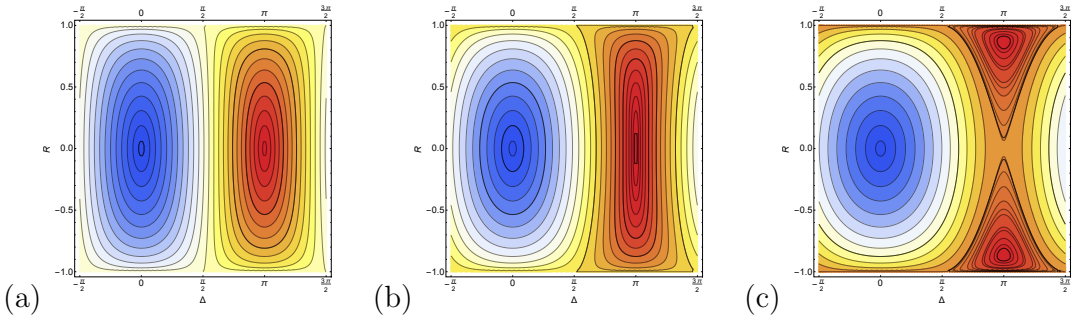

Figure 1: Phase portraits (2) in the terms of variables R and Δ at different oscillation amplitudes $Q = \pi/10$(a). $Q = 2\pi/10$ (b), $Q = 3.2\pi/10$ (c). $\sigma = 1$, $N = 32$.

References

[1] Braun, O. M. and Kivshar, Yu. S., The Frenkel Kontorova Model: Concepts, Methods, and Applications, Berlin: Springer, 2004.

[2] The sine-Gordon Model and Its Applications: From Pendula and Josephson Junctions to Gravity and High-Energy Physics, J. Cuevas-Maraver, P.Kevrekidis, F. Williams (Eds.), Cham: Springer, 2014.

[3] Takeno, Sh. and Homma, Sh., A sine-Lattice (sine-Form Discrete sine-Gordon) Equation: One- and Two-Kink Solutions and Physical Models, J. Phys. Soc. Japan, 1986, vol. 55, no. 1, pp. 6575.

[4] Smirnov, V. V. and Manevitch, L. I., Large-amplitude nonlinear normal modes of the discrete sine lattices, Phys. Rev. E, 2017, vol. 95, no. 2, 022212, 8 pp.

[5] Smirnov V. V. and Kovaleva M. A. and Manevitch L. I., Nonlinear Dynamics of Torsion Lattices, Russian J Nonlinear Dynamics, 2018, vol. 14, no. 2, pp. 179193.

[6] Manevitch L.I., Kovaleva A.S., Smirnov V.V. and Starosvetsky Yu, Nonstationary Resonant Dynamics of Oscillatory Chains and Nanostructures, 2018, Springer Nature, Singapore

Weakly and Strongly Nonlinear Periodic Materials: Tunable Dispersion, Non-Reciprocity, and Device Implications

A. Darabi[1] and M. J. Leamy[2]

Georgia Institute of Technology
Atlanta, USA
[1]amirdarabi@gatech.edu
[2]michael.leamy@me.gatech.edu

Abstract This talk will discuss research aimed at analyzing, simulating, and experimentally exploring weakly and strongly nonlinear acoustic periodic materials. In particular, the talk will focus on the manner in which these materials can be used to create novel wave-control devices for the purposes of wave guiding and filtering.

Weak and strong nonlinearity provide additional design degrees of freedom for achieving novel behavior in periodic elastic media. In weakly nonlinear media, perturbation techniques [1, 2] have recently been employed to uncover amplitude-dependent dispersion and spatial propagation – see Fig. 1 for representative results. These techniques asymptotically expand the displacement field and frequency (or, equivalently, time) and result in a cascading set of linear equations. Removal of secular terms yield updates to the dispersion relationship, while particular solutions at higher orders lead to multiharmonic content. Recent interpretations [3, 4] of these higher-order waves have shown that they can propagate through weakly nonlinear media with little to no generation of higher harmonics, similar to the invariance displayed by solitons.

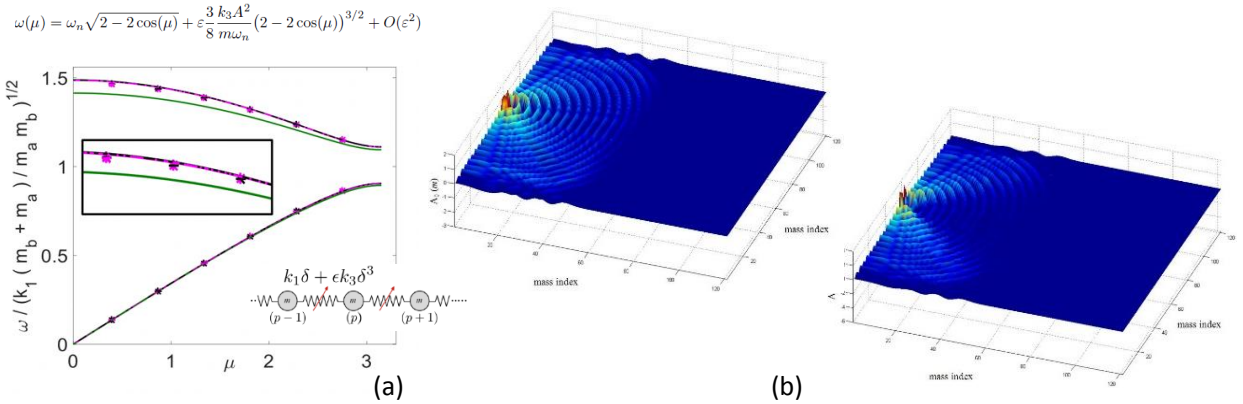

Figure 1: (a) Weakly nonlinear periodic media give rise to amplitude-dependent dispersion and (b) amplitude-dependent spatial dead-zones for (left) small and (right) large amplitude waves.

Experimental confirmation of these and other findings are an open area of investigation. Manktelow *et al.* [5] provided an indirect measurement of amplitude-dependent dispersion in a periodic string by placing evenly-spaced lead masses on a taut string, which was then excited by a shaker and measured using a laser Doppler vibrometer. The taut string exhibits a well-known cubic stiffening, which leads to positive shifts to the string's dispersion with increasing amplitude. The analysis connected the system's natural frequencies to the dispersion relationship in the first Brillouin zone using a phase closure argument. Measurements of the nonlinear backbones then resulted in amplitude-dependent dispersion curves – see Fig. 2. While successful, the experiment was limited

to relatively small motions due to the string's tendency to exhibit a whirling instability. Experimental studies have yet to appear which confirm the other richness observed both analytically and numerically.

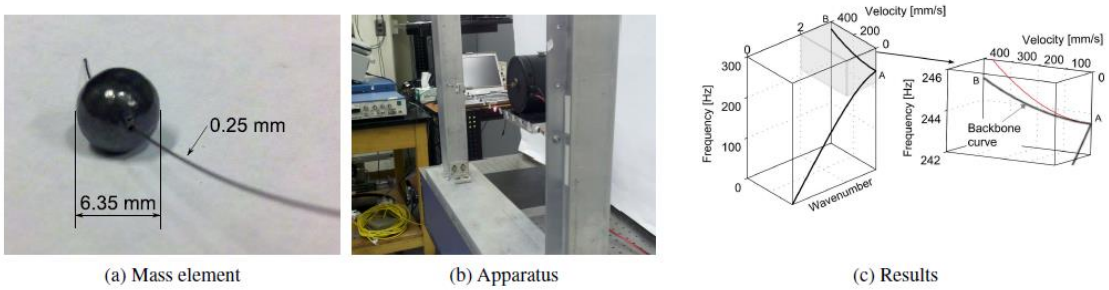

Figure 2: Experimental apparatus and results: (a) lead bead and steel wire, (b) periodic string fixed to two upright aluminium beams, (c) experimentally measured backbone curve AB (black) and theoretical backbone curve for a simplified model (red).

Strongly nonlinear periodic systems exhibit additional advantageous behavior, particularly as concerns non-reciprocal wave propagation. Boechler *et al.* [6] showed that a granular chain with a defect near one end could passively break reciprocity due to a bifurcation involving the defect mass. More recently, strongly nonlinear systems incorporating hierarchical scales and asymmetry have been shown theoretically and experimentally to passively break reciprocity over a large range of impulse-like excitation [7]. Figure 3 illustrates representative results for such systems in which excitation on the left yields propagation, while excitation on the right leads to localization and no propagation. This is an ongoing area of research which is currently being extended to strongly nonlinear systems which passively break plane wave reciprocity.

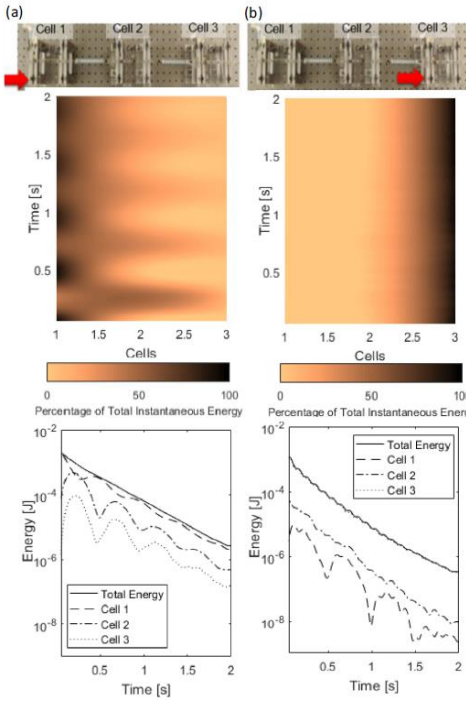

Figure 3: Experimental demonstration non-reciprocity in a chain consisting o unit cells, each unit cell containing tw scales coupled by strongly nonlinear stiffness. Excitation on the left end cle shows propagation to the right, while excitation on the right remains localize and no transmission to the left occurs.

References

[1]. Narisetti, R.K., M.J. Leamy, and M. Ruzzene, *A Perturbation Approach for Predicting Wave Propagation in One-Dimensional Nonlinear Periodic Structures,* Journal of Vibration and Acoustics 132(3), 2010.

[2]. Vakakis, A.F. and M.E. King, *Nonlinear-Wave Transmission in a Monocoupled Elastic Periodic System*, Journal of the Acoustical Society of America 98(3), 1534-1546, 1995.

[3]. Fronk, M. and M.J. Leamy, *Waveform Invariance in Nonlinear Periodic Systems Using Higher Order Multiple Scales,* ASME IDETC 2016.

[4]. Fronk, M.D. and M.J. Leamy, *Direction-dependent invariant waveforms and stability in two-dimensional, weakly nonlinear lattices,* Journal of Sound and Vibration 447, 137-154, 2019.

[5]. Manktelow, K.L., M.J. Leamy, and M. Ruzzene, *Analysis and Experimental Estimation of Nonlinear Dispersion in a Periodic String,* Journal of Vibration and Acoustics 136(3), 2014.

[6]. Boechler, N., G. Theocharis, and C. Daraio, *Bifurcation-based acoustic switching and rectification.* Nature Materials 10(9), 665-668, 2011.

[7]. Bunyan, J., et al., *Acoustic nonreciprocity in a lattice incorporating nonlinearity, asymmetry, and internal scale hierarchy: Experimental study*, Physical Review E 97(5), 2018.

Wave propagation on a beam resting on a unilateral soil

S. Lenci[1] **and F. Clementi**[2]

[1]Polytechnic University of Marche
Ancona, Italy
lenci@univpm.it

[2]Polytechnic University of Marche
Ancona, Italy
francesco.clementi@univpm.it

Abstract The wave propagation problem of an Euler-Bernoulli beam resting on a tensionless foundation is addressed. The exact solution of the governing equation is obtained, selecting among the various mathematical solutions only those having a physical meaning. It is investigated how the stiffness of the unilateral soil influence the wave velocity.

The flexural wave propagation in beams is a classical problem [1], that is characterized by the velocity of propagation $c_{low} = \frac{\sqrt{EJ}}{L\sqrt{\rho A}}2\pi$, L being the wavelenght. When the beam rests on a bilateral elastic soil, of stiffness k, this velocity changes to $c_{up} = \frac{\sqrt{EJ}}{L\sqrt{\rho A}}\sqrt{4\pi^2 + \left(\frac{kL^4}{EJ}\right)\frac{1}{4\pi^2}}$. This problem has been investigated since long time ago, too [2].

Much less investigated is the problem of a beam resting on a unilateral soil, in which the foundation reach in traction (or compression) only [3], while the problem of wave propagation in this case has been studied in [4], a paper that constitutes the background of this work.

The mechanical problem is illustrated in Fig. 1, and is governed by the equation of motion

$$EJw'''' + \hat{k}w + \rho A\ddot{w} = 0, \tag{1}$$

$$\hat{k} = \begin{cases} k, & w > 0, \\ 0, & w \leq 0, \end{cases} \tag{2}$$

where $w(x,t)$ is the transversal displacement of the Euler-Bernoulli beam, EJ the bending stiffness, ρA the mass per unit length and $\hat{k}$ the stiffness of the foundation. We consider *undamped free* wave propagation.

The solution is sought after in the form

$$w(x,t) = \begin{cases} w_1(x,t) = W_1(\gamma_1 x - \omega_1 t), & \text{in the contact part,} \\ w_2(x,t) = W_2(\gamma_2 x - \omega_2 t), & \text{in the detached part,} \end{cases} \tag{3}$$

where

$$\omega_1 = \sqrt{\frac{EJ\gamma_1^4 + k}{\rho A}}, \qquad \omega_2 = \sqrt{\frac{EJ}{\rho A}}\gamma_2^2, \tag{4}$$

with relevant continuity/periodicity conditions for $x = L_1$ and $x = L_2$.

After long mathematical developments, that are reported in [4] and that require to add a physical admissibility condition to the purely mathematical solution of (1)-(2), it is possible to determine the wave velocity c_{unil} as a function of the soil stiffness k.

The solution is made of many branches, the first three being reported in Fig. 2. The first branch start from 2π for $k = 0$, increases for increasing k, reaches a maximum and then approaches π for k going back to $k = 0$. The other branches, on the other hand, are increasing functions of k, and, apart from the initial part, are always below the case of bilateral soil,

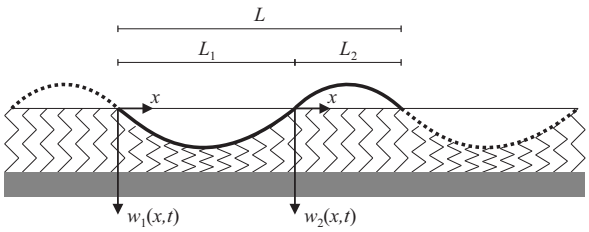

Figure 1: The considered mechanical problem.

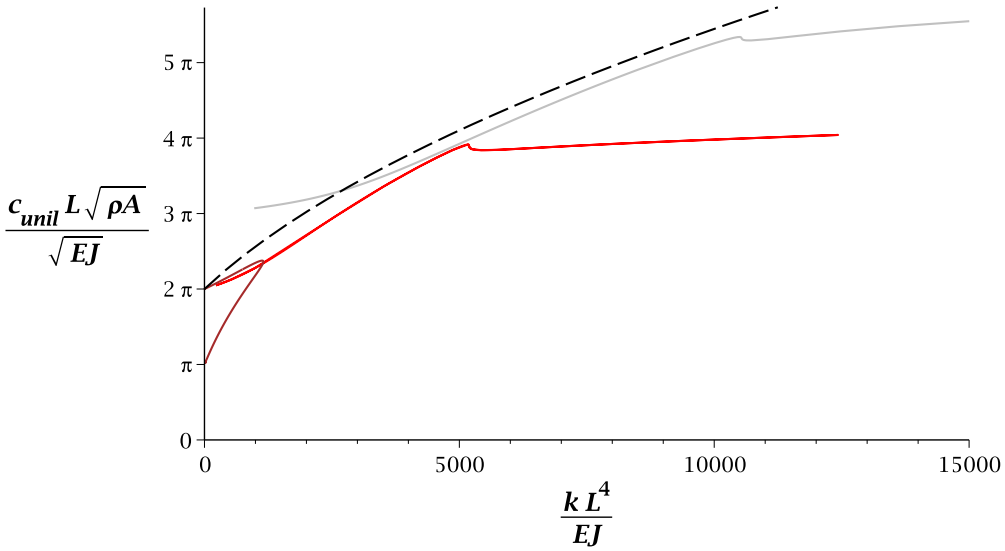

Figure 2: Wave velocity c_{unil} as a function of the soil stiffness. The dash line corresponds to the case of bilateral soil c_{up}.

according to the fact that waves propagate faster on stiffer systems; in fact, the bilateral foundation is stiffer than the unilateral one.

When the solution is close to the dashed line, the wave shape resembles (qualitatively) that reported in Fig. 1, i.e. the detached and in contact parts have about the same length, while far from it one of the two parts becomes predominant.

References

[1] H. Kolsky, Stress Waves in Solids, Dover, 1963.

[2] P.M. Mathews, *Vibration of a beam on elastic foundation*, Zeitschrift für Angewandte Mathematik und Mechanik 38, 105-115, 1958.

[3] L. Demeio, S. Lenci, *Forced nonlinear oscillations of semi-infinite cables and beams resting on a unilateral elastic substrate*, Nonlinear Dynamics 49, 203-215, 2007.

[4] S. Lenci, F. Clementi, *Flexural wave propagation in infinite beams on a unilateral elastic foundation*, Nonlinear Dynamics, accepted, 2019.

Musical acoustics

Wednesday, 3rd July 2019

Chairman: O.Thomas

Nonlinear dynamics in musical acoustics : characteristics, models and sound synthesis

C. Touzé

IMSIA, ENSTA ParisTech-CNRS-EDF-CEA
Palaiseau, France
cyril.touze@ensta-paristech.fr

Abstract Musical instruments are all concerned with a nonlinear characteristics, making the sound interesting to the ear and the problems challenging for the physician. In this presentation, we will give an overview of the nonlinear phenomena appearing in a number of musical instruments, without the aim of exhaustivity. The sound of friction, the acoustic nonlinearity occuring in brass instruments and giving rise to their particular rich tone will be surveyed, and a particular emphasis will be given to contact and geometric nonlinearity.

The physics of musical instruments always present a nonlinear characteristics, making the sound interesting and pleasant to the ear with the generation of a peculiar timbre [1–3]. Consequently the understanding and modeling has to cope with various and complex nonlinear phenomena that will be surveyed in this talk. When one thinks of the particular sound of a brass instrument, the high-frequency content generated by contact dynamics in indian stringed instruments such as tanpoura and sitar, or the wave turbulence at hand in the nonlinear dynamics of gongs and cymbals, one has to face a number of smooth and non smooth nonlinearities that are key in the sound production and cannot be neglected. Moreover, the sensitivity of the human perception makes the problems difficult to solve for sound synthesis as any small amount of numerical dispersion, or any mismodeling in the loss mechanisms and resulting decay rates, are immediately recognized by the ear as non physical, resulting in poor and unrealistic sound synthesis.

The talk will survey the main nonlinear characteristics in musical instruments. Without the aim of exhaustivity, the key components creating the typical sound of bow instruments, brass instruments, gongs and cymbals, and the problems of collisions, will be overviewed. More particularly:

- the sound of friction is key to understand the bowed string dynamics. The Helmholtz motion and the particular stick/slip dynamics will be reviewed, as well as the effect of rosin. The playability of the bowed string, which gives an idea of the boundary limits where Helmholtz motion occurs as function of the dynamical input parameters, will be explained [4–6].
- the brassy sound is generated by nonlinear acoustics propagation in tubes. The effect will be briefly explained [7]. For wind instruments, another interesting nonlinearity also occurs in reed instruments, where a nonlinear characteristics between pressure and air flow velocity is needed to ensure the birth of oscillations through a Hopf bifurcation [8].
- Collisions are present in a number of musical instruments. A special emphasis will be given to contact dynamics occuring in stringed instruments and used in order to create a specific tone, such as the one of indian instruments (sitar, tanpura) [9–12].

- The sound of turbulence is typical of percussion instruments such as gongs and cymbals. These instruments are characterized by a a broadband Fourier spectrum instead of having a definite pitch. Geometric nonlinearity occuring due to large-amplitude vibration of those thin structures, generates a wave turbulent regime with an energy flux from the low to the high frequencies, resulting in the particular sound of these instruments [13, 14].

Models used for sound synthesis of these instruments will then be exemplified and a particular emphasis on contact dynamics and thin plates dynamics including geometric nonlinearity will be shown with dedicated sound synthesis examples.

References

[1] N. H. Fletcher and T. D. Rossing, The Physics of musical instruments, Springer Verlag, 1991.

[2] A. Chaigne and J. Kergomard: Acoustics of musical instruments, Springer, 2016.

[3] S. Bilbao, Numerical Sound Synthesis: Finite Difference Schemes and Simulation in Musical Acoustics, Wiley, Chichester, 2009.

[4] J. H. Smith and J. Woodhouse: The tribology of rosin, Journal of the Mechanics and Physics of Solids, vol. 48, pp. 1633–1681, 2000.

[5] C. Desvages: Physical modelling of the bowed string and applications to sound synthesis, PhD thesis, University of Edinburgh, 2018.

[6] S. Serafin: The sound of friction: real-time models, playability and musical applications, PhD thesis, Stanford university, 2004.

[7] A. Myers, R. Pyle, J. Gilbert, M. Campbell, J. Chick and S. Logie: Effects of nonlinear sound propagation on the characteristic timbres of brass instruments, The Journal of the Acoustical Society of America, 131(1), 678-688, 2012.

[8] A. Hirschberg, J. Gilbert, A. P. J. Wijnands, and A. M. C. Valkering: Musical aero-acoustics of the clarinet, Journal de Physique IV 4:C5559:C5568, 1994.

[9] S. Bilbao, A. Torin and V. Chatziioannou: Numerical modeling of collisions in musical instruments. Acta Acustica, 101:15573, 2015.

[10] V. Chatziioannou and M. van Walstijn: Energy conserving schemes for the simulation of musical instrument contact dynamics. Journal of Sound and Vibration, 339:26279, 2015.

[11] C. Issanchou, S. Bilbao, J.-L. Le Carrou, C. Touzé and O. Doaré : A modal-based approach to the nonlinear vibration of strings against a unilateral obstacle: Simulations and experiments in the pointwise case, Journal of Sound and Vibration, vol. 393, 229-251, 2017.

[12] C. Issanchou, J-L. Le Carrou, C. Touzé, B. Fabre and O. Doaré, String/frets contacts in the electric bass sound: Simulations and experiments, Applied Acoustics 129, 217-228, 2018.

[13] M. Ducceschi and C. Touzé: Modal approach for nonlinear vibrations of damped impacted plates: Application to sound synthesis of gongs and cymbals, Journal of Sound and Vibration, vol. 344, 313-331, 2015.

[14] Q-B. Nguyen and C. Touzé : Nonlinear vibrations of thin plates with variable thickness : application to sound synthesis of cymbals, Journal of the Acoustical Society of America, 145(2), 977-988, 2019.

Non linear vibration of strings against obstacles in plucked string instruments

J-L. Le Carrou[1], C. Issanchou[1,2], C. Touzé[2] and O. Doaré[2]

[1]Sorbonne Université, CNRS, Institut ∂'Alembert, Equipe Lutheries-Acoustique-Musique
Paris, France
jean-loic.le_carrou@sorbonne-universite.fr

[2]IMSIA, ENSTA ParisTech-CNRS-EDF-CEA
Palaiseau, France

Abstract Contacts occurring during the string vibration provide a non linear effect which shapes a specific tone and contributes to the sound identity of the instrument. A conservative scheme based on a modal representation of the string displacement is presented, allowing the simulation of a stiff, damped string vibrating against an obstacle with an arbitrary geometry. Applications on the tanpura and the medieval harp with one contact point and on the electric bass with numerous contact points are proposed.

Collisions in musical string instruments play a fundamental role in the sound production in numerous instruments. These collisions are either expected, for specific musical instruments design or instrumentalist gesture, or undesired and related to adjustment issues. Taking into account these collisions is then essential to insure the realism of the sound simulation of musical instruments. An abundant literature [1] exists on numerical simulations of a string vibrating against an obstacle but a few studies include the two transverse polarisations, physical parameters of the string and a comparison with experimental data. The talk aims at presenting a numerical tool to simulate musical strings vibrating against a unilateral distributed obstacle, and confronting it to experiments in detail for various instruments.

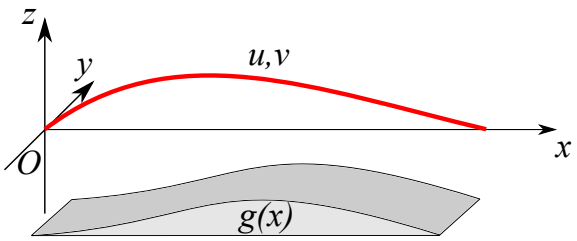

Figure 1: Drawing of a string vibrating against a unilateral obstacle described by $g(x)$.

The numerical method is based on a modal description of the string considered stiff, damped and simply supported at both ends [2]. The string collides with an obstacle having a profile $g(x)$ which is constant along (Oy). The contact force is modeled by a penalty approach where a small amount of interpenetration is allowed. Note also that an alternative modeling using nonsmooth numerical integration has also been investigated [3], showing equivalent results for the considered cases. Along the (Oy)-polarisation, a friction force is selected as a regularized empirical Tresca friction law [4]. In order to take into account the vibrations of the instrument body, the mobility at the string ends is then added to complete the model. In the case of solid-body electric guitars and basses, it has been shown that the bridge mobility is negligible as compared to that at the nut [5].

For the experimental approach, the mobility at the nut and the string characteristics (modal parameters, damping, stiffness) have to be obtained to feed the numerical model. String characteristics are identified using the ESPRIT algorithm from the measured vibration of the string stretched on a frame guaranteeing rigid-end conditions [5]. In order to compare numerical results to experimental ones, both displacements along (Oz) and (Oy) are recorded simultaneously, with optical sensors calibrated according to the procedure described in [6]. The profile $g(x)$ is also measured using a ruler or an optical profilometer. The initial condition is provided by pulling the string with a copper wire until it breaks.

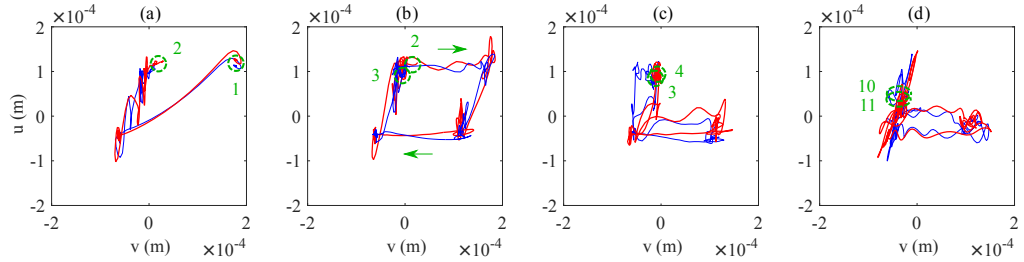

Figure 2: String displacement in the plane (Oyz) at x=854 mm and at y=845 mm, showing two u and v components. Blue: experiments, Red: numerics for four oscillation periods: 1 to 2 (a); 2 to 3 (b); 3 to 4 (c) and 10 to 11 (d) [1]

In figure 2 is shown an example of a very good agreement between numerical and experimental data measured on an electric bass. The friction force was adjusted empirically. As we can see in this figure, numerical and experimental string displacements overlap at each time step from the first period of oscillation to the tenth after colliding many times with 20 frets.

During the talk, other examples will be shown on the tanpura, the medival harp and the electric bass to understand their specific sound and to see how numerical simulations can be used as a tool for helping instrument makers to adjust or design musical instruments.

References

[1] C. Issanchou. Vibrations non linaires de cordes avec contact unilatral. Application aux instruments de musique. Thse de doctorat de l'Universit Pierre et Marie Curie. 2017

[2] C. Issanchou, S. Bilbao, J-L. Le Carrou, C. Touzé and O. Doaré, *A modal-based approach for the non linear vibration of strings against a unilateral obstacle: simulations and experiments in the pointless case*, Journal of Sound and Vibration 393, 229-251, 2017.

[3] C. Issanchou, V. Acary, F. Pémignon, C. Touzé and J-L. Le Carrou, *Nonsmooth contact dynamics for the numerical simulation of collisions in musical string instruments*. Journal of the Acoustical Society of America 143(5), 3195-3205, 2018.

[4] C. Issanchou, J-L. Le Carrou, C. Touzé, B. Fabre and O. Doaré, *String/frets contacts in the electric bass sound: Simulations and experiments*, Applied Acoustics 129, 217-228, 2018.

[5] A. Paté, J-L. Le Carrou and B. Fabre, *Predicting the decay time of solid body electric guitar tones*. Journal of the Acoustical Society of America 135(5), 3045-3055, 2014.

[6] J-L. Le Carrou, D. Chadefaux, L. Seydoux et B. Fabre. *A low-cost high-precision measurement method of string motion*. Journal of Sound and Vibration 333(17), 3881-3888, 2014.

From the bifurcation diagrams to the ease of playing of reed musical instruments. Application to a reed-like instrument having two quasi-harmonic resonances

J. Gilbert[1], **S. Maugeais**[2] **and C. Vergez**[3]

[1]Laboratoire d'Acoustique de l'Université du Mans - UMR 6613 CNRS
Le Mans, France
joel.gilbert@univ-lemans.fr

[2]Laboratoire Manceau de Mathématiques - Le Mans Université
Le Mans, France
sylvain.maugeais@univ-lemans.fr

[3]Aix-Marseille Univ, CNRS, Centrale Marseille, LMA, UMR 7031
Marseille, France
vergez@lma.cnrs-mrs.fr

Abstract A reed-like instrument having two quasi-harmonic resonances, represented by a 4-dimensional dynamical system, is studied using the continuation and bifurcation software AUTO. Bifurcation diagrams are explored with respect to the blowing pressure, with focus on amplitude and frequency evolutions along the different solution branches.

Wind musical instruments are nonlinear dynamical systems with a large diversity of oscillating behaviours. Among these, musicians know how to control their instrument in order to select periodic oscillating regimes, which correspond to notes when their frequency is properly adjusted. Understanding the conditions required to obtain the desired oscillating regime, in terms both of control by the musician and of the acoustic properties of the instrument is an interesting and intricate problem of nonlinear dynamics. In this study we focus on reed instruments. The use of the AUTO continuation package allows to revisit and extend the analytical approach proposed in [1].

Reed musical instruments can be described in terms of conceptually separate linear and nonlinear mechanisms: a localized nonlinear element (the valve effect due to the reed) excites a linear, passive acoustical multimode element (the musical instrument usually represented in the frequency domain by its input impedance). The linear element in turn influences the operation of the nonlinear element. The reed musical instruments are self-sustained oscillators. They generate an oscillating acoustical pressure (the note played) from a static overpressure in the player's mouth (the blowing pressure).

A reed instrument having N acoustical modes can be described as a $2N$-dimensional autonomous nonlinear dynamical system [2]. For instance a reed-like instrument having two quasi-harmonic resonances, represented by a 4-dimensional dynamical system, is considered in this study, in order to be able to use the AUTO continuation method. The modulus of the corresponding acoustic input impedance of the resonator is shown in figure 1. The acoustic input impedance is defined in the frequency domain by the ratio between the pressure and the volume flow at the input of the instrument, so that :

$$P(\omega) = Z(\omega)U(\omega), \qquad \text{where } \omega \text{ is the angular frequency.} \tag{1}$$

On the other hand, the reed-valve nonlinear behaviour can be modelled by the following polynomial nonlinearity in the time domain, where the volume flow $u(t)$ is defined as a function of the acoustic pressure $p(t)$ [2]:

$$u = u_0 + Ap + Bp^2 + Cp^3, \tag{2}$$

where u_0 is the mean volume flow and A, B and C are real numbers that depend on the control of the musician.

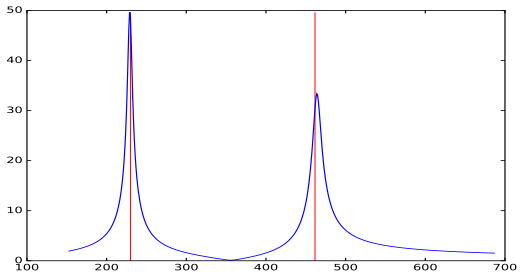

Figure 1: Modulus of the dimensionless input impedance of the resonator with respect to frequency. The two resonances are quasi-harmonic: first resonance frequency $229Hz$ (left red vertical line), second resonance frequency $463.5Hz$ slightly higher than the octave $458Hz$ (right red vertical line), corresponding to an inharmonicity of 0.012.

Bifurcation diagrams are explored with respect to the blowing pressure, with focus on amplitude and frequency evolutions along the different solution branches (see examples on figure 2). The ratio between the two acoustic resonance frequencies of the instrument (also called inharmonicity) appears to be of crucial importance.

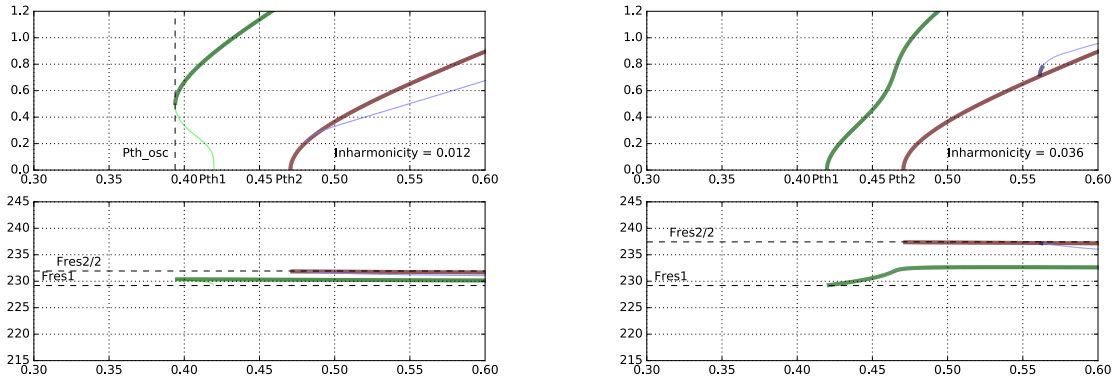

Figure 2: Bifurcation diagrams corresponding to the case of an input instrument with a 1^{st} peak 50% larger than the 2^{nd} one, like in figure 1. The ratio between the two resonance frequencies is 2.024, inharmonicity 0.012 (left) or 2.072, inharmonicity 0.036 (right). Top plots represent the amplitude of the periodic oscillation branches with respect to the blowing pressure. Bottom plots represent the frequency of the corresponding periodic solutions with respect to the blowing pressure. Green (red) lines correspond to periodic oscillations resulting from the instability of the first (second) acoustic resonance and are called 1^{st} and 2^{nd} registers respectively. Blue lines correspond to periodic oscillations of the 1^{st} register resulting from the period doubling of the 2^{nd} register.

The oral presentation will show how some of these results can be interpreted in terms of the ease of playing of the reed instrument.

References

[1] J-P. Dalmont, J. Gilbert and J. Kergomard, *Reed Instruments, from Small to Large Amplitude Periodic Oscillations and the Helmholtz Motion Analogy*, Acta Acustica united with Acustica, 86, 671-684, 2000.

[2] A. Chaigne, J. Kergomard, *Acoustics of Musical Instruments*, Springer, 2016.

Continuation of a physical model of brass instrument: application to trumpet categorization

V. Fréour[1], H. Masuda[1], S. Usa[1], E. Tominaga[1], Y. Tohgi[1], B. Cochelin[2] and C. Vergez[2]

[1]YAMAHA Corporation, R&D division, Hamamatsu, Japan
vincent.freour@music.yamaha.com

[2]Aix Marseille Univ., CNRS, Centrale Marseille, LMA UMR7031, Marseille, France
last@lma.cnrs-mrs.fr

Abstract The system formed by the couple {player - trumpet} falls into the class of non-linear dynamical systems likely to be studied using different numerical tools such as numerical continuation methods. In this study we illustrate the interest of this approach for the categorization of Bb trumpets in the space of some performance descriptors obtained from continuation by the ANM method combined to the Harmonic Balance Method (HBM).

The model considered is based on one-dimensional lip model, coupled to the resonator impedance described by a series of complex modes similar to what proposed in [1]. The coupling between the mechanical oscillator and the acoustic resonator is achieved by a Bernoulli flow equation, considering turbulent mixing in the mouthpiece with no pressure recovery [2]. The mechanical and acoustic equations are given in system 1, where y is the vertical lip position (y_0 is the lip position at rest), ω_l, Q_l, μ_l and b the mechanical lip parameters, s_k and C_k with $k \in [1, N]$ the modal parameters of the N resonances of the acoustic impedance of the instrument, Z_c the characteristic impedance, u the volume flow, p the downstream pressure at the input of the instrument (in the mouthpiece), and p_0 the upstream (mouth) static pressure.

$$\begin{cases} \ddot{y}(t) + \frac{\omega_l}{Q_l}\dot{y}(t) + {\omega_l}^2(y(t) - y_0) = \frac{1}{\mu_l}(p_0 - p(t)) \\ \dot{p}_k(t) = Z_c C_k u(t) + s_k p_k(t), \forall k \in [1, N] \end{cases} \tag{1}$$

with $p(t) = 2\sum_{k=1}^{N} \Re(p_k(t))$ and $u = \sqrt{\frac{2|p_0 - p|}{\rho}} b \cdot sign(p_0 - p) \cdot \theta(y)$, where $\theta(y) = \frac{|y|+y}{2}$, b is the lip width and ρ is the air density.

The case of a negative opening of the lips is managed by introducing the Heaviside function $\theta(y)$. The modal parameters of the N modes of the impedance are extracted from measured impedances, using the high resolution method ESPRIT [3].

The specificity of the approach proposed in this paper is based on combining the ANM method [4, 5] with the Harmonic Balance Method (HBM) for the search of periodic solutions of the system. The HBM allows to approximate the unknowns by truncated Fourier series. The new unknowns of the problem are the Fourier coefficients of each element of $\mathbf{U}$. For more details about the continuations of periodic solutions using ANM and HBM, the reader is invited to refer to [6].

The calculation of bifurcation diagrams of system 1 is performed using the Matlab library MANLAB developed at LMA[1]. The natural frequency of the lips $f_l = 2\pi\omega_l$ is set to excite the fourth regime of the instrument in open fingering (no valve pressed). In a first step the stationary solution of the system is calculated in order to identify a Hopf bifurcation from which a periodic solution emerges. This periodic solution is then followed by continuation using the method described previously. A bifurcation diagram obtained for a Bb4 on a Bb trumpet is represented in Fig. 1.

[1] http://manlab.lma.cnrs-mrs.fr/

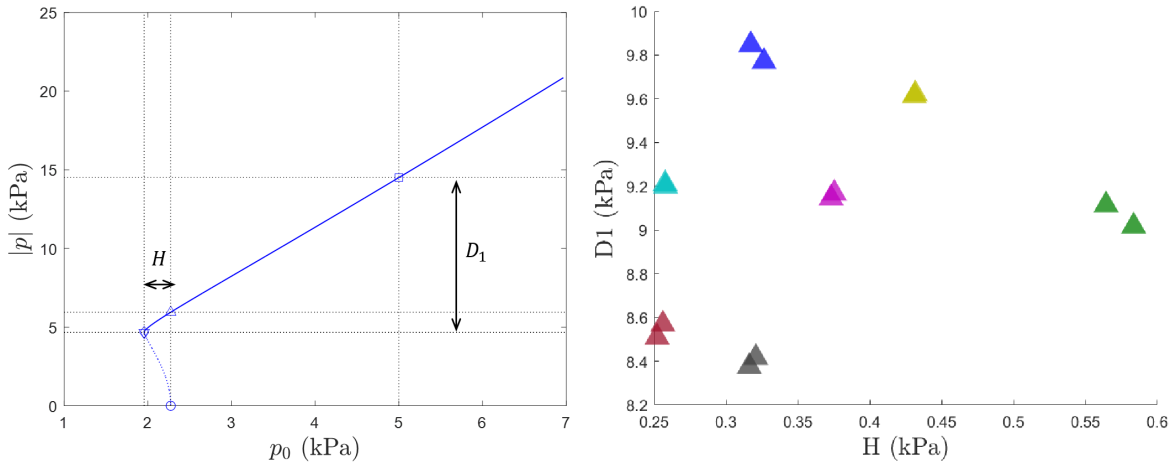

Figure 1: Left: bifurcation diagram of a Bb4 for a Bb trumpet: amplitude of the mouthpiece pressure p as a function of the static mouth pressure p_0. The dotted line indicates unstable portions of the branch, while the solid line indicates the stable branch. Right: categorization of trumpets in the (H, D_1) space. The different colors correspond to the different trumpets. To each trumpet, two points are associated, corresponding to two impedance measurements of the instrument.

The obtained diagram is characterized by an inverse bifurcation that induces an hysteresis H. A quantity D_1 associated to the dynamic range of p can also be defined from the stable part of the solution. By extracting H and D_1 on different trumpets, and locating the corresponding points in the (H, D_1) 2D space, the categorization represented in Fig. 1 is obtained. For each instrument, two impedance measurements are used for calculation. The categorization obtained clearly allows to differentiate instruments in the 2D space, showing the ability of the method to provide discriminating descriptors.

Acknowledgments

The authors would like to thank Louis Guillot for his precious support on the use of MANLAB.

References

[1] Silva, F., Vergez, C., Guillemain, P., Kergomard, J., and Debut, V., MoReeSC: A Framework for the Simulation and Analysis of Sound Production in Reed and Brass Instruments. *Acta Acustica united with Acustica*, **100**, 126-138, (2014).

[2] Elliot, S. J., and Bowsher, J. M., Regeneration in brass instruments. *Journal of Sound and Vibration*, **83**, 2, 181-217, (1982).

[3] Roy, R., and Kailath, T., Esprit: Estimation of signal parameters via rotational invariance techniques. *IEEE Trans. Acoust. Speech, Signal Process.*, **37**, 7, 984-995, (1989).

[4] Cochelin, B., Damil, N., and Poitier-Ferry, M., *Méthode asymptotique numérique*, Lavoisier, Cachan, France, (2007).

[5] Cochelin, B., A path-following technique via an asymptotic-numerical method. *Computers & structures*, **53**, 5, 1181–1192, (1994).

[6] Cochelin, B., and Vergez, C., A high-order purely frequency based harmonic balance formulation for continuation of periodic solutions. *Journal of Sound and Vibration*, **324**, 243-262, (2009).

NES & TET

Thursday, 4th July 2019

Chairman: G. Kerschen

Design criterion and finite element analysis of pure cubic system

A. Zhenhang WU[1], B. Sébastien SEGUY[1], C. Manuel PAREDES[1] and D. Donghai QIU[2]

[1] Institut Clément Ader (ICA), CNRS-INSA-ISAE-Mines Albi-UPS
Université de Toulouse, France
zhenhang.wu@insa-toulouse.fr
sebastien.seguy@insa-toulouse.fr
manuel.paredes@insa-toulouse.fr

[2] Suzhou Institute of Biomedical Engineering and Technology
Chinese Academy of Sciences, Suzhou, China
qiudh@sibet.ac.cn

Abstract The purpose of this abstract is to report a novel design of pure cubic stiffness system and general methodology to parameterize variable pitch spring. The performance of the improved design will be tested by finite element analysis (FEA).

In the studies of machining accuracies, devices that work under complex load conditions, and comfort, to name a few, vibration mitigation, is an inevitable issue. The traditional vibration absorber can be divided into three types: passive, active, and semi-active. Among these, the passive absorber Nonlinear Energy Sink (NES) attracts researcher's attention because of its lighter attachment and performance in a broader band of frequency.

This type absorber is characterized by a damped linear oscillator coupled to an essentially nonlinear attachment. When the NES meets certain conditions, such as proper mass ratio, nonlinear stiffness, and external excitation, it can be activated [1]. There exists regimes of the quasi-periodic response and leads to a passive irreversible transfer of primary structural energy (referred as energy pumping) towards secondary highly coupled mass via a nonlinear element [2].

The mastery of nonlinearity is a key issue to obtain the optimal vibration absorption performance. To obtain an optimally strong nonlinearity, a generalized methodology for designing a novel Nonlinear Energy Sink was established [3].

Firstly, a designed parameterization of variable pitch spring is implemented. Accordingly, the objective nonlinear Force-displacement function was divided into sections, whose stiffness were considered to be constant. The core of generating a variable pitch spring is adjusting its variable active coils during the compression. A symmetrical design method is applied to overcome the inaccuracy in the end of curve fitting.

Secondly, it is very challenging to produce a purely cubic stiffness by using variable pitch spring directly i.e., without a linear part (Figure 1). In order to overcome this shortcoming, two important steps were implemented: 1) a method of axial combination of two variable pitch springs and pre-compression at transition point was proposed. This produced the force polynomial component with only linear terms and cubic terms. 2) With the help of a negative stiffness mechanism that was designed with an axial coincidence having two cylindrical springs whose direction of movement is perpendicular to their axis. This mechanism can counterbalance the linear term and obtain the pure cubical stiffness.

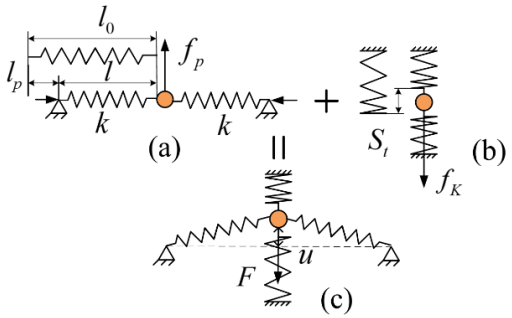

Figure 1: Detailed realization of NES system.

A finite element model of variable pitch spring was built by optimizing the geometry, adjusting and refining the mesh type, resetting the boundary conditions to carry out simulations (Figure 2). These parameters of simulations were adjusted to closely match the theoretical results. The current simulation results show that Abaqus can effectively simulate the compression characteristics of variable pitch springs (Figure 3)

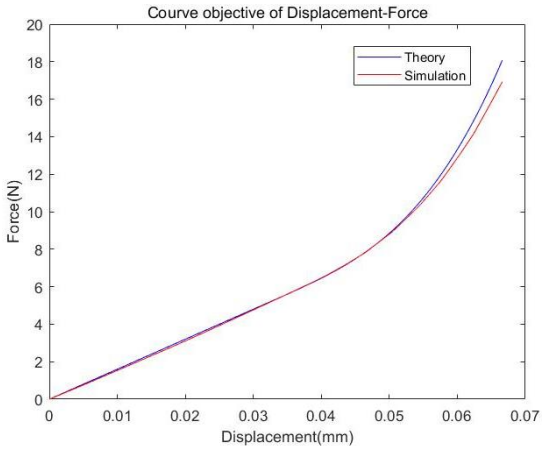

Figure 2: 3D model of variable pitch spring Figure 3: Comparison of theory and simulation

In the future, the following steps will be carried out：

1) Complete analysis of the whole system. Study the error between model predictions and experiments.

2) Study the dynamic behaviour of models in Abaqus, and investigate the possibility to simulate the phenomena of energy pumping.

After verifying the effectiveness of finite element models, we will develop an optimized NES system by experimentation with the aim towards industrial applications.

References

[1] Starosvetsky, Y., & Gendelman, O. V. (2010). *Bifurcations of attractors in forced system with nonlinear energy sink: the effect of mass asymmetry.* Nonlinear Dynamics, 59(4), 711-731.

[2] Bellet, R., Cochelin, B., Herzog, P., & Mattei, P. O. (2010). *Experimental study of targeted energy transfer from an acoustic system to a nonlinear membrane absorber.* Journal of Sound and Vibration, 329(14), 2768-2791.

[3] Qiu, D., Paredes, M., & Seguy, S. (2019). *Variable pitch spring for nonlinear energy sink: Application to passive vibration control.* Proceedings of the Institution of Mechanical Engineers, Part C: Journal of Mechanical Engineering Science, 233(2), 611-622.

Bistable nonlinear energy sink dynamics via high-dimensional invariant manifolds

G. Habib[1] **and F. Romeo**[2]

[1]Dept. of Applied Mechanics, Budapest University of Technology and Economics
Budapest, Hungary
habib@mm.bme.hu

[2]Dept. of Structural and Geotechnical Engineering, Sapienza University of Rome
Rome, Italy
francesco.romeo@uniroma1.it

Abstract A bistable nonlinear energy sink, conceived to mitigate the vibrations of a multi-degree-of-freedom host mechanical system, is considered. Under impulsive excitation, the invariant manifolds describing the high amplitude slow dynamics are generalised. Results illustrate that the absorber is generally unable to resonate with more than one mode of the primary system at a time, experiencing instead a sort of "modal cascade" from higher to lower modes.

Nonlinear vibration absorbers, designed to resonate for broad frequency band, have received considerable attention in the last decade. A wide spectrum of nonlinearity sources have been so far addressed, encompassing a variety of excitations, host structure typology, design constraints and objectives [1,2]. Within this context the nonlinear energy sink (NES), consisting of a small mass connected to the primary system by an essential nonlinear spring, has been extensively studied. Recently, the NES capabilities for the mitigation of broadband impulsive energy was studied by the authors exploiting the four-dimensional invariant manifold of a two-DoF host system [3]. Stemming from the latter study, a bistable NES (BNES) connected to a multi-degree-of-freedom (MDOF) system is here considered. Invariant manifolds describing the high amplitude slow dynamics are analytically identified. These consist in high dimensional surfaces, which relate the absorber vibration amplitude to the primary system ones.

The dynamics of the BNES attached to an undamped linear n-DOF primary system is modelled by the following system of differential equations

$$\begin{aligned}
&\sum_{j=1}^{n} m_{ij}\ddot{x}_j + \sum_{j=1}^{n} k_{ij}x_j = 0 \quad \text{for } i = 1,...,n,\ i \neq l \\
&\sum_{j=1}^{n} m_{lj}\ddot{x}_j + \sum_{j=1}^{n} k_{lj}x_j - k_a\left(x_l - x_{n+1}\right) + c_a\left(\dot{x}_l - \dot{x}_{n+1}\right) + k_{nl}\left(x_l - x_{n+1}\right)^3 = 0 \\
&m_a\ddot{x}_{n+1} + c_a\left(\dot{x}_{n+1} - \dot{x}_l\right) - k_a\left(x_{n+1} - x_l\right) + k_{nl}\left(x_{n+1} - x_l\right)^3 = 0,
\end{aligned} \tag{1}$$

where $m_{ij} = m_{ji}$ and $k_{ij} = k_{ji}$ are the primary system mass and stiffness matrices terms, m_a is the absorber mass, k_a, c_a and k_{nl} are the absorber negative linear stiffness, linear damping and cubic stiffness coefficients. m_a is assumed small with respect to the primary system masses.

We perform a modal analysis according to the primary system modes and we scale amplitudes by the absorber nonlinearity. Then, aiming at characterizing the behavior of the BNES against impulsive excitation, the invariant manifolds describing the high amplitude slow dynamics are identified, following the procedure adopted in [3]. The obtained invariant manifolds have the form

$$v_{li}^2\omega_{ni}^4 a_i^2 = b_i^2\left(\omega_{ni}^2 + \omega_a^2 + \frac{3}{4}b_i^2 - \frac{3}{2}\sum_{i=1}^{n} b_j^2\right)^2 + 4\zeta_a\omega_a^2\omega_{ni}^2 b_i^2 \quad \text{for } i = 1,...,n \tag{2}$$

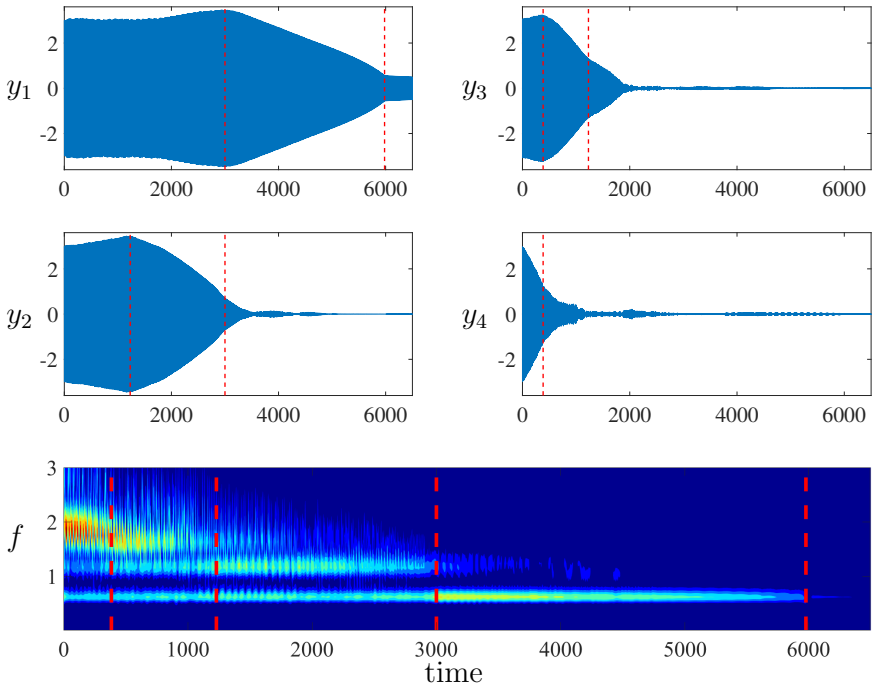

Figure 1: Time series for a 4-DoF primary system with an attached BNES. y_1, y_2, y_3, y_4 indicate modal amplitudes and f the absorber relative displacement wavelet transformation.

where a_i is the vibration amplitude of the i^{th} mode in the primary system, while b_i is the relative vibration amplitude of the absorber with frequency ω_{ni}, ω_{ni} are the primary system natural frequencies, v_{lj} are terms of the transformation matrix utilized for the modal analysis, $\zeta_a = c_a/(2m_a\omega_a)$ and $\omega_a^2 = k_a/m_a$.

Results illustrate that the BNES, although is capable of interacting with all modes of the primary system, it is generally unable to resonate with more than one mode of the primary system at the same time. It experiences instead a sort of "modal cascade", dissipating first energy of higher modes and then of lower ones. Modal interaction between the absorber and more than one mode of the primary system seems to be possible only at very specific energy levels. This is clearly illustrated in Fig. 1 for a 4-DOF primary system. The figure shows how modal energy of the 4^{th} mode is first dissipated (y_4). Then, the BNES disengages from the 4^{th} mode and starts interacting with y_3 ($t \approx 385$, first vertical dashed line), until it disengages also from y_3 and interacts with y_2 ($t \approx 1230$, second vertical dashed line). The process goes on until energy is dissipated on the lowest mode. At $t \approx 6000$ the energy level is so low that the BNES is confined to oscillate in-well.

References

[1] A.F. Vakakis, *Shock isolation through the use of nonlinear energy sinks*, Modal Analysis 9, 7993, 2003.

[2] Y. Starosvetsky and O.V. Gendelman, *Vibration absorption in systems with a nonlinear energy sink: nonlinear damping*, Journal of Sound and Vibration 324, 916-939, 2009.

[3] G. Habib and F. Romeo, *The tuned bistable nonlinear energy sink*, Nonlinear Dynamics 89, 179-196, 2017.

Nonlinear energy pumping in Acoustics using multistable absorbers

I. Bouzid[1,2], R. Côte[1] and P.-O. Mattei[1]

[1]Aix Marseille Univ, CNRS, Centrale Marseille, LMA
Marseille, France
bouzid@lma.cnrs-mrs.fr, cote@lma.cnrs-mrs.fr, mattei@lma.cnrs-mrs.fr

[2]Ecole Nationale d'Ingénieurs de Sfax
Sfax, Tunisie
islem.bouzid@enis.tn

Abstract This work addresses the development of a vibroacoustics nonlinear absorber based on the concept of a Nonlinear Energy Sink (NES) under multi-stable configuration. Numerical experiments show that adding a bistable property to a NES permits to lower its activation threshold compared to NESs with only one stable position.

Since the seminal papers by Vakakis *et al* [1, 2], energy pumping has become a subject of growing interest. Despite highly efficient energy dissipation, the main drawback is that the higher the frequency of the primary linear system to control, the higher the amplitude for activation of non linear passive dissipation. Recent theoretical and numerical works by Manevitch *et al* [3], Romeo *et al* [4] and experimental work by Mattei *et al* [5] showed that a bi-stable NES (B-NES) provides improved robustness in frequency and amplitude range over existing NESs by lowering the activation threshold. This work aims at improving the absorber developed by R. Bellet *et al* [6]. The developed absorber is made of a high amplitude vibrating membrane that is described by linear and cubic stiffnesses and a dissipation described by linear and quadratic terms. The bistable NES developed in this work can be described by linear quadratic and cubic stiffness terms. The presence of this quadratic damping conplexifies the theoretical analysis but doesn't prevent numerical experiments. The absorber equation developed in [6] is written as

$$m_m\ddot{q}(t) + k_1\left[(1+\chi)q(t) + \eta\dot{q}(t)\right] + k_3(2\eta q^2(t)\dot{q}(t) + q^3(t)) = S_m/(2h)p(t) \quad (1)$$

where $m_m = \rho_m h S_m/3$ is the dynamic membrane mass, S_m its section, η its viscous damping and $p(t)$ is the forcing term. The parameter $\chi = 3R^2e_0/h^2$ is the ratio between the pre-strain e_0 and the (strain) buckling load of the membrane and the coefficients k_1 and k_3 that respectively stand for the linear and nonlinear stiffnesses are defined as $k_1 \approx \frac{1.015^4\pi^5}{12}\frac{Eh^3}{3(1-\nu^2)R^2}, k_3 = 8\pi\frac{Eh^3}{3(1-\nu^2)R^2}$. It is worth noting that $1.015^4\pi^5/12 = 8.24 \approx 8$ and thus $k1 \approx k_3$. By denoting $1+\chi = -\zeta$ with $\zeta > 0$ for a buckled membrane, the Eq. (1) is then written as $m_m\ddot{q}(t) + k_1\left[-\zeta q(t) + q^3(t) + \eta(1+2q^2(t))\dot{q}(t)\right] = S_m/(2h)p(t)$. By the change of variable $q_m(t) = \sqrt{\zeta}(y(t)+1)$, one obtains a Helmholtz-Duffing like nonlinear equation for the buckled membrane, very similar to that obtained in [5]

$$\ddot{y}(t) + f_1^2\left[y(t) + 3/2\,y^2(t) + 1/2\,y^3(t) + \eta\left(1/(2\zeta) + (1+y(t))^2\right)\dot{y}(t)\right] = S_m/(2\sqrt{\zeta}hm_m)p(t) \quad (2)$$

where $f_1 = \sqrt{2\zeta k_1/m_m}$ is the linear frequency of the buckled membrane. Such an equation with a non-linearity of the form $y + 3/2y^2 + 1/2y^3$ possesses two stable equilibrium points (0 and -2) and one unstable (-1). We investigated the targeted energy transfer occurring between the acoustic medium (the one-dimensional tube of length L around its first acoustic mode) and the bistable membrane during both the sinusoidal forced regime and the free oscillations as proposed in [6]. Using non-dimensional quantities defined as $\tau = \omega t$, $\omega = c_0\pi/L$, and

$u = u_a 2S_t/(hS_m)$ if u_a is the acoustic velocity inside the tube and S_t its section, with the notations of [6], the two d.o.f. non-dimensional system is given by

$$\begin{aligned} \frac{d^2u(\tau)}{d\tau^2} + \lambda\frac{du(\tau)}{d\tau} + u(\tau) + \beta\left(u(\tau) - \sqrt{\zeta}(y(t)+1)\right) &= F\cos(\tfrac{\Omega}{\omega}\tau) \\ \gamma\sqrt{\zeta}\frac{d^2y(\tau)}{d\tau^2} + c_1\sqrt{\zeta}\left[\eta\omega\left(1+2\zeta(1+y(\tau))^2\right)\frac{dy(\tau)}{d\tau}\right. & \\ \left.+\zeta\left(2y(\tau)+3y(\tau)^2+y(\tau)^3\right)\right] - \beta\left(u(\tau) - \sqrt{\zeta}(y(t)+1)\right) &= 0 \end{aligned} \tag{3}$$

The numerical results for this system are compared to the numerical results for the system (22) given in [6]. The simulation had been obtained for the numerical values: $\lambda \approx 0.014$, $\beta \approx 0.12$, $\omega \approx 545$, $\Omega = 1.06\omega$, $\gamma \approx 1.73$, $\zeta = 10$, $\eta = 10^{-4}$, $c_1 = 0.04$, $c_3 \approx 0.036$, $f_1 = 57$ and $f_1/f_0 \approx 4.4$. The last three coefficients are used for the Bellet's model.The results are presented in Figure 1. It is worth noting that the classical membrane do not show any particular modulation while the bistable membrane show strongly modulated response which is characteristic of dissipation by NES. As the forcing are identical in the two cases, the threshold for energy pumping has been lowered by the bi-stable membrane.

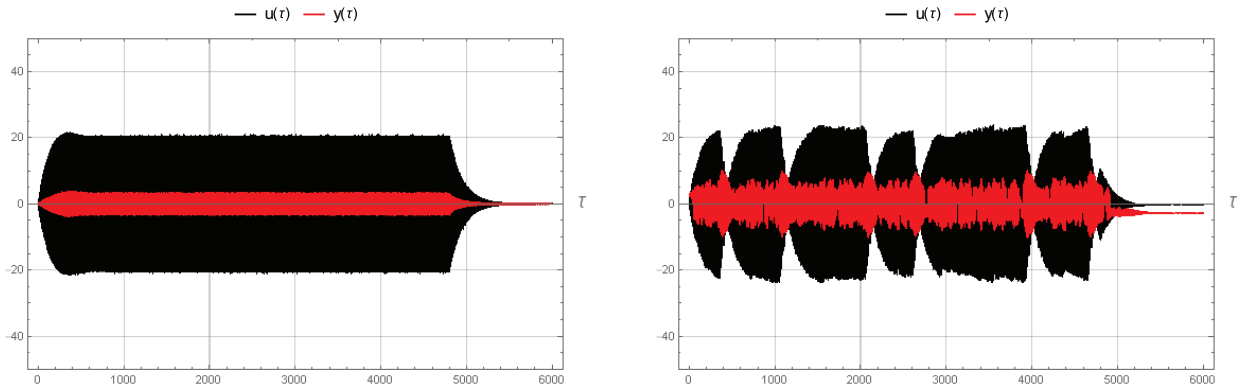

(a) (b)

Figure 1: Time response of the system (22) in [6] figure (a) and 3 figure (b). The forcing of amplitude $F = 13$ is stopped at $t = 4800$.

References

[1] O. Gendelman, L.I. Manevitch, A.F. Vakakis, R.M. Closkey, Energy Pumping in Nonlinear Mechanical Oscillators: Part I–Dynamics of the underlying Hamiltonian systems. ASME Journal of Applied Mechanics 68 (2011) 34-42. doi:10.1115/1.1345524.

[2] A.F. Vakakis, O.V. Gendelman, Energy Pumping in Nonlinear Mechanical Oscillators: Part II–Resonance Capture. ASME Journal of Applied Mechanics 68 (2011) 42-48. doi:10.1115/1.1345525.

[3] L.I. Manevitch, G. Sigalov, F. Romeo, L.A. Bergman, A. Vakakis, Dynamics of a Linear Oscillator Coupled to a Bistable Light Attachment: Analytical Study. ASME Journal of Applied Mechanics 81 (2014) 041011-1-9. doi:10.1115/1.4025150.

[4] F. Romeo, L.I. Manevitch, L.A. Bergman, A. Vakakis, Transient and chaotic low-energy transfers in a system with bistable nonlinearity. Chaos 25 (2015) 053109. doi:10.1063/1.4921193.

[5] P.-O. Mattei, R. Ponçot, M. Pachebat, R. Côte, Nonlinear Targeted Energy Transfer of Two Coupled Cantilever Beams Coupled to a Bistable light Attachment. Journal of Sound and Vibration 373 (2016) 29-51. doi.org/10.1016/j.jsv.2016.03.008

[6] R. Bellet, B. Cochelin, Ph. Herzog, P.-O. Mattei, Experimental study of targeted energy transfer from an acoustic system to a nonlinear membrane absorber. Journal of Sound and Vibration, 329(14):2768-2791. doi.org/10.1016/j.jsv.2010.01.029

Targeted nonlinear energy transfer for electroacoustic absorbers

D. Bitar[1,2], A. Ture Savadkoohi[1], E. Gourdon[1], C. H. Lamarque[1] and M. Collet[2]

[1]LTDS UMR CNRS 5513, Ecole Nationale des Travaux Publics de l'Etat, Univ Lyon
3 Rue Maurice Audin, 69518 Vaulx en Velin Cedex, France
diala.bitar@entpe.fr, alireza.turesavadkoohi@entpe.fr, emmanuel.gourdon@entpe.fr, claude-henri.lamarque@entpe.fr

[2]LTDS UMR CNRS 5513, Ecole Centrale de Lyon, Univ Lyon
36 avenue Guy de Collongue, 69134 Ecully Cedex, France
manuel.collet@ec-lyon.fr

Abstract An electroacoustic loudspeaker linearly coupled to an electric nonlinear shunt circuit acting as a nonlinear energy sink is considered. An analytical treatment enabling to analyze the behavior of the system around the 1:1 resonance at different time scales is performed. Extended form of Manevitch's complex variables is introduced, taking into account higher harmonics. Periodic and strongly modulated responses are well predicted.

We consider an electroacoustic loudspeaker, shunted to an electrical nonlinear circuit (cubic nonlinearity is chosen to use the nonlinear energy sink concept developed in [1]) and subjected to an external periodically varying sound pressure. The dynamics can be described by the following equations [2]:

$$\begin{cases} M_{ms}\ddot{\boldsymbol{x}}(t) + R_{ms}\dot{\boldsymbol{x}}(t) + C_{mc}^{-1}\boldsymbol{x}(t) - CBl\dot{\boldsymbol{V}}_{\boldsymbol{c}}(t) = SA_m\cos(\omega t), \\ C(L_e + L_c)\ddot{\boldsymbol{V}}_{\boldsymbol{c}}(t) + C(R_e + R_c)\dot{\boldsymbol{V}}_{\boldsymbol{c}}(t) + k\boldsymbol{V}_{\boldsymbol{c}}^{\boldsymbol{3}} + Bl\dot{\boldsymbol{x}}(t) = 0, \end{cases} \quad (1)$$

where $\boldsymbol{x}$ and $\boldsymbol{V_c}$ describe the small displacement of the loudspeaker membrane and the electrical potential applied to the capacitor in the nonlinear shunt circuit, with $\dot{\boldsymbol{x}}(t) = \frac{d\,\boldsymbol{x}(t)}{dt}$. M_{ms}, R_{ms} and C_{mc} are the mass, the mechanical resistance of the moving bodies and the equivalent compliance of the enclosed loudspeaker. Bl is the force factor of the transducer, B represents the magnetic field magnitude and l stands for the length of the wire in the voice coil. A_m stands for the pressure amplitude, ω the angular frequency and S the diaphragm area. From the electrical side, R_e and L_e are respectively the DC resistance and the inductance of the voice coil and $Bl\dot{\boldsymbol{V}}_{\boldsymbol{c}}(t)$ is the back electromotive force. R_c, L_c and C are the inductor, resistor and capacitance of the corresponding nonlinear shunt circuit. k is the nonlinear coefficient (related to the design of the electronic circuit). Then we introduce the following non-dimensional time variable $T = \omega_0 t$ with $\omega_0 = \sqrt{1/(M_{ms} + C_{mc})}$ and $\Omega = \omega/\omega_0$. We denote $\boldsymbol{x}'(t) = \frac{d\,\boldsymbol{x}(t)}{dT}$. Then, scaling of parameters is also done by considering their physical range and by expressing them in function of a small parameter $\varepsilon = L_e + L_c \ll 1$.

The Slow Invariant Manifold (SIM) of the system is generally obtained by treating the system (1) analytically after introducing the classical Manevitch's complex variables [3]. However, with the present system, we can show (by looking at results by direct numerical integration of the system) that the contribution of the third harmonic for $d\boldsymbol{V_c}/dT$ in the transient regime is not negligible and that the contribution of the third harmonic for $d\boldsymbol{x}/dT$ in the transient regime is

negligible. That is why we propose to extend the method by introducing higher harmonics of the present system:

$$\begin{cases} \boldsymbol{x}' + i\Omega\boldsymbol{x} = \varphi_{11}(T)e^{i\Omega T}, \\ \boldsymbol{V_c}' + i\Omega\boldsymbol{V_c} = \varphi_{21}(T)e^{i\Omega T} + \varphi_{23}(T)e^{3i\Omega T}. \end{cases} \quad (2)$$

We also write the complex variables into their polar form as $\varphi_{jm} = N_{jm}e^{i\delta_{jm}}$.

The analytical treatment allows to detect time multi-scale energy pumping between the primary system that describes the displacement of the loudspeaker and the shunt nonlinear circuit. It permits the detection of the SIM of the system at fast time scale, in addition to the equilibrium and fold singularities identification of the obtained reduced order system at slow time scales. Figure 1 (a) illustrates the fact that the extended method allows to better predict the SIM than the classical one.

Figure 1 (b) shows the normalized admittance according to frequency for different cases of coupling. The classical shunt optimal resistor permits a significant decrease in the normalized admittance with a perfect absorption at the resonance. However, this approach is limited to a narrow range of frequency with no possible broadening control of the bandwidth. In the vicinity of 1:1 resonance, an optimal response frequency of the system can be identified through a selected threshold. It corresponds to the maximum of energy that the primary system can reach during an energy exchange process with the NES. Thus, the optimal design defined in terms of normalized admittance is represented by the horizontal line. The added passive nonlinear shunt circuit allowed a significant decrease of the admittance, principally at the vicinity of the resonance frequency where the targeted energy transfer prevents the velocity to exceed a certain amplitude. Moreover, we can identify that the frequency bandwidth undergoes a 45% of relative increase.

(a) (b)

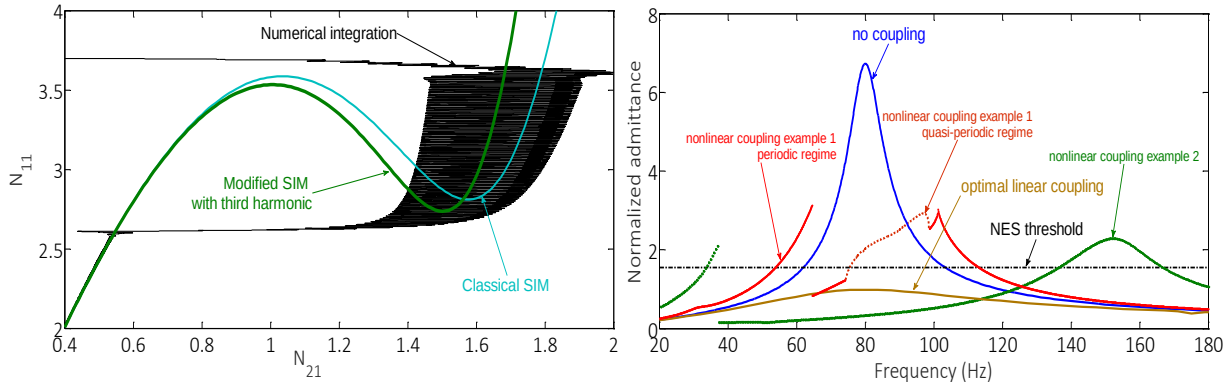

Figure 1: (a) Comparison between the analytical classical SIM, the new one obtained by ing into account the third harmonic and the direct numerical integration of the initial system; (b) Comparison of the normalized admittance as function of frequency between the cases of)pen circuit, optimal linear resonator and the shunt nonlinear circuits with two examples of nonlinear coupling (two different amplitudes for sound incident wave).

References

[1] A.F. Vakakis, O. Gendelman, L.A. Bergman, D.M. McFarland, G. Kerschen, Y.S. Lee. *Nonlinear Targeted Energy Transfer in Mechanical and Structural Systems*, Springer, Dordrecht, ISBN 978-1-4020-9125-4, 2009.

[2] D. Bitar, A. Ture Savadkoohi, C.-H. Lamarque, E. Gourdon and M. Collet. *Targeted nonlinear energy transfer for electroacoustic absorbers*. In Stefano Lenci and Ivana Kovacic, editors, IUTAM Symposium on Exploiting Nonlinear Dynamics for Engineering Systems. Springer, 2019.

[3] L. I. Manevitch. *The description of localized normal modes in a chain of nonlinear coupled oscillators using complex variables*. Nonlinear Dynamics, 25(1), 95-109, 2001.

Poster session 2

Thursday, 4th July 2019

Chairman: B. Cochelin

Predicting Frequency Response as Perturbation from the Conservative Limit

M. Cenedese and G. Haller

Institute for Mechanical Systems, ETH Zürich
Leonhardstrasse 21, 8092 Zürich, Switzerland
mattiac@ethz.ch georgehaller@ethz.ch

Abstract Conservative backbone curves are often observed to shape forced-damped frequency responses for multi-degree-of-freedom nonlinear vibratory systems. This relationship, however, is generally inferred a posteriori from experiments or numerical simulations. Here we discuss an analytic criterion to predict the bifurcation of frequency-amplitude plots from their conservative limits without assumptions on the amplitude or the number of degrees of freedom.

Conservative families of periodic orbits, or nonlinear normal modes, are commonly described in the analysis of nonlinear oscillations [1]. Among their properties, such oscillations are noted to act as backbones of forced-damped frequency responses. Analytic calculations supporting this observation are only available for specific, low-dimensional oscillators under the assumption of small response amplitudes.

Establishing a rigorous mathematical relation between conservative oscillations and frequency responses would have important numerical and experimental implications. Indeed, a qualitative description of the frequency response starting from conservative backbone curves would avoid computationally expensive simulations for several parameters value or shapes of the dissipative contributions. Moreover, there are experimental routines (e.g. force appropriation, [2]) that explicitly rely on the observed relation between conservative backbone curves and forced response, thus an analytic criterion could determine the range of applicability of such methods.

In this contribution, we clarify the persistence and bifurcations of conservative periodic orbits under small non-conservative perturbations [3]. We reduce the problem to the analysis of a bifurcation function that turns out to be the classic subharmonic Melnikov function [4]. When our analysis is applied to mechanical systems featuring pure forcing and arbitrary dissipative terms, it proves that either two, one or no isochronous or isoenergetic periodic orbit can arise from the conservative limit.

As an example, we apply this generalized Melnikov method to a three-degree-of-freedom system whose equations of motion read:

$$\begin{cases} \ddot{q}_1 + 3q_1 - q_2 - 0.75q_1^3 + 0.25q_1^5 = f_0\cos(\omega t) - 0.005(3\dot{q}_1 - \dot{q}_2) \\ \ddot{q}_2 + 3q_2 - q_1 - 2q_3 = -0.005(3\dot{q}_2 - \dot{q}_1 - 2\dot{q}_3) \\ \ddot{q}_3 + 4q_3 - 2q_2 + 0.5q_3^3 = -0.01(2\dot{q}_3 - \dot{q}_2) \end{cases} \qquad q = \begin{pmatrix} q_1 \\ q_2 \\ q_3 \end{pmatrix} \quad . \quad (1)$$

Linearization around the origin reveals that three families of periodic orbits emanate from the origin under zero forcing and damping terms are zero. By analyzing each conservative orbit family separately, we obtain rigorous predictions for the frequency response as illustrated in the left plot of Figure 1. Using different colors for each mode, we depict the analytic relation between the maximum of the frequency response and the forcing parameter. Such relation can be extracted identifying limit points of a suitable bifurcation function evaluated using conservative trajectories only. Moreover, when these trajectories have lower amplitudes then the maximum value, two orbits laying the frequency response with the same energy bifurcate from the conservative limit, while no solution persists for higher amplitudes. We illustrate

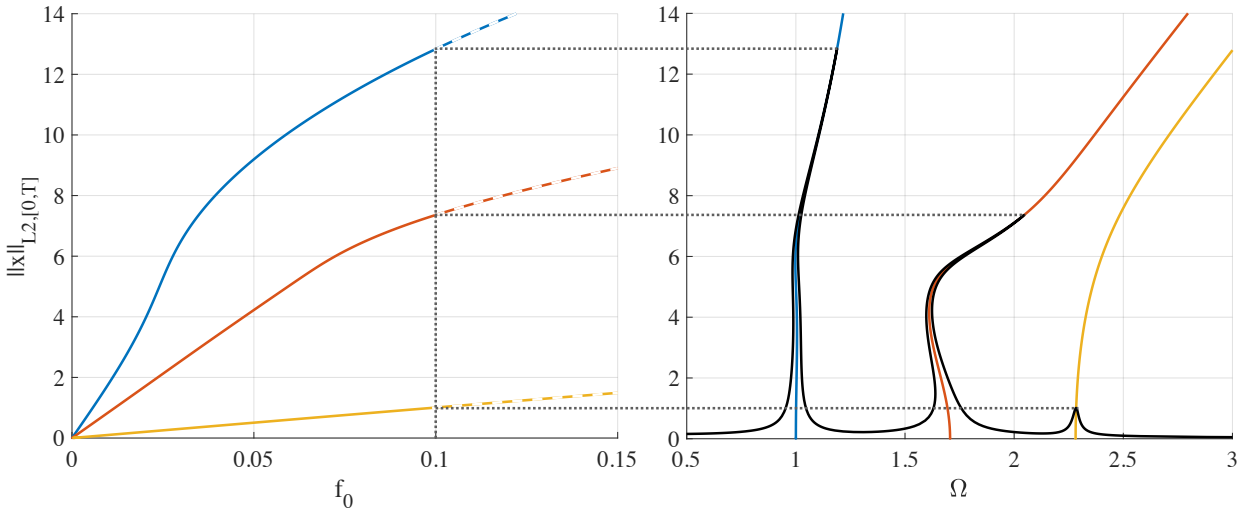

Figure 1: Left: analytic relation between the maximum value in the frequency response of the L_2-norm of the full trajectory $x = (q, \dot{q})$ and the forcing amplitude obtained from a Melnikov analysis of conservative nonlinear normal modes for the three modes; mode 1 in blue, mode 2 in orange and mode 3 in yellow. Right: the black line depicts a frequency response simulation with $f_0 = 0.1$ including three colored lines for the conservative backbone curves. The frequency is normalized with that of the first linear mode. The analytic predictions are also carried over from the left plot using gray dotted lines.

this behavior using solid and dashed lines respectively, selecting maximal modal amplitudes corresponding to $f_0 = 0.1$. Our predictions are confirmed in the right plot of Figure 1 where the black line illustrates the frequency response computed with numerical continuation. This plot is completed with conservative backbone curves with the same colors used for the left plot. Our conclusions assume that the non conservative terms are small enough and that there is no interaction between single modes.

References

[1] G. Kerschen, M. Peeters, J.C. Golinval, and A.F. Vakakis. Nonlinear normal modes, part I: A useful framework for the structural dynamicist. *Mechanical Systems and Signal Processing*, 23(1):170 – 194, 2009.

[2] M. Peeters, G. Kerschen, and J.C. Golinval. Dynamic testing of nonlinear vibrating structures using nonlinear normal modes. *Journal of Sound and Vibration*, 330(3):486 – 509, 2011.

[3] M. Cenedese and G. Haller. How do conservative backbone curves perturb into forced responses? A Melnikov's function approach. *Preprint*, 2019.

[4] V.K. Melnikov. On the stability of a center for time-periodic perturbations. *Tr. Mosk. Mat. Obs.*, 12:3 – 52, 1963.

Modelling, Exploration and Mitigation of Partially Liquid-Filled Tanks Using Various Passive Energy Absorbers

Maor Farid and Oleg Gendelman

Faculty of Mechanical Engineering, Technion – Israel Institute of Technology

Haifa, Israel

maorfarid@gmail.com

Abstract This study treats oscillations of a liquid in partially filled vessel under horizontal harmonic ground excitation. Such excitation may lead to hydraulic impacts applied on the tank walls. Different equivalent mechanical models are suggested to mimic the most essential sloshing regimes of the overall tank-liquid system. Then, the contribution of Nonlinear Energy Sink (NES) to the overall system mitigation is firstly examined.

We introduce the equivalent mechanical model for liquid sloshing in cylindrical tank with the well explored TMD attached **[1]**. Parameters *K* and *C* are modal stiffness and damping of the vessel fundamental (1,1) beam-type mode, respectively. The tank is of radius *R* and height *H* and exposed to arbitrary external excitation of u_g.

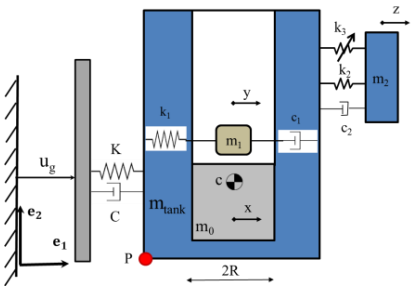

Figure 1: Scheme of cylindrical tank with liquid interacting with structure walls, and attached TMD

The liquid static and dynamic portions heights and the combined tank-static liquid portion center of gravity height are denoted by h_0 and h_1, respectively. Parameters k_2 and k_3 represent the coupling stiffness associated with the TMD and NES, respectively. c_2 is the linear damping coefficient. The PEA installation height h_2 is determined by the designer. Masses $m_{\tan k}$ and m_0 are the tank shell mass and the liquid 'static' portion mass, respectively. The sloshing dynamics combines infinite number of sloshing modes with mass of m_n. However, as shown by Abramson **[2]**, the modal mass decreases rapidly with increasing mode number. Then, to reveal most important aspects of dynamics, one can take into account only the first sloshing mode and the static-like portion of the fluid in the mechanical equivalent model, as long as the excitation frequency is far from the natural frequencies of the higher modes. The normalized displacement coordinate of the sloshing mass *m* with respect to the tank axis is denoted by v. Impact takes place for the absolute value of v reaches unity. The liquid-structure interaction involves energy dissipation due to wave breaking and fluid viscosity, which exhibits VI behavior. Interaction between the sloshing mass and the tank walls is described by a strongly nonlinear power-form forces with high exponents potential and dissipation force

functions **[3-5]**, fully-defined by empirical positive integers, which are going to be assessed both numerically and experimentally. Seismically-induced tank failure modes are explained extensively by Maekawa **[6]**. Based on the ROM, Von-Mises equivalent stresses were calculated in the tank critical point **P**. We separately apply both the well-known TMD and the cubic NES as vibration mitigation solutions. The following equations of motion are obtained for the overall tank-PEA system:

$$\begin{aligned}
&\ddot{u}+u+\varepsilon_1 v+Z\dot{u}+\varepsilon_1 Z\dot{v}-\varepsilon_2(1+\varepsilon_1)\beta_2^2 w-\varepsilon_2\kappa_2 w^3-2\varepsilon_2\beta_2\zeta_2\dot{w}=-\frac{(1+\varepsilon_1)^2}{R\Omega^2}u_{g,tt}(t)\\
&\ddot{v}+u+\left(\varepsilon_1+(1+\varepsilon_1)^2\beta_1^2\right)v+Z\dot{u}+\left(\varepsilon_1 Z+2(1+\varepsilon_1)\beta_1\zeta_1\right)\dot{v}-\varepsilon_2(1+\varepsilon_1)\beta_2^2 w-\varepsilon_2\kappa_2 w^3-2\varepsilon_2\beta_2\zeta_2\dot{w}+(1+\varepsilon_1)\kappa v^{4n+1}+(1+\varepsilon_1)\lambda\dot{v}v^{2n}=0\\
&\ddot{w}-u-\varepsilon_1\left(1+(1+\varepsilon_1)\beta_1^2\right)v+(1+\varepsilon_1)(1+\varepsilon_2)\beta_2^2 w+(1+\varepsilon_2)\kappa_2 w^3-Z\dot{u}-\varepsilon_1(Z+2\beta_1\zeta_1)\dot{v}+2(1+\varepsilon_2)\beta_2\zeta_2\dot{w}-\varepsilon_1\kappa v^{4n+1}-\varepsilon_1\lambda\dot{v}v^{2n}=0
\end{aligned} \quad (1)$$

While the TMD is examined, we take $\kappa_2=0$, when κ_2 is the parameter associated with the coupling between the NES and the tank structure, and in the same manner, when the NES is examined, we take $\beta_2=0$. The performances of both PEAs are evaluated with the help of two criteria; stress reduction and time of vibration decay. At this stage, the PEAs optimization is performed numerically; the TMD with mass about 10% of the total mass of the system allows up to 40% stress level reduction and 95% reduction of characteristic decay time in conditions of an optimal tuning.

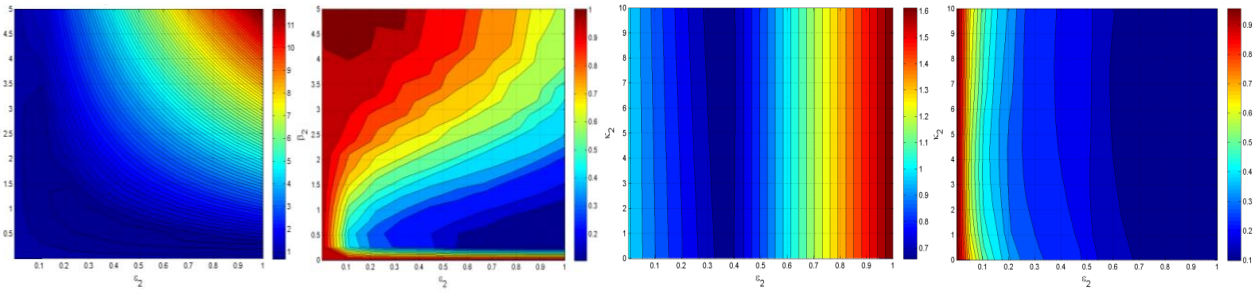

Figure 2: Example of performance optimization graph for impulsive excitation vs. PEA design parameters (stiffness and dissipation): from left to right: TMD optimization graph with respect to stress mitigation and time of decay, respectively; cubic NES optimization graph with respect to identical evaluation criteria.

Conclusions ROM is used to describe main most hazardous dynamical regimes taking place in cylindrical tank subjected to horizontal ground excitation, and internal impact regime on particular. Additional TMD and NES vibration mitigation performances were primarily examined and exhibit promising results, in term of both decay time and stresses mitigation in the tank critical location.

References

[1] J.P. Den Hartog, *Mechanical Vibrations*, 1985.
[2] H.N. Abramson, *The Dynamic Behavior of Liquids in Moving Containers*. NASA SP-106, NASA Spec. Publ. 106 (1966).
[3] V.N. Pilipchuk, R.A. Ibrahim, *The dynamics of a non-linear system simulating liquid sloshing impact in moving structures*, J. Sound Vib. 205 (1997) 593–615.
[4] V. Babitsky, *Theory of vibro-impact systems and applications*. Springer Science & Business Media, 2013
[5] M.A. El-Sayad, S.N. Hanna, R.A. Ibrahim, *Parametric Excitation of Nonlinear Elastic Systems Involving Hydrodynamic Sloshing Impact*, Nonlinear Dyn. 18 (1999) 25–50.
[6] A. Maekawa, *Recent Advances in Seismic Response Analysis of Cylindrical Liquid Storage Tanks*, INTECH Open Access Publisher (2011).

Experimental observation of localisation in a symmetric structure with non-smooth nonlinearities

F. Fontanela[1], A. Vizzaccaro[1], J. Auvray[2], A. Grolet[4], L. Salles[1] and N. Hoffmann[5]

[1]Imperial College London
London, UK
a.vizzaccaro17@imperial.ac.uk

[2]Centrale Marseille
Marseille, France

[4]Arts et Métiers ParisTech
Lille, France

[5]Hamburg University of Technology
Hamburg, Germany

Abstract In this work we investigate experimentally the localisation of energy that occurs in a symmetric structure composed of two weakly coupled identical beams impacting against bilateral rigid stoppers. The nonlinear modes of the underlying simplified model display localised solutions bifurcating from the homogeneous out-of-phase mode. In the range of frequencies where in-phase and out-of-phase nonlinear modes can interact, four stable branches are observed both numerically and experimentally, two of which consist of localised vibrating states.

This work aims at investigating, both numerically and experimentally, the existence of localised vibrations in a symmetric structure subject to piecewise-smooth nonlinearities.
Energy localisation in two degrees of freedom systems with cubic-type spring nonlinearities has been widely investigated (see e.g. Refs. [1]). Here a minimal model composed of two weakly coupled oscillators subject to bilinear springs is studied (1).

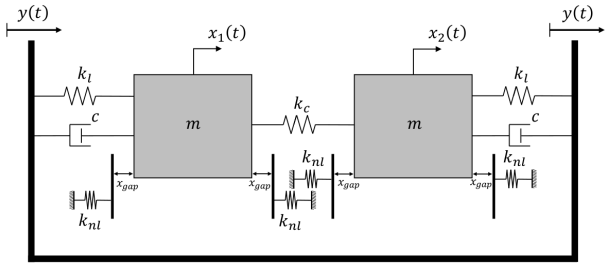

Figure 1: Minimal model of a symmetric piecewise linear system with two degrees of freedom subjected to base displacements.

Nonlinear modal analysis of this system has been performed and the existence of localised states bifurcating from the homogeneous out-of-phase mode is assessed. The out-of-phase solution, stable in the linear regime, loses stability at the grazing point and bifurcates in two localised solution branches. These branches only exist in a restricted range of frequencies that coincides with the range where in-phase and out-of-phase mode coexist. The localised branches then merge back onto the out-of-phase solution branch when the in-phase mode reaches its asymptotic limit frequency. The response of the system to a symmetric excitation also shows stable branches of localised solutions coexisting with the main branch of in-phase vibration.

A test-rig composed of two weakly coupled cantilever beams touching symmetrical stoppers, has been designed to reproduce the localisation phenomenon described above. The piecewise

stiffness, which introduces the nonlinear effect in the minimal model of Fig. 1, is obtained by means of impactors placed on each side of each beams at a fixed distance from the beam equilibrium position (cfr Refs. [2]). Two masses attached at the tip of each blade ensure that each beam behaves as a simple oscillator. The base excitation provides the symmetric forcing of both oscillators. Experimental results demonstrated the existence of four stable branches: the lower main branch where both masses vibrates in phase at low amplitude without impacts, the higher main branch where they both touch the stoppers, and two localised branches where they possess an out-of-phase component and either the first or the second beam is impacting and the other is not.

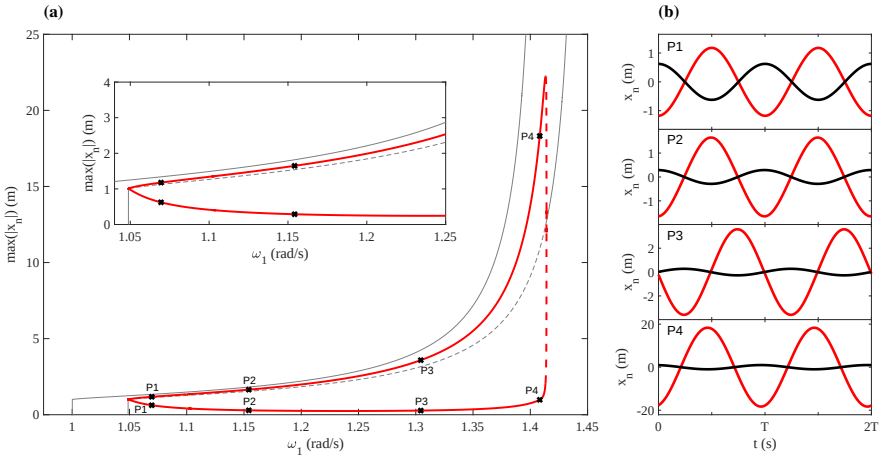

Figure 2: (a) Backbone curves of in-phase ond out-of-phase mode (gray) and localised solutions branch bifurcating at grazing point and merging at limit frequency and (b) displacement of the two masses over time at bifurcated branches

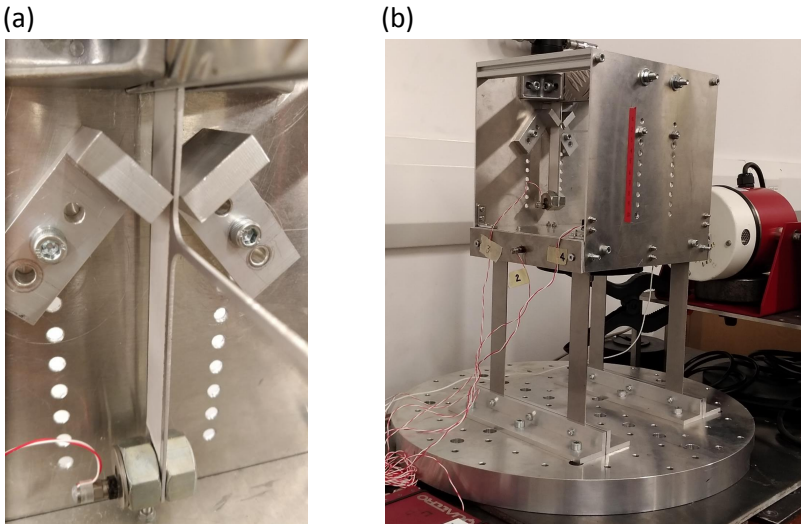

Figure 3: Test rig. Panel (b) shows the platform connected to the shaker, while Panel (a) depicts the stoppers near one of the two beams.

References

[1] T.Ikeda, Y. Harata, and K. Nishimura, *Intrinsic Localized Modes of Harmonic Oscillations in Nonlinear Oscillator Arrays*, Journal of Computational and Nonlinear Dynamics, 8, 041009, 2013.

[2] G. F. S. Rebouas, I. F. Santos and J. J. Thomsen, *Validation of vibro-impact force models by numerical simulation perturbation methods and experiments*, Journal of Sound and Vibration, 413, 291-307, 2018.

Characterization of a nonlinear sound absorber at low frequencies and high sound levels

M. Volpe[1], **S. Bellizzi**[1] **and R. Côte**[1]

[1]Aix Marseille Univ, CNRS, Centrale Marseille, LMA
Marseille, France
volpe@lma.cnrs-mrs.fr, bellizzi@lma.cnrs-mrs.fr, cote@lma.cnrs-mrs.fr

Abstract To characterize nonlinear acoustic loads identification techniques have been developed. A specific setup of impedance tube named "Short Kundt's Tube" (SKT) was built to reach high sound levels at low frequencies. Two approaches, developed in the frequency domain, are discussed : a linearization method giving access to the acoustic impedance and a nonlinear model which is able to characterize energy transfer to higher harmonics. Both are excitation level dependent.

Numerous sound absorbers dedicated to noise reduction at low frequencies are based on nonlinear properties, such as nonlinear vibroacoustic absorbers also known as Nonlinear Energy Sinks (see for example [1,2]). In this work, nonlinear elements are characterized at low frequencies and very high levels using a SKT [3] composed of a complex acoustic source connected to a tube wich support the device under test (DUT) (see Figure 1.(a,b)).

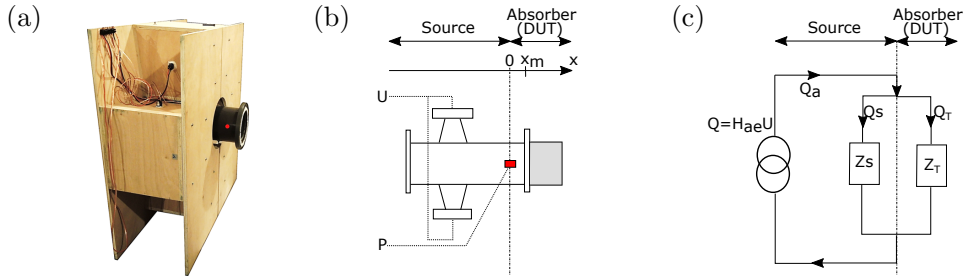

Figure 1: (a) Picture of the source. (b) Scheme of the experimental set-up and (c) the equivalent electroacoustic circuit of the one-microphone identification method.

A first identification technique is a linearization method and gives access to the acoustic impedance and/or the reflection coefficient which are excitation level dependent. After a source calibration step [3], the nonlinear DUT is characterized by an equivalent impedance $Z_T(f)$ (and the reflection coefficient $R_T(f)$). $Z_T(f)$ is definied as a linear approximation of the transfert between the pressure $P(f)$ and volume velocity $Q(f)$. They are both considered over the tube section in the measurement plane (see Figure 1.(c)). Two nonlinear acoustic absorbers, a thin viscoelastic circular membrane and the same membrane with a plywood box clamped on its rear face described in [2], have been studied. We observe that resonance frequencies of the two absorbers increase with the excitation level, characterizing a nonlinear behaviour of the systems and their hardening nature. Moreover, the energy extracted by the absorbers increase with the excitation level, over a frequency range widening.

A second technique is based on a nonlinear model which is able to characterize energy transfer to higher harmonics, by defining an impedance or a scattering matrix [4]. We assume that the acoustic source generates an excitation at only one frequency f (the fundamental frequency). The impedance formulation of multi-port model characterizes the relationship between the harmonic terms ($P_n(f)$) of the acoustic pressure at the microphone position and

the harmonic terms ($Q_n(f)$) of the corresponding acoustic volume velocity as

$$P_n(f) = \sum_{k=1}^{\infty} Z_{nk}(f, |P_1(f)|) Q_k(f) \text{ for } n = 1, 2, \cdots \tag{1}$$

The impedance term, $Z_{nk}(f, |P_1(f)|)$, represents the opposition at the frequency nf that the acoustic load presents to the acoustic flow at the frequency kf from a source signal at frequency f. This term depends on the excitation frequency f and on the amplitude level of the acoustic pressure represented by $|P_1(f)|$ (amplitude of the first harmonics). An equivalent formulation can be obtained using a scattering-matrix approach and Eq.(1) can be simplified by assuming that energy exchange can occur only from low to high frequency and that the DUT satisfies the harmonic superposition principle [5]. This method has been applied to an adjustable nonlinear acoustic absorber, made of a loudspeaker membrane described in [1]. Coefficients of the impedance matrice are reported Figure.2. Nonlinear behaviour of the absorber is visible on $|Z_{11}|$ where we can observe the frequency shift of the apparent resonance when the excitation level increases (see Figure2.(a)). $|Z_{22}(f)|$ is equivalent to a $|Z_{11}(f)|$ associated to a lower excitation level (level of $P_2(f)$) and shifted in frequency with a ratio of $f/2$ (see Figure.2(b)). Finally, $|Z_{21}|$ shows the transfer of energy between the fundamental and the second harmonics, which increases with the excitation level (see Figure.2(c)).

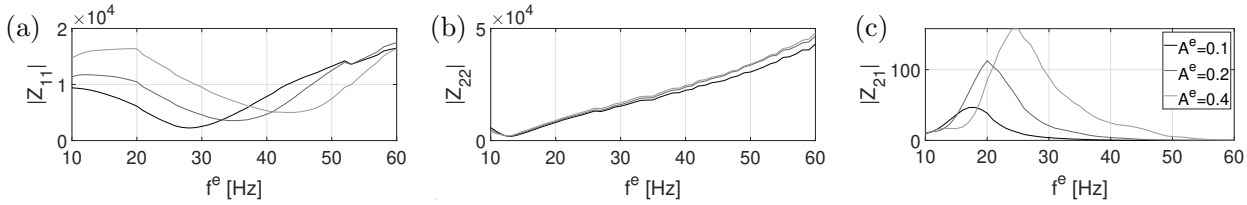

Figure 2: Estimation of impedance coefficients for three excitation levels.

These experimental results have been compared to numerical simulations results. In future works the quantification of energy transfer will be done with a larger number of harmonics, in order to quantify all the wave conversions present in the tube. A synchronized swept-sine method will be developed to improve experimental procedure.

References

[1] R. Mariani, S. Bellizzi, B. Cochelin, Ph. Herzog and P.O. Mattei, *Toward an adjustable nonlinear low frequency acoustic absorber*, Journal of Sound and Vibration 330, 5245-5258, 2011.

[2] P.Y. Bryk, S. Bellizzi and R. Côte, *Experimental study of a hybrid electro-acoustic nonlinear membrane absorber*, Journal of Sound and Vibration 424, 224-237, 2018.

[3] A. Chauvin, M. Monteil, S. Bellizzi, R. Côte, Ph. Herzog and M. Pachebat, *Acoustic characterization of a nonlinear vibroacoustic absorber at low frequencies and high sound levels*, Journal of Sound and Vibration 416, 244-257, 2018.

[4] H. Bodèn, *One-sided multi-port techniques for characterisation of in-duct samples with nonlinear acoustic properties*, Journal of Sound and Vibration 330, 3050-3067, 2012.

[5] Verspecht, J. and Root, D.E., Polyharmonic Distortion Modeling, *IEEE Microwave Magazine*, **7**(3), 44–57, (2006).

Using Complex Nonlinear Normal Mode to Design a Frictional Damper for Bladed Disk

Y. Sun, J. Yuan, L. Pesaresi, E. Denimal and L. Salles

Dynamics Research Group
Imperial College London
London, United Kingdom
ys5113@ic.ac.uk

Abstract A numerical methodology is described to design a frictional damper for blade structure within aircraft engine. A finite element beam-platform model is used for preliminary design stage. The frictional damper is designed based on two parameters, contact angle and vertical position of the platform. Nonlinear modal analysis is used to investigate the nonlinear dynamic behaviour and damping performance.

High cycle fatigue (HCF) is one of the common failure of turbines bladed disks within aircraft engines and normally caused by large vibrational stress. Dry friction dampers are widely used in turbomachinery industrial, since vibrational energy can be released through rubbing motion between the contact surfaces. The placement of dry friction damper is also important. In literature, there are several types of dry friction dampers within blade-disks [3]: root joints in Fig.1a [6], tip shrouds in Fig.1b [4] and underplatform dampers in Fig.1c [5]. Those interaction force, friction, between contact surfaces are strongly nonlinear due to stick-slide and separation, leading to complex dynamic behaviour. Therefore, after taking the friction into consideration, the techniques for nonlinear dynamic analysis are required to solve this complex problem.

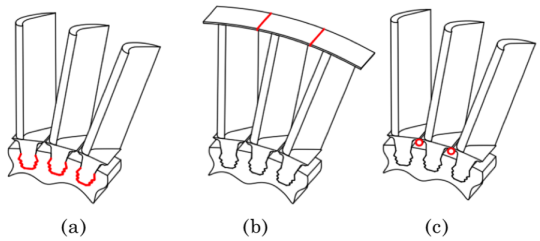

Figure 1: Different frictional dampers [1]

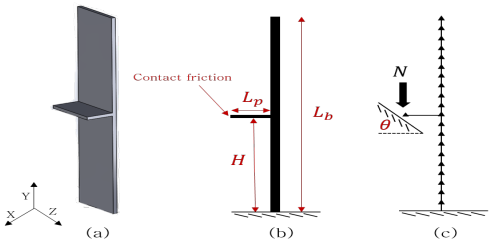

Figure 2: Beam-Platform Model

The objective is to determine the influence of the position of the damper on nonlinear dynamic behaviour of the system. Hence, a 2-D case is investigated. The blade is modelled with finite element beam-platform model displayed in Fig.2, where the platform can be located between the ground and tip of the beam. The position of platform is characterized by its vertical position H. The tip of the platform is in contact with frictional damper, the contact is characterized by the contact angle denoted θ. Therefore, this frictional damper is designed based on two parameters, contact angle $\theta \in [0°, 90°]$ and vertical position of the platform $H/L_b \in (0, 1]$. By varying the design parameters, all three types dampers given in Fig.1 can be modelled. A 2-D contact model is used to simulate the contact forces. Ideally, there are three contact status: separation, sticking and sliding.

Complex nonlinear normal modes are computed through the nonlinear modal analysis based on the method proposed by Krack [2]. Harmonic Balanced Method with continuation technique is the numerical approach used to solve the autonomous equation of motion in Eq.1, where $\mathcal{Q}$ is mass normalized displacements; $\mathcal{F}_c$ is contact forces. ζ is a negative artificial damping to

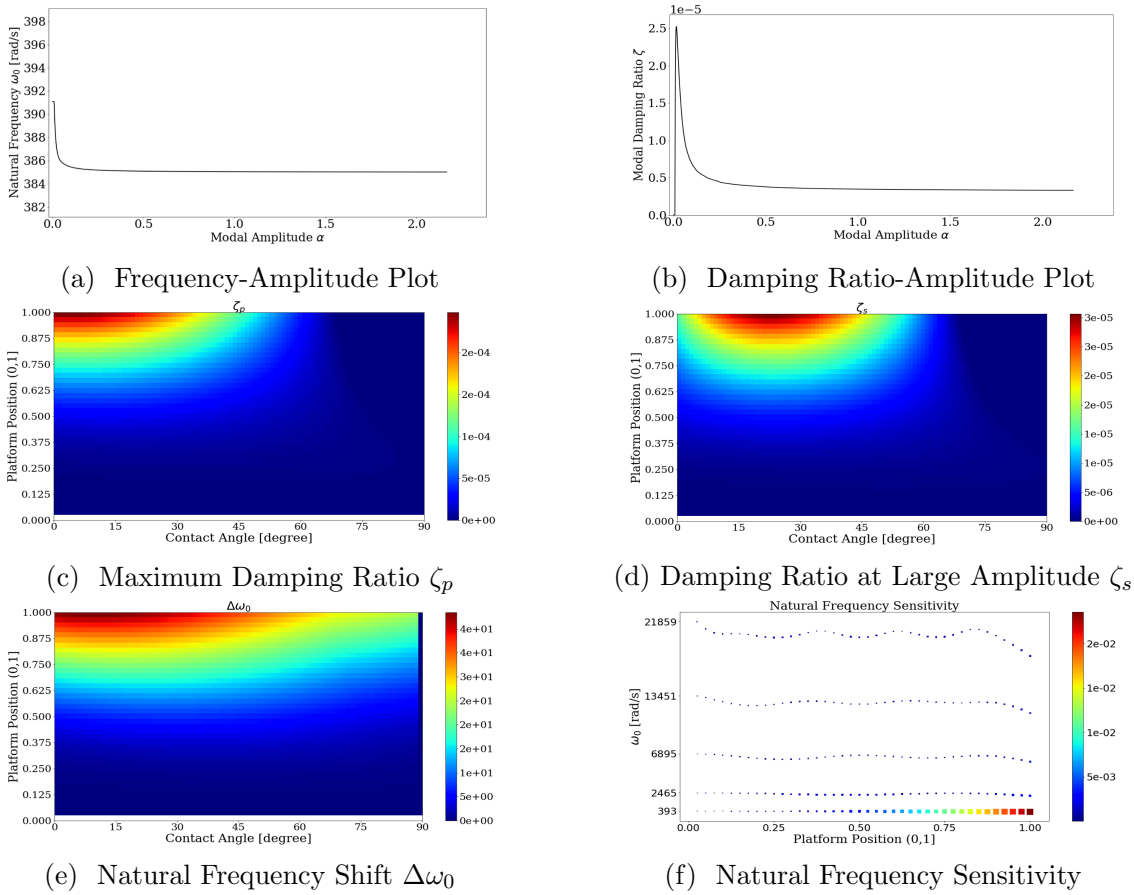

(a) Frequency-Amplitude Plot

(b) Damping Ratio-Amplitude Plot

(c) Maximum Damping Ratio ζ_p

(d) Damping Ratio at Large Amplitude ζ_s

(e) Natural Frequency Shift $\Delta\omega_0$

(f) Natural Frequency Sensitivity

Figure 3: Overview of the results

compensate the energy lost due to friction [2]. System vibrates at its natural frequency ω_0 and α is modal amplitude. Detailed description of numerical approach can be found in [7].

$$\mathbf{M}\alpha\ddot{\mathcal{Q}}(t) - (\zeta \times \mathbf{K})\alpha\dot{\mathcal{Q}}(t) + \mathbf{K}\alpha\mathcal{Q}(t) + \mathcal{F}_c(\alpha\mathcal{Q}, t) = 0 \tag{1}$$

The 1^{st} bending mode is chosen to assess the damping performance. After the nonlinear modal analysis, natural frequency ω_0 and modal damping ratio ζ are calculated within range of modal amplitude α. As shown in Fig.3a and 3b, the natural frequency and modal damping ratio are plotted against the modal amplitude. When the modal amplitude is low, the contact status is sticking and the whole system is purely linear. The natural frequency of the system is constant and there is no energy lost due to the friction. Then, the modal amplitude is increased to certain value, the platform starts to slide. In this case, two contact points are partial-sliding-partial-sticking. In this case, both natural frequency and modal damping ratio reach to a steady value. The softening effect is caused by change of the stiffness at the contact points. To assess the damping performance, three objectives are chosen: modal damping ratio at peak ζ_p and stable region ($\alpha = 2$) ζ_s as well as the shift of natural frequency $\Delta\omega_0$ in Fig.3c, 3d, 3e.

The damping performance is evaluated for whole design space and it appears that it is highly sensitive to both design parameters. The optimized damping performance is achieved while the contact angle θ is around 25°-30°. Shift of natural frequency can be explained by natural frequency sensitivity to the contact stiffness as shown in Fig.3f. Generally, underpaltform damper with desired contact angle is able to provide effective damping and acceptable shift of natural frequency. Uncertainty Quantification with Latin Hypercube Simulation will be investigated in near future to taking wearing effect and manufacturing tolerance of frictional damper into consideration.

A Taylor series based continuation method for equilibrium, periodic, quasi-periodic and transient solutions of dynamical systems

L. Guillot, B. Cochelin and C. Vergez

Aix Marseille Univ, CNRS, Centrale Marseille, LMA, UMR 7031,
Marseille, France,
guillot@lma.cnrs-mrs.fr, bruno-cochelin@centrale-marseille.fr, vergez@lma.cnrs-mrs.fr

Abstract. This paper emphasizes how a quadratic rewriting of ordinary differential equations (ODE) allows different types of solutions to be easily continued by asymptotic numerical method (ANM). The focus will be especially on the continuation of quasi-periodic steady state solutions and transient solutions. A toy model of saxophone is studied in detail to illustrate the methods presented.

Introduction. The ANM relies on a high-order Taylor series representation of the solution-branch. This technique has already proven its efficiency for a lot of applications in engineering, mechanics or acoustics for example. As opposed to standard predictor-corrector algorithm, the high order prediction of ANM series does not need a correction step in most cases. While some implementations relying on automatic differentiation do exist the choice is made here to work with a quadratic framework. A generic implementation of this latest approach which minimizes problem-dependent implementation has been developed [3, 4]. A simplified scheme is represented in figure 1. It is based on the numerical continuation of algebraic systems of the form

$$R(V) = 0, \qquad \text{where } V \in \mathbb{R}^{n+1} \text{ and } R(V) \in \mathbb{R}^n \text{ is analytic} \tag{1}$$

This system is always written in a quadratic format as a prerequisite of the method. This formalism is not a constraint that we suffer but a choice that allows to treat a very wide range of problems as shown in [3].

The quadratic framework. The quadratic rewriting of the system is a key point of our approach since it allows to compute the terms in the development of the series explicitly and very efficiently (see [3] for details). Here, the focus is on ODE :

$$\dot{X} = F(X, \lambda, t), \qquad \text{where } X \text{ and } F \in \mathbb{R}^n \text{ and } \lambda \in \mathbb{R} \tag{2}$$

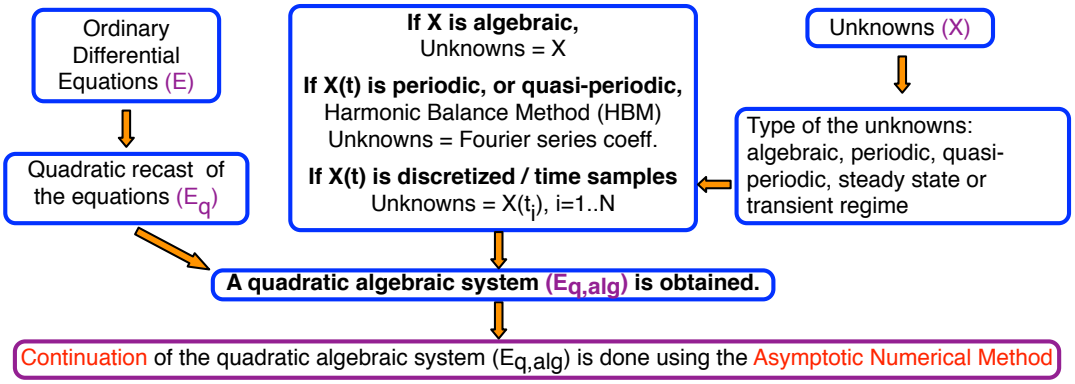

Figure 1: Different types of ODE solutions that can be easily continued by Asymptotic Numerical Method using quadratic rewriting.

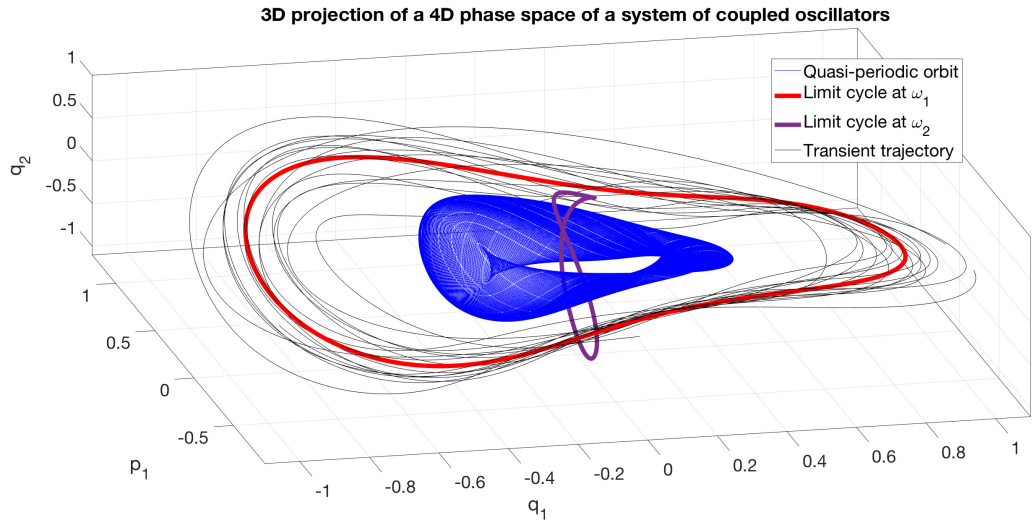

Figure 2: The two limit cycles and a quasi-periodic orbit of a system of a toy model of saxophone [4] obtained with our method. A transient that goes to one of the limit cycles is also represented.

Equ. (2) is solved using a quadratic recast. The equilibrium of ODEs and their stability can be classically treated by solving $F(X, \lambda, t) = 0$ and is not detailed. The periodic solutions and their stability is addressed with the harmonic balance method [4] and Hill's method [1]. The focus is on quasi-periodic and transient solutions.

A quasi-periodic solution can be sought for under the form of a truncated double Fourier series

$$X(t) = \sum_{k_1=-H}^{H} \sum_{k_2=-H}^{H} X_{k_1,k_2} e^{j(k_1\omega_1 + k_2\omega_2)t}, \qquad \text{where } X_{k_1,k_2} \in \mathbb{C},\ \omega_1, \omega_2 \in \mathbb{R}_+^\star. \tag{3}$$

Replacing $X(t)$ by (3) in equ (2) and deriving a quadratic algebraic system from the recast of equ. (2) can be automatized [2]. Continuation is then possible on unknowns X_{k_1,k_2}, ω_1 and possibly ω_2 if the system is autonomous.

To continue transient regimes of ODEs, the solution X is discretized on time samples

$$X(t_i), 1 \leq i \leq N, N \in \mathbb{N}^\star. \tag{4}$$

Then, the quadratic rewriting of equ. (2) is written on each time step so that the equations are automatically quadratic. A wide range of discretization schemes can be used : Runge-Kutta, Euler, Newmark, finite-differences*etc...* Once the initial value is specified, continuation is possible on unknowns $X(t_i)$ and possibly t_i for schemes with auto-adaptive time steps.

Conclusion. The details of the methods discussed above are available in the journal article [4]. The method requires very few effort to switch between the different types of solutions since the original ODE is rewritten quadratically by the user once and for all. It can also be applied to implicit differential-algebraic systems with time-delay or fractional order derivatives. An implementation of this approach is freely available online on a dedicated website http://manlab.lma.cnrs-mrs.fr/.

References

[1] Bentvelsen, B. and Lazarus, A. (2018). Modal and stability analysis of structures in periodic elastic states: application to the Ziegler column. Nonlinear Dynamics, 91(2), 1349-1370.

[2] Guillot, L., Vigué, P., Vergez, C. and Cochelin, B. (2017). Continuation of quasi-periodic solutions with two-frequency Harmonic Balance Method. Journal of Sound and Vibration, 394, 434-450.

[3] Guillot, L, Cochelin, B, Vergez, C. (2019). A generic and efficient Taylor seriesbased continuation method using a quadratic recast of smooth nonlinear systems. Int J Numer Methods Eng. ; 1 20. https://doi.org/10.1002/nme.6049

[4] Guillot, L. , Cochelin, B., Vergez, C. (2019). A Taylor series-based continuation method for solutions of dynamical systems. Nonlinear Dyn. https://doi.org/10.1007/s11071-019-04989-5

NNM & Forced responses

Thursday, 4th July 2019

Chairman: G. Rega

Nonlinear Vibration in Aircraft Engines

L. Salles[1], **A. Vizzaccaro**[1] **and Y. Sun**[2]

[1]Dynamics Group, Department of Mechanical Engineering Imperial College
London,UK
l.salles@imperial.ac.uk

Abstract Several component of turbomachinery operate in nonlinear regime of vibration during operation. We present in this work the state of the art techniques for analysing nonlinear vibration of turbomachinery. Most of the vibration anlayses are performed using frequency response for forced response problem. It is possible to use the concept of nonlinear normal modes and their adaptation for non conservative system. The periodic response are calculated using boundary value problem (BVP) solvers. We will present results using harmonic balance method and finite element in time techniques for non smooth dynamic problem. The work will conclude with presentation of challenge for the future in turbomachinery vibration analysis.

Turbomachinery are very complicated systems and undergo a large level of vibration during operation that leads to nonlinear behavior. Several kinds of nonlinearity are present in an aircraft engine as shown in Figure 1.

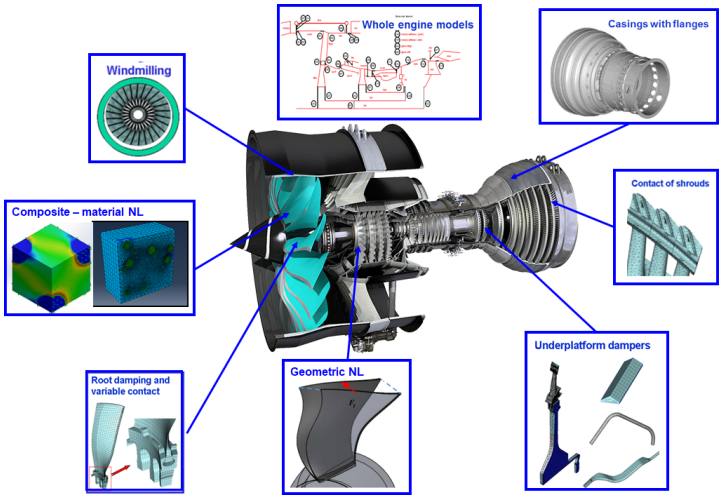

Figure 1: Nonlinearities in aircraft engine (pictures courtesy Rolls-Royce Plc)

An in-house code named FORSE has been developed at Imperial College for twenty years to deal with nonlinear vibration and different types of nonlinearity. The code was first designed to treat localized nonlinearities: contact, friction, impact, bearings... and was recently extended to distributed nonlinearities: material nonlinearities and geometric nonlinearities. FORSE is based on harmonic balance method coupled with continuation method and permits to compute frequency response, (complex) nonlinear normal modes and limit cycle oscillation. The software is based on object oriented programming using Modern Fortran. Some feature of the code are presented in this work and results for different applications. FORSE permit to solve boundary value problem in time defined by the following equation

$$\mathbf{M}\ddot{\mathbf{U}} + \mathbf{C}\dot{\mathbf{U}} + \mathbf{F}_{\text{int}}(\mathbf{U}) = \mathbf{F}_{\text{nl}}(\mathbf{U}, \dot{\mathbf{U}}) + \alpha\mathbf{F}_{ex}(t) \tag{1}$$

where $\mathbf{M}$ and $\mathbf{C}$ are the mass and damping matrices, $\mathbf{U}$ is the vector of displacement, $\mathbf{F}_{\text{int}}$ represents the internal forces due to large deformation or material nonlinearities, $\mathbf{F}_{\text{nl}}$ is the

vector of localized nonlinearities, $\alpha \mathbf{F}_{ex}(t)$ are the excitation forces and α is a cefficient used to switch between autonomous and non-autonomous system. The ordinary differential equation Eq. 1 is transformed to nonlinear algeabric system using Fourier Galerkin method and reduced order modelling (ROM) based on Component Mode Synthesis. The proposed ROM depends on the nonlinearities [2, 7]. The proposed techniques permits to calculate frequency response with detection and path following of bifurcated branches [4]. The code has been modified to calculate (complex) nonlinear normal modes for different applications [5, 6]. It is possible to extend the technique for analysing stability of rotating system [1]. Figure 2 shows results for a blade tip rub application [3].

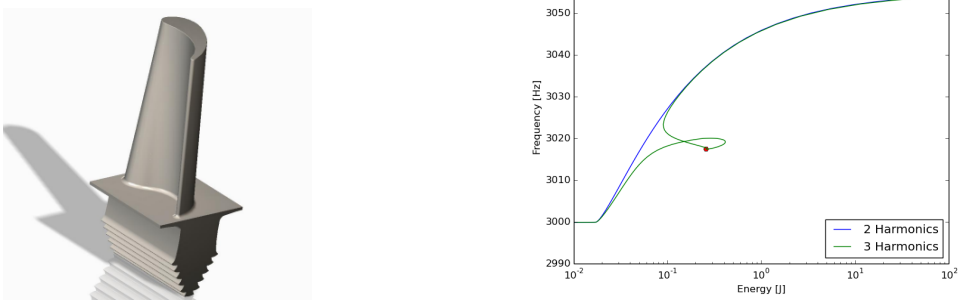

(a) turbine blade (b) FEP

Figure 2: Nonlinear Normal Mode of blade of first bending mode due to tip rub

Acknowledgment The first and second authors are grateful EPRSC and Rolls-Royce Plc for providing the financial support through prosperity partnerships Cornerstone (EP/R004951/1). The third author is grateful to China Scholarship Council (File NO. 201708060239) for providing the financial support for this project.

References

[1] J. Hong, P. Yu, D. Zhang, and Y. Ma, *Nonlinear dynamic analysis using the complex nonlinear modes for a rotor system with an additional constraint due to rub-impact*, Mechanical Systems and Signal Processing 116. 443-461, 2019.

[2] P. Longobardi, *Asymptotic Numerical Method for Nonlinear Vibration of Bladed-Disk including Geometric Nonlinearities*, Master thesis, Torino, 2019

[3] A. Panunzio, L.Salles, C. Schwingshackl and M. Gola, *Asymptotic numerical method and polynomial chaos expansion for the study of stochastic non-linear normal modes*, ASME TurboExpo, 2015.

[4] L. Salles, B. Staples, N. Hoffmann, C. Schwingshackl *Continuation techniques for analysis of whole aeroengine dynamics with imperfect bifurcations and isolated solutions*, Nonlinear Dynamics, 86, 3, 1897-1911, 2016

[5] A. Vizzaccaro and L. Salles, *Friction-induced vibrations due to mode-coupling instability in open gap systems* , (under review)

[6] Y. Sun, J. Yuan, L. Pesaresi and L. Salles, *Using Complex Nonlinear Normal Mode to Design a Frictional Damper for Bladed Disk*, 7 International Conference on Nonlinear Vibrations, Localization and Energy Transfer 2019.

[7] J. Yuan, F. El-Haddad, L. Salles, C. Wong, *Numerical Assessment of Reduced Order Modeling Techniques for Dynamic Analysis of Jointed Structures With Contact Nonlinearities*, Journal of Engineering for Gas Turbines and Power 141, 3, 2019.

Dynamics of a Rotating Nonlinear Hub-Beam Structure

J. Warminski[1]

[1]Department of Applied Mechanics, Faculty of Mechanical Engineering
Lublin University of Technology, Lublin, Poland
j.warminski@pollub.pl

Abstract Dynamics of a beam attached to a rotating rigid hub is presented in the paper. A beam model, based on extended Bernoulli-Euler theory, takes into account a nonlinear curvature, coupled transversal and longitudinal oscillations and non-constant angular velocity of the hub. Natural and forced vibrations are studied on the basis of exact equations of motion and associated dynamic boundary conditions derived from Hamilton principle.

The development of modern materials and design of lightweight and flexible rotating structures give rise to better understanding their dynamic response. Thus, more precise mathematical models which take into account nonlinearity of the system are required. Derivation of equations of motion of nonlinear flexural-torsional vibrations of a beam has been presented in [1] where a nonlinear beam curvature has been taken into account. However, inextensibility condition has been applied in the mathematical formulation. This resulted in a constraint relation between transversal and longitudinal displacements. Similar approach to the rotating structure with attached tip mass is presented in [2], but additionally quasi-static elongation of the beam and tension force occurring due to beam rotation have been considered. A rotating thin–walled composite beam has been studied in [3] but because of structural complexity only a linear deformation field has been included in the mathematical description. Nonlinear vibrations of a rotating cantilever beam have been studied recently in [4] where hardening or softening phenomenon has been demonstrated for reduced nonlinear Bernoulli-Euler beam based on the inextensionality condition.

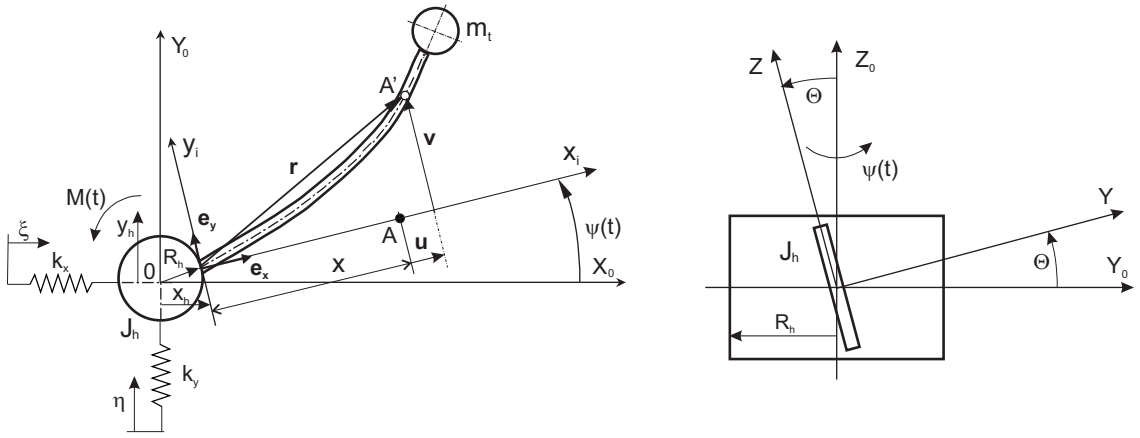

Figure 1: A model of a rotating hub-beam system with attached tip mass m_t, (a) top view with indicated deformations and (b) side view with preset angle Θ.

In the present paper we will develop a model of a rotating beam presented in [5] however, apart from rotation of the hub also translation of its center is considered. Equations of motion are based on assumptions of Bernoulli-Euler beam theory extended for axial elongation of the beam and nonlinear curvature based on the strict definition.

The model with global and local coordinate sets as well as displacements of an elementary beam point (u, v) are presented in Fig. 1(a) while the beam preset angle Θ is shown in side

view (Fig. 1b). The strain of the elementary segment and beam's curvature are defined as:

$$\varepsilon = \sqrt{\left(1+u'\right)^2 + v'^2} - 1, \quad \kappa = \frac{\partial \phi}{\partial s} = \frac{v''\left(1+u'\right) - v'u''}{\left[\left(1+u'\right)^2 + v'^2\right]^{3/2}} \tag{1}$$

Components of velocity vector $\dot{\mathbf{R}}$ of an arbitrary beam point in the absolute coordinates frame is defined as:

$$\begin{aligned} \dot{R}_{X_0} &= \dot{X}_h - \left[\left(R_h + s + u\right)\dot{\psi} + \dot{v}\cos\Theta\right]\sin\psi - v\cos\Theta\dot{\psi}\cos\psi \\ \dot{R}_{Y_0} &= \dot{Y}_h - \left[\left(R_h + s + u\right)\dot{\psi} + \dot{v}\cos\Theta\right]\cos\psi - v\cos\Theta\dot{\psi}\sin\psi \\ \dot{R}_{Z_0} &= \dot{v}\sin\Theta \end{aligned} \tag{2}$$

The differential equations of motion are derived on the basis of the extended Hamilton principle of least action

$$\int_{t_1}^{t_2} \left(\delta T - \delta V + \delta W_{nc}\right) dt = 0 \tag{3}$$

where T and V are kinetic and potential energies

$$T = \frac{1}{2}J_h\dot{\psi}^2 + \frac{1}{2}\int_0^L \rho_1\dot{R}^2 ds + \frac{1}{2}m_t\dot{R}_t^2\,, V = \frac{1}{2}\int_0^L \left(EI\kappa^2 + EA\varepsilon^2\right) ds + \frac{1}{2}k_X\left(X_0 - \xi\right)^2 + \frac{1}{2}k_Y\left(Y_0 - \eta\right)^2 \tag{4}$$

and δW_{nc} is virtual work of other nonconservative forces.

Substituting definitions for the strain, curvature and velocity into potential and kinetic energies as well as considering nonconservative forces, damping and excitations, we derive partial differential equations (PDEs) of motion of the rotating nonlinear hub–beam structure and associated dynamical boundary conditions for transversal and longitudinal vibrations. Due to long and complex forms the equations are not presented in the abstract. The ongoing work is to solve the equations by the direct attempt to PDEs by the multiple time scale method and then to determine natural and forced vibrations for fixed and varied angular velocity.

Acknowledgments The work is financially supported by grant 2016/23/B/ST8/01865 from the National Science Centre, Poland.

References

[1] M. R. M. Crespo da Silva and C. C. Glynn *Nonlinear flexural-flexural-torsional dynamics of inextensional beams, I. Equations of motion*, Journal of Structural Mechanics 6, 437-448, 1978.

[2] J. Warminski and J. M. Balthazar *Nonlinear vibrations of a beam with a tip mass attached to a rotating hub*, Proceedings of 20th ASME: Biennial Conference on Mechanical Vibrations and Noise, Long Beach, California, USA, DETC2005-84518:1-6, 2005.

[3] J. Latalski, J.Warminski and G. Rega, *Bending-twisting vibrations of a rotating hub–thin-walled composite beam system*, Mathematics and Mechanics of Solids, 22(6), 1303-1325, 2016.

[4] O. Thomas, A. Senechal and J.F. Deu, *Hardening/softening behavior and reduced order modeling of nonlinear vibrations of rotating cantilever beams*, Nonlinear Dynamics, 86, 1293-1318, 2016.

[5] J. Warminski, *Nonlinear Model of a Rotating Hub-Beams Structure:Equations of Motion*, Computer Methods in Mechanics (CMM2017), AIP Conf. Proc. 1922, 100006-1100006-7, 2017.

Phase driven modal synthesis for forced response evaluation

E. Sarrouy[1]

[1]Aix Marseille Univ, CNRS, Centrale Marseille, LMA UMR 7031, Marseille, France
emmanuelle.sarrouy@centrale-marseille.rr

Abstract A new definition is proposed for the Nonlinear Normal Modes, close to the one developed by Bellizzi & Bouc [1]. Theses NNMs are the used to evaluate the forced responses using a modal phase parametrization rather than the classical forcing frequency parametrization.

The basic dynamic equation considered for nonlinear dynamics writes

$$\mathbf{M}\ddot{\mathbf{u}} + \mathbf{C}\dot{\mathbf{u}} + \mathbf{K}\mathbf{u} + \mathbf{f}_{\mathrm{nl}}(\mathbf{u}, \dot{\mathbf{u}}) = \mathbf{f}_{\mathrm{e}}(t) \tag{1}$$

where $\mathbf{f}_{\mathrm{nl}}$ gathers nonlinear forces while $\mathbf{f}_{\mathrm{e}}$ denotes a periodic external forcing.

Damped nonlinear normal modes (dNNMs) are the solutions of Eq. (1) when the forcing $\mathbf{f}_{\mathrm{e}}$ is nullified [3]. Several methods to compute these solutions where proposed. The one exposed and used here is close to the amplitude and phase parameterization described by Bellizzi and Bouc [1]. Displacements $\mathbf{u}$ and velocities $\mathbf{v}$ have the same dependency to an amplitude α and a dimensionless time τ than in [1] but the amplitude decay function η and the pseudo circular frequency ω only depend on amplitude here:

$$\mathbf{u}(t) = \alpha(t)\boldsymbol{\psi}^u(\alpha(t), \tau(t)),\ \mathbf{v}(t) = \alpha(t)\boldsymbol{\psi}^v(\alpha(t), \tau(t)),\ \dot{\alpha}(t) = \eta(\alpha(t))\alpha(t),\ \dot{\tau}(t) = \omega(\alpha(t)) \tag{2}$$

Once injected in Eq. (1), and adding $\mathbf{v} = \dot{\mathbf{u}}$ condition leads to

$$\alpha\boldsymbol{\psi}^v(\alpha,\tau) = \eta(\alpha)\alpha\boldsymbol{\psi}^u(\alpha,\tau) + \alpha\left(D_\alpha\boldsymbol{\psi}^u(\alpha,\tau)\eta(\alpha)\alpha + D_\tau\boldsymbol{\psi}^u(\alpha,\tau)\omega(\alpha)\right) \tag{3a}$$

$$\begin{aligned}\mathbf{M}\left(\eta(\alpha)\alpha\boldsymbol{\psi}^v(\alpha,\tau) + \alpha\left(D_\alpha\boldsymbol{\psi}^v(\alpha,\tau)\eta(\alpha)\alpha + D_\tau\boldsymbol{\psi}^v(\alpha,\tau)\omega(\alpha)\right)\right) + \\ \mathbf{C}\left(\alpha\boldsymbol{\psi}^v(\alpha,\tau)\right) + \mathbf{K}\left(\alpha\boldsymbol{\psi}^u(\alpha,\tau)\right) + \mathbf{f}_{\mathrm{nl}}(\alpha\boldsymbol{\psi}^u(\alpha,\tau), \alpha\boldsymbol{\psi}^v(\alpha,\tau)) \ &= \ \mathbf{0}\end{aligned} \tag{3b}$$

Instead of seeking for the various quantities as a power series in α and a Fourier series in τ which leads to a very large system of equations, a "point-by-point" approach is preferred in the α dimension: a branch is defined by successive points gathering $\alpha^{(i)}$ (modal amplitude), $\mathbf{Q}^{u^{(i)}}$ (Fourier coefficients for $\boldsymbol{\psi}^{u^{(i)}}$), $\mathbf{Q}^{v^{(i)}}$ (Fourier coefficients for $\boldsymbol{\psi}^{v^{(i)}}$), $\eta^{(i)}$ (modal amplitude decay function) and $\omega^{(i)}$ (modal circular frequency). While $D_\tau\bullet = \partial\bullet/\partial\tau$ quantities can be evaluated exactly via Fourier series derivation, $D_\alpha\bullet = \partial\bullet/\partial\alpha$ is evaluated using a linear interpolation between the previous and the current points. The two necessary normalization conditions are defined by

$$\boldsymbol{\psi}^u(\alpha,0)^{\mathrm{T}}\mathbf{M}\boldsymbol{\psi}^u(\alpha,0) + \boldsymbol{\psi}^u(\alpha,\pi/2)^{\mathrm{T}}\mathbf{M}\boldsymbol{\psi}^u(\alpha,\pi/2) = 1 \tag{4a}$$

$$\boldsymbol{\psi}^u(\alpha,0)^{\mathrm{T}}\mathbf{M}\boldsymbol{\psi}^u(\alpha,\pi/2) = 0 \tag{4b}$$

Lastly, points on the branch are index by their (discrete) arclength $s^{(i)}$:

$$\begin{aligned}s^{(i)} = s^{(i-1)} + \Big(&\left(\alpha^{(i)} - \alpha^{(i-1)}\right)^2 + \left(\eta^{(i)} - \eta^{(i-1)}\right)^2 + \left(\omega^{(i)} - \omega^{(i-1)}\right)^2 \\ &+ \left|\left|\mathbf{Q}^{u^{(i)}} - \mathbf{Q}^{u^{(i-1)}}\right|\right|^2 + \left|\left|\mathbf{Q}^{v^{(i)}} - \mathbf{Q}^{v^{(i-1)}}\right|\right|^2\Big)^{1/2}\end{aligned} \tag{5}$$

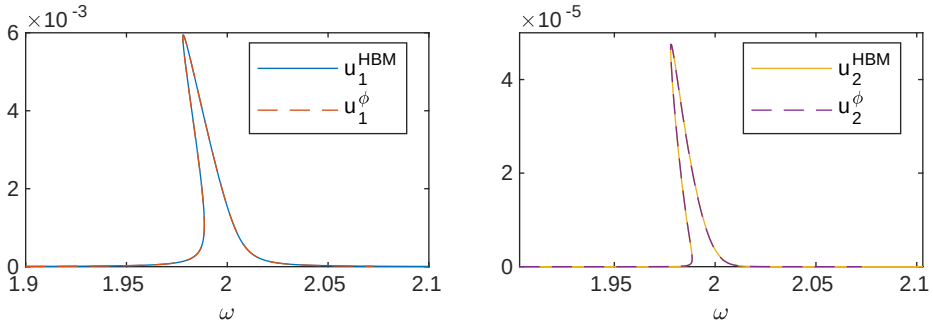

Figure 1: Illustration: modal synthesis around first mode for a 2-dofs system.

Once a dNNM is calculated, it offers a first understanding of the structure as well as a rough prediction of its behavior when forcing is introduced. It can also be used to compute the forced response effectively using modal synthesis.
Let us assume that $\mathbf{f}_e(t) = \mathbf{f}_{e_0}\cos(\omega t)$. Using a dimensionless time $\tau = \omega t$ and denoting $\mathbf{u}_\tau(\tau) = \mathbf{u}(t)$, $\bullet' = d\bullet/d\tau$, Eq. (1) becomes

$$\omega^2\mathbf{M}\mathbf{u}_\tau'' + \omega\mathbf{C}\mathbf{u}_\tau' + \mathbf{K}\mathbf{u}_\tau + \mathbf{f}_{\text{nl}}(\mathbf{u}_\tau, \omega\mathbf{u}_\tau') = \mathbf{f}_{e_\tau}(\tau) \tag{6}$$

Then, $\mathbf{u}_\tau$ is naturally sought as

$$\mathbf{u}_\tau(\tau) = \tilde{\mathbf{u}}(s, \tau + \phi) \tag{7}$$

where the 2 unknowns are s which defines the location on the dNNM branch and ϕ, the phase with respect to the excitation as in the linear case.
Equations used to find these 2 unknowns are

$$\int_0^{2\pi} \mathbf{r}(\tau)\,\tilde{\mathbf{u}}(s, \tau+\phi)\,d\tau = 0 \text{ and } \int_0^{2\pi} \mathbf{r}(\tau)\,\left(\omega\tilde{\mathbf{u}}'(s, \tau+\phi)\right)\,d\tau = 0 \tag{8}$$

with $\mathbf{r}(\tau)$ being the residue of the dynamical equation (6):

$$\mathbf{r}(\tau) = \omega^2\mathbf{M}\mathbf{u}_\tau'' + \omega\mathbf{C}\mathbf{u}_\tau' + \mathbf{K}\mathbf{u}_\tau + \mathbf{f}_{\text{nl}}(\mathbf{u}_\tau, \omega\mathbf{u}_\tau') - \mathbf{f}_{e_\tau}(\tau) \tag{9}$$

This system can be solved using any continuation method in the variables ω, s, ϕ.

Another approach is to consider that, as in the linear case, ϕ will vary from 0 to $-\pi$ with a continuous decrease along the frequency function response (FRF). Hence, the FRF can be computed by solving for ω and s only for discrete values of $\phi \in]-\pi, 0]$ avoiding the use of a continuation scheme. This approach was applied to compute the first mode and the FRF around this first mode for the 2-dofs example used by Touzé and Amabili [4] and return very accurate results as illustrated in Figure 1 for which reference results are HBM results with up to 5 harmonics. This phase parameterization can be very interesting in the stochastic case to link points of different realizations as explained in [2] for the linear case.

References

[1] S. Bellizzi and R. Bouc. "An amplitude-phase formulation for nonlinear modes and limit cycles through invariant manifolds". In: *Journal of Sound and Vibration* 300.3–5 (2007), pp. 896 –915. DOI: 10.1016/j.jsv.2006.09.004.

[2] E. Sarrouy. "Phase driven study for stochastic linear multi-dofs dynamic response". In: *Mechanical Systems and Signal Processing* 129 (2019), pp. 717–740. DOI: 10.1016/j.ymssp.2019.04.042.

[3] S.W. Shaw and C. Pierre. "Normal Modes for Non-Linear Vibratory Systems". In: *Journal of Sound and Vibration* 164.1 (1993), pp. 85–124. DOI: 10.1006/jsvi.1993.1198.

[4] C. Touzé and M. Amabili. "Nonlinear normal modes for damped geometrically nonlinear systems: Application to reduced-order modelling of harmonically forced structures". In: *Journal of Sound and Vibration* 298.4–5 (2006), pp. 958–981. DOI: 10.1016/j.jsv.2006.06.032.

Computing nonlinear modes of geometrically nonlinear structures

B. Cochelin, L. Guillot and C. Vergez

Aix Marseille Univ, CNRS, Centrale Marseille, LMA, UMR 7031
Marseille, France
bruno.cochelin@centrale-marseille.fr

Abstract The harmonic balance method is combined to the asymptotic numerical method to compute the nonlinear modes of geometrically nonlinear structural mechanical systems discretized by the finite element method. The method is first described on a toy duffing model and then applied to a beam formulation with large displacements, large rotations but small strain. Various examples computed with the V4 Manlab software are presented.

Let us described the numerical method on a toy duffing equation $\ddot{u} + \lambda\dot{u} + u + u^3 = 0$. Introducing the velocity $v = \dot{u}$ and the auxiliary variable $w = u^2$ the system is recasted as a first order ODE with quadratic nonlinearities

$$\begin{array}{lll} \dot{u} = & v & \\ \dot{v} = & -\lambda v & -u * w \\ 0 = & w & -u * u \end{array}$$

The harmonic balance method aims at determining periodic solutions of the system using Fourier expansion of the unknowns $u(t), v(t)$ and $w(t)$. Denoting $\hat{u}$ the vector of Fourier coefficients of $u(t)$ and ω the angular freuency, the balance of the harmonics yields the following quadratic algebraic system

$$\begin{array}{lll} \omega\, D\, \hat{u} & = & \hat{v} \\ \omega\, D\, \hat{v} & = -\lambda\hat{v} & -\mathrm{conv}(\hat{u}, \hat{w})_{same} \\ 0 & = & \hat{w} \quad -\mathrm{conv}(\hat{u}, \hat{u})_{same} \end{array}$$

where D and 'conv' are operators for derivative and convolution (same : means that the output has the same harmonic truncature as the two inputs). A phase condition is added to close the system. The computation of the solution branches of this algebraic system is performed by the so-called asymptotic-numerical method,ie , a high order Taylor series based computation method.

The key point of the method is the quadratic recast of the governing equation. This can be achieved for almost any model by following the procedure presented in [1] . It is illustrated here for a beam model with large displacements and rotations. Let $u(x)$, $w(x)$, $\theta(x)$ denote the displacements and the rotation of the cross-section. By introducing the following auxiliary variables (quadratic equation)

$$\begin{array}{ll|ll} C(x) & = \cos(\theta) \rightarrow dC = -Sd\theta & N(x) & = ESe \\ S(x) & = \sin(\theta) \rightarrow dS = Cd\theta & M(x) & = EIk \\ e(x) & = (1+u') * C + w' * S - 1 & T(x) & = GS\gamma \\ k(x) & = \theta' & F_x(x) & = N * C - T * S \\ \gamma(x) & = -(1+u') * S + w' * C & F_y(x) & = N * S - T * C \\ & & T_2 & = N * \gamma - (1+e) * T \end{array}$$

the governing equations of the beam reads (linear equation)

$$\int_0^L \rho S\ddot{u}\delta u + \rho S\ddot{w}\delta w + \rho I\ddot{\theta}\delta\theta \mathrm{dv} + \int_0^L F_x\delta u' + F_y\delta w' + M\delta\theta' + T_2\delta\theta \mathrm{dv} = 0$$

A finite element discretization is performed with the element descrtibed in [2]. Several nonlinear mode examples will be presented at the conference as in the figure below. The well-known difficulty of dealing with the numerous bifurcations associated with modal interactions will be adressed for NNMs and for forced responses.

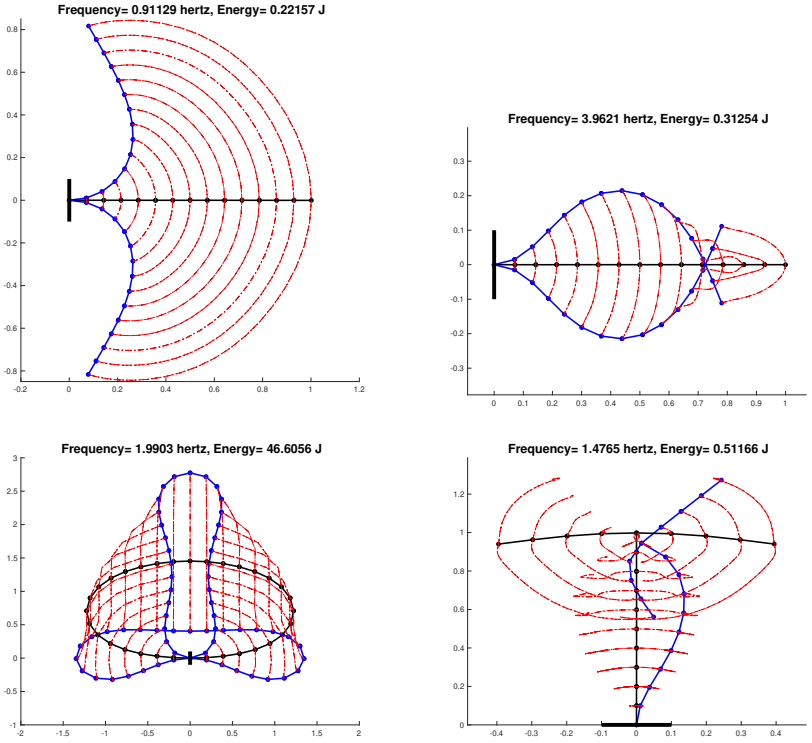

Figure 1: Nonlinear mode periodic motion of various beam structures. In blue : extreme position at $t = 0$ and $t = \frac{T}{2}$, in black : position at $t = \frac{T}{4}$ and $t = \frac{3T}{4}$, in red : trajectory of the nodes. left up : first mode of a clamped-free beam. right up : Second mode of a clamped-free beam with a mass at the end. Left bottom : Second mode of a circular beam. Right bottom : second mode of a T-shape frame. A pure harmonic balance with H=14 harmonics has been used for these computation

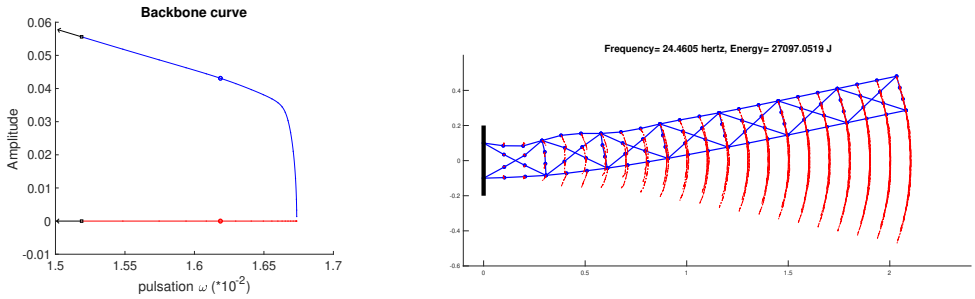

Figure 2: The first nonlinear mode of a this frame structure is softening because of local buckling near the attached end, The model has 258 d.o.f., H=8 harmonics

References

[1] L. Guillot, B. Cochelin and C. Vergez *A generic and efficient Taylor series–based continuation method using a quadratic recast of smooth nonlinear systems*, Inter. J. Numer. Methods Eng, 1-20, 2019.

[2] 0.Thomas, A. Sénéchal, J.F. Deü, *Hardening/softening behaviour and reduced order modeling of nonlinear vibrations of rotating cantilever beams*, Nonlinear Dynamics, 86:1293-1318, 2016.

Author Index

Publications du LMA n° 160
ISSN 1159-0947 - ISBN 978-2-909669-26-7
Résumés étendus / Extended Abstracts
7th International Conference on
Nonlinear Vibrations, Localization and Energy Transfer
1st - 4th July 2019, Marseille (France)